

Particalized Eggshell Membrane (PEM) for Biomedical Applications

Ling Wu

Thesis submitted to the University of Ottawa
in partial fulfillment of the requirements for the
Master's degree

Department of Cellular and Molecular Medicine
Faculty of Medicine
University of Ottawa



uOttawa

L'Université canadienne
Canada's university

© **Ling Wu, Ottawa, Canada, 2021**

TABLE OF CONTENTS

TABLE OF CONTENTS	II
LIST OF TABLES	VI
LIST OF FIGURES	VII
ABBREVIATIONS	IX
ABSTRACT.....	XII
DEDICATIONS	XIII
ACKNOWLEDGEMENTS	XIV
CHAPTER 1 INTRODUCTION.....	1
1.1 Avian egg	1
1.2 Eggshell membrane	4
1.3 Multifunctional proteins	6
<i>Collagen.....</i>	<i>6</i>
<i>Cysteine-rich eggshell membrane proteins (CREMPs).....</i>	<i>7</i>
<i>Ovocalyxin-36 (OCX-36).....</i>	<i>9</i>
<i>Avian Beta-Defensins (AvBDs).....</i>	<i>10</i>
1.4 Biomedical applications of ESM.....	10
1.5 Skin immune system.....	12
1.6 Antimicrobial protein/peptides.....	17
1.7 Antimicrobial resistance	17
1.8 Skin inflammation	18
1.9 Oxidative stress	23
CHAPTER 2 HYPOTHESIS AND OBJECTIVES.....	26
2.1 Hypothesis	26
2.2 Objectives	26

CHAPTER 3 MATERIAL AND METHODS.....	27
3.1 Preparation of PEM	27
<i>Moisture content</i>	<i>27</i>
<i>Cryo-Grinding (CG) of ESM</i>	<i>27</i>
<i>Sieving and further processing</i>	<i>28</i>
<i>Assessment of microbial contamination</i>	<i>28</i>
3.2 Characterization of PEM.....	29
<i>Evaluation of surface morphology (Performed by G. Kulshreshtha).....</i>	<i>29</i>
<i>PEM particle size analysis (Performed by G. Kulshreshtha).....</i>	<i>29</i>
<i>Calcium content (Performed by T. Ahmed and L. Wu).....</i>	<i>29</i>
3.3 Evaluation of antimicrobial activity.....	30
<i>Bacterial strains and growth conditions.....</i>	<i>30</i>
3.4 Evaluation of anti-inflammatory activity	30
<i>Cell culture</i>	<i>30</i>
<i>Preparation of LPS.....</i>	<i>31</i>
<i>Cell viability assay.....</i>	<i>31</i>
<i>Nitric oxide assay</i>	<i>32</i>
3.5 Evaluation of antioxidant activity	33
<i>PEM Hydrolysis.....</i>	<i>33</i>
<i>Total antioxidant assay.....</i>	<i>33</i>
<i>Protein quantification.....</i>	<i>34</i>
3.6 Statistical analysis.....	35
CHAPTER 4 PRODUCTION AND CHARACTERIZATION OF PEM	38
4.1 Introduction.....	38
4.2 Results.....	39
4.2.1 <i>Production of PEM</i>	<i>39</i>
<i>Moisture content</i>	<i>42</i>
<i>Cryo-Grinding and further process.....</i>	<i>44</i>
<i>Assessment of microbial contamination</i>	<i>47</i>
4.2.2 <i>Characterization of PEM.....</i>	<i>48</i>

Morphology and particle size	48
Calcium content	51
4.3 Discussion	58
CHAPTER 5 EVALUATION OF THE ANTIMICROBIAL ACTIVITY OF PEM	64
5.1 Introduction.....	64
5.2 Results.....	66
5.2.1 Dose-dependent antimicrobial activity of PEM versus <i>E. coli</i>	66
5.2.2 Size-dependent antimicrobial activity of PEM versus <i>E. coli</i>	66
5.4 Discussion	72
CHAPTER 6 IN VITRO EVALUATION OF THE ANTI-INFLAMMATORY ACTIVITY OF PEM.....	77
6.1 Introduction.....	77
6.2 Results.....	78
6.2.1 The effect of PEM on LPS-activated murine macrophages.....	78
Cell viability	78
Proinflammatory mediator NO level	79
6.3 Discussion	83
CHAPTER 7 IN VITRO EVALUATION OF ANTIOXIDANT ACTIVITY OF PEM	87
7.1 Introduction.....	87
7.2 Results.....	89
7.2.1 Specific antioxidant activity of PEM	89
7.2.2 Effect of NaOH hydrolysis on the specific antioxidant activity of PEM.....	89
7.2.3 Effect of hydrolysis parameters on the antioxidant activity of PEM-H.....	93
Macroscopic appearance changes in response to different hydrolysis conditions	93
TEAC levels and protein concentrations in the PEM-H samples.....	93
Specific antioxidant activity	95
Summary of the correlation between three parameters and antioxidant activity index.....	96

7.3 Discussion104

CHAPTER 8 CONCLUSIONS..... 115

COPYRIGHTED CONTENT..... 116

REFERENCES..... 121

LIST OF TABLES

Table 1-1 Various protein families identified in ESM	5
Table 3-1 Hydrolysis conditions of PEM-H (permutations and combinations are described in the text)	37
Table 4-1 Moisture loss of ESM during drying.....	43
Table 4-2 Summary of the yield of PEM obtained after cryo-grinding and sieving.....	45
Table 4-3 Impact of top-down approach on PEM particle size	50
Table 4-4 Calcium content of PEP and I-ESM	52
Table 4-5 Elemental analysis of PEM in various preparations analyzed by energy-dispersive x-ray spectroscopy (EDS).....	53
Table 4-6 Amino acid composition of PEM in various sizes as compared to literature values for ESM.....	54
Table 7-1 Analysis of the correlation between three parameters and specific antioxidant activity	103

LIST OF FIGURES

Figure 1-1 Longitudinal section to depict the interior contents of a chicken egg	2
Figure 1-2 Stylized depiction of the reproductive system of the hen, containing an incomplete egg in the uterus.....	3
Figure 1-3 Schematic of skin histology viewed in cross-section with microorganisms and skin appendages	15
Figure 1-4 Levels and Components of the Cutaneous Barrier	16
Figure 1-5 Inflammatory triggers (LPS) activate the expression of proinflammatory genes	22
Figure 3-1 Flowchart of production of PEM.....	36
Figure 4-1 Macroscopic appearance of dried ESM and the resultant PEM after grinding and sieving	41
Figure 4-2 Particle size distribution of industrial ESM (I-ESM) and PEM obtained from top-down processing, including cryo-grinding for different times followed by sieving.	46
Figure 4-3 Scanning electron microscopy (SEM) of ESM in various size ranges	49
Figure 4-4 Cross-sectional views homogenized PEM hollow fibers	56
Figure 4-5 Hypothetical mechanisms for the formation of PEM hollow fibers after Emulsiflex homogenization	57
Figure 5-1 Dose-dependent antimicrobial activity of PEM<53 μm against <i>E. coli</i>.....	69
Figure 5-2 Size-dependent antimicrobial activity of various sizes PEM against <i>E. coli</i>.....	71
Figure 6-1 Effect of PEM on cell viability of RAW 264.7 macrophages.....	81
Figure 6-2 Effect of PEM on NO production in LPS-stimulated RAW 264.7.....	82
Figure 7-1 Specific antioxidant activity of various sizes of PEM	91

Figure 7-2 Effect of PEM dose and PEM size on specific antioxidant activity of PEM-H... 92

Figure 7-3 Effects of time-, dose- and temperature-dependent NaOH hydrolysis on TEAC level and protein concentration of PEM-H<53 μm 100

Figure 7-4 Effects of time-, dose- and temperature-dependent NaOH hydrolysis on specific antioxidant activity of PEM-H<53 μm 102

ABBREVIATIONS

3-MPA	3-mercapto-propionic acid; C ₃ H ₆ O ₂ S
AD	Atopic Dermatitis
AMP	Antimicrobial Peptide
ANOVA	Analysis of Variance
ATCC	American Type Culture Collection
AvBDs	Avian Beta-Defensins
BCA	Bicinchoninic Acid
BHA	Butylated Hydroxyanisole
BHT	Butylated Hydroxytoluene
BPI	Bactericidal Permeability-Increasing Protein
BSA	Bovine Serum Albumin
CAT	Catalase
CCl ₄	Carbon Tetrachloride
CFU	Colony Forming Unit
CG	Cryo-Grinding
CREMP	Cysteine-Rich Eggshell Membrane Protein
CRP	Cysteine-Rich Protein/Peptide
DNA	Deoxyribonucleic Acid
DTT	Dithiothreitol
EDTA	Ethylenediaminetetraacetic Acid
ES	Eggshell
ESM	Eggshell Membrane

FBS	Fetal Bovine Serum
GAGs	Glycosaminoglycans
GPx	Glutathione Peroxidase
GuHCl	Guanidine Hydrochloride
HCl	Hydrochloric Acid
HSC	Hepatic Stellate Cells
Ig	Immunoglobulin
IL	Interleukin
LB broth	Luria-Bertani Broth
LBP	Lipopolysaccharide-Binding Protein
LOXL2	Lysyl Oxidase-Like 2
LPS	Lipopolysaccharide
MRSA	Methicillin-resistant <i>Staphylococcus aureus</i>
MSSA	Methicillin-sensitive <i>Staphylococcus aureus</i>
NADPH	Nicotinamide Adenine Dinucleotide Phosphate
NF- κ B	Nuclear factor-kappa B
OCX	Ovocalyxin
OD	Optical Density
PAMP	Pathogen-associated Molecular Patterns
PBS	Phosphate Buffered Saline
PEM	Particalized Eggshell Membrane
PEP	Processed Eggshell Membrane Powder
PFA	Performic Acid

PLUNC	Palate, Lung and Nasal Epithelial Clone
PRR	Pattern Recognition Receptors
RJF	Red Junglefowl
RNS	Reactive Nitrogen Species
ROS	Reactive Oxygen Species
SEM	Scanning Electron Microscopy
SEP	Soluble Eggshell Membrane Protein
SOD	Superoxide Dismutase
spp.	Species
TBARS	Thiobarbituric Acid Reactive Substances
TEAC	Trolox Equivalent Antioxidant Capacity
TNF	Tumor Necrosis Factor
WHO	World Health Organization
WSEM	Water-soluble Eggshell Membrane

ABSTRACT

Eggshell membrane (ESM) provides a physical and bioactive barrier to protect the developing embryo. Proteomics and bioinformatics analyses have revealed that the collagen-rich ESM is composed of >500 proteins with multiple functionalities. The goal of this study was to produce novel particalized ESM (PEM) with enhanced bioactivities for focused applications on positive skin health. A novel top-down method was developed to produce the PEM from table eggs, in a submicron size range. PEM exhibited dose- and size-dependent antimicrobial activity against Gram-positive *Staphylococcus aureus* (*S. aureus*), and Gram-negative *Pseudomonas aeruginosa* (*P. aeruginosa*) and *Escherichia coli* (*E. coli*) species. A dose-dependent anti-inflammatory activity for PEM was observed in an *in vitro* model but no significant difference between two finest sizes. Additionally, the antioxidant activity of PEM was significantly improved by optimized chemical hydrolysis with size-dependent activity. Taken together, the eco-friendly PEM has great potential as a novel topical ingredient for cosmetics/ skincare applications.

DEDICATIONS

This thesis is dedicated to the loving memory of my grandparents, Zhu Hongyuan (朱鸿元) and Liu Zhifeng (刘芝凤). Surviving the war, my grandpa never stopped absorbing knowledge and loving others and enjoyed high prestige and respect. His immense knowledge and insightful thoughts helped me achieve higher levels and to see the bigger picture. He will always be the light of my life guiding me to be a righteous, kind, brave, insightful, modest, and independent person. And I know we are still together in the multiverse.

I also dedicate this thesis to my parents who unconditionally respect and support all my decisions and always create the best environment for me, so that I can stick to the things I love. I want to tell them: I have no regrets and I can do well in biology, just as well as I could have done in math and physics.

I would also dedicate this thesis to my best friend and also boyfriend Su Qiran, for his constant company to help me get through sadness, anger and depression.

Lastly, I would dedicate this thesis to world peace.

ACKNOWLEDGEMENTS

I would like to express my sincere gratitude to my supervisor Dr. Maxwell Hincke for the trust and support of my research in uOttawa. His patience, encouragement, and guidance throughout these two years have made this work much more meaningful and helped me to become closer to my dream.

I also deeply and truly appreciate my committee members, Dr. Qiao Li, Dr. Riadh Hammami and Dr. Erik Suuronen for their insightful advice and support of my research.

In addition, I would like to thank my lab members for their priceless help in both my research and life, making these two years an unforgettable memory.

This research was funded by the Natural Sciences and Engineering Research Council of Canada (NSERC), Egg Farmers of Canada (EFC), and Burnbrae Farms.

CHAPTER 1 INTRODUCTION

1.1 Avian egg

The domesticated chicken (*Gallus gallus domesticus*), a subspecies of the red junglefowl (RJF), appeared in the human record many millennia ago. A recent genomics study revealed that domestic chickens were initially derived from the RJF subspecies *Gallus gallus spadiceous*, at least six thousand years ago, which is now predominantly distributed in southwestern China, northern Thailand and Myanmar (M. Wang et al., 2020). Following their domestication, chickens interbred locally with both RJF subspecies and other junglefowl species when they travelled across Southeast and South Asia. Since then, chickens have been selectively bred for meat and egg production and are a critically important component of food production for human consumption.

From inside to outside, the avian egg is composed of a central yolk, egg white (albumen), eggshell membranes (ESM), calcified eggshell (ES) and cuticle (Figure 1-1). Egg formation is a complex but well-organized process (Figure 1-2) (Hincke et al., 2012). Briefly, after ovulation, the yolk travels through specialized regions of the oviduct to collect components of the forming egg, such as the vitelline membrane surrounding the yolk (infundibulum) and the albumen (magnum). Next, the precursors of the highly cross-linked meshwork of ESM fibres are secreted and assembled around the albumen (white isthmus) (Hincke et al., 2012). The double-layered ESM is formed on the surface of the rotating egg with an inner thin membrane (15–26 μm thick) and outer thick membrane (50-70 μm thick) (Cordeiro & Hincke, 2011; Liong et al., 1997), which are similar in terms of general morphology and amino acid composition (Kodali et al., 2011).

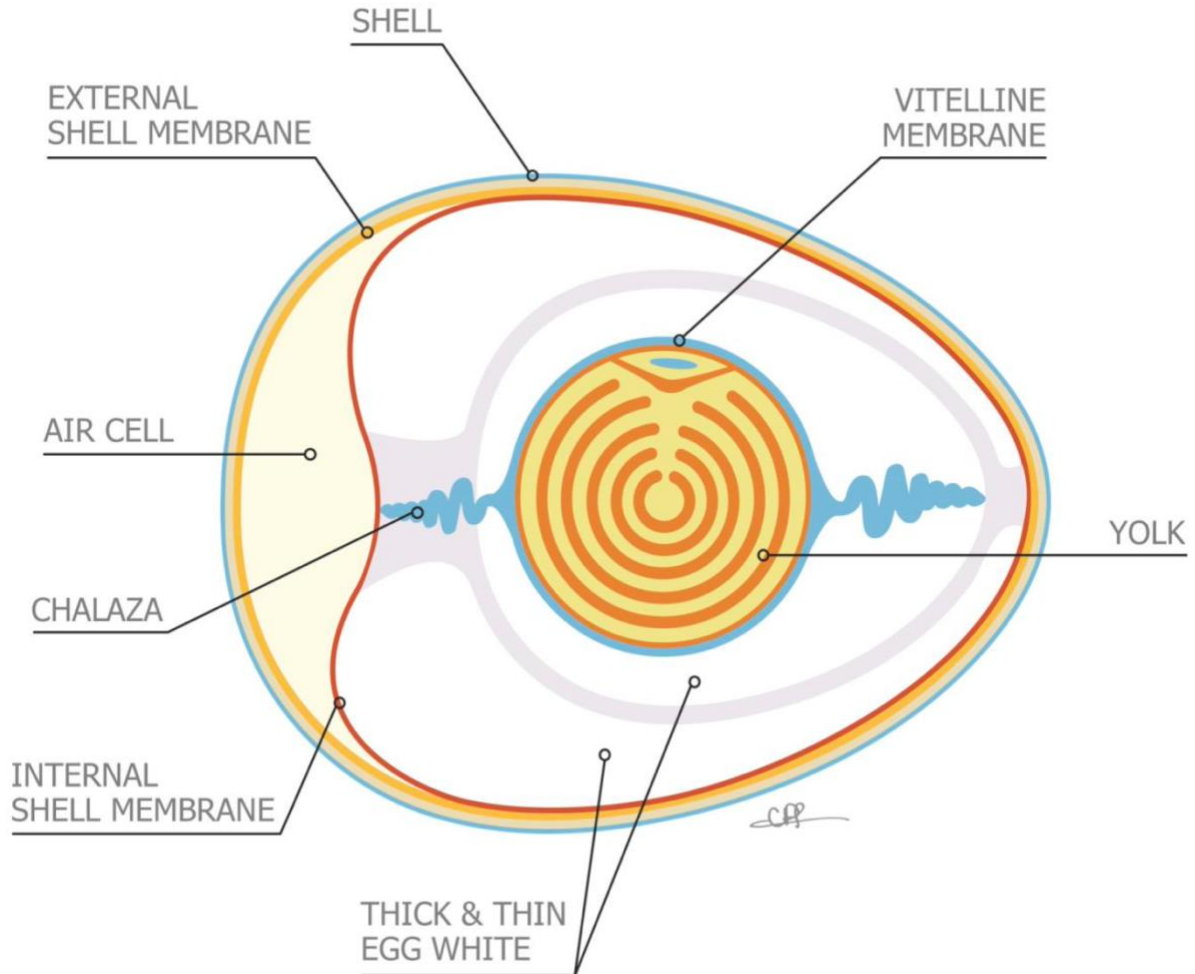


Figure 1-1 Longitudinal section to depict the interior contents of a chicken egg

Source: Hincke et al., 2012. The eggshell: structure, composition and mineralization. *Frontiers in Bioscience*. 17:1266-80. With permission from *Frontiers in Bioscience*.

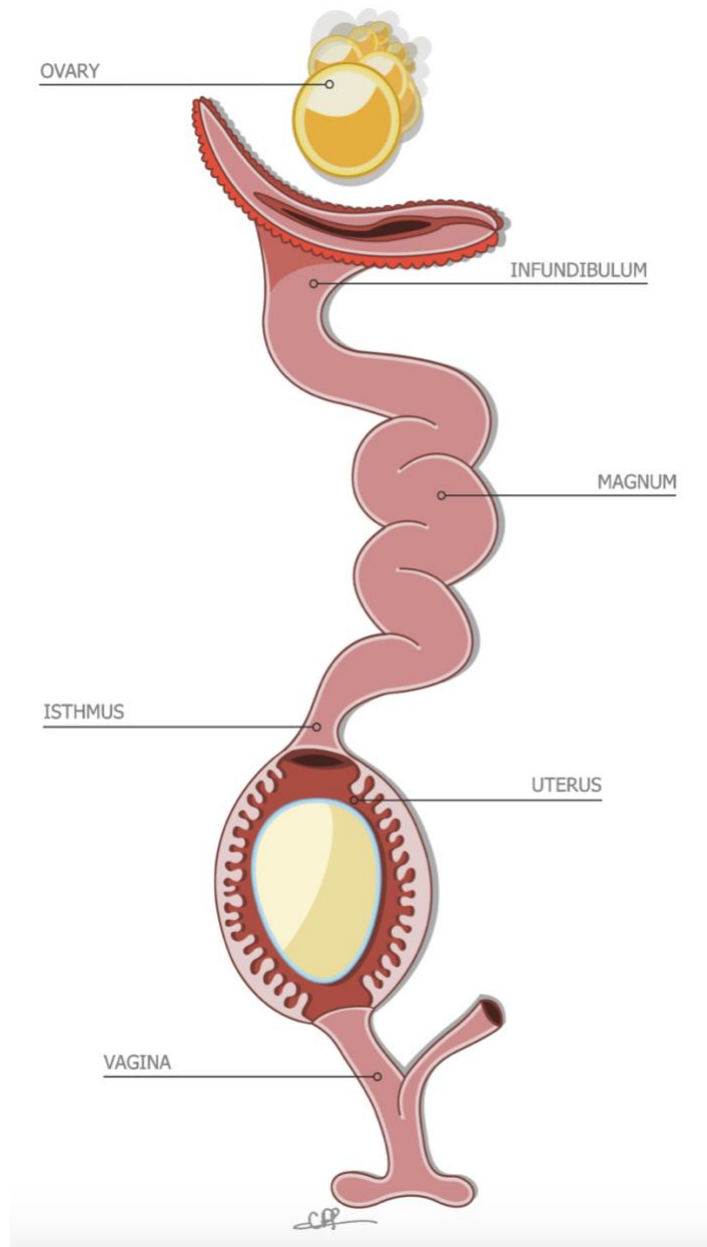


Figure 1-2 Stylized depiction of the reproductive system of the hen, containing an incomplete egg in the uterus

Source: Hincke et al., 2012. *The eggshell: structure, composition and mineralization. Frontiers in Bioscience*. 17:1266-80. With permission from *Frontiers in Bioscience*.

1.2 Eggshell membrane

In eggs, the ESM functions to maintain the albumen and plays an essential role in the formation of the ES by providing the structural support upon which biomineralization occurs (Ahmed et al., 2017). Lysine-derived cross-linkages in ESM contribute to the structure and mechanical properties. ESM also provides a biological homeostatic environment which supports the developing embryo in fertilized eggs (Rose-Martel et al., 2015). The ESM is mainly constituted by various proteins, of which approximately 10% are types I, V and X collagens, in addition to lysozyme, CREMPs (cysteine-rich eggshell membrane proteins) and many other proteins and glycoproteins [e.g. ovotransferrin, lysozyme, lysyl oxidase-like type 2 (LOXL2), etc.] (Ahmed et al., 2017; Makkar et al., 2015), and high levels of functional groups (e.g. lysine-derived desmosine and isodesmosine cross-linkages) (Ahmed et al., 2017; Gharibi & Abdolmaleki, 2018). Lysine-derived cross-linkages in ESM fibres render them intractable to dissolving in reducing agents and detergents, and subsequently the ESM fibres possess poor solubility and low bioavailability, which hinder the identification of their proteins and their applications. Hincke et al. (2000) previously identified and located lysozyme as an ESM component using colloidal-gold immunocytochemical staining. Kodali et al. (2011) identified a major disulfide-rich structural protein termed CREMP by digesting reductively alkylated proteins of ESM. Recently, Ahmed et al. (2017) identified 472 proteins in ESM by merging the results from different extraction/solubilization conditions with various proteomic approaches. Of this, 163 and 124 proteins were relatively or highly specific to ESM compared to other egg compartments. Various families of ESM-enriched proteins were identified (Table 1-1) namely collagens, CREMPs, histones, avian β defensins (AvBDs), LOXL2, ovocalyxin-36 (OCX-36), etc. (Ahmed et al., 2017).

Table 1-1 Various protein families identified in ESM

No.	Protein family name	Family members identified in ESM
1	Avian β -defensins	Avian β -defensins 9 and 10
2	Collagens	Collagens III (α 1 chain), IV (α 1, α 3, and α 6 chains), V (α 2 chain), VII (α 1 chain), VIII (α 1 chain), X (α 1 chain), XII (α 1 chain), XXII (α 1 chain).
3	Cysteine-rich eggshell membrane proteins (CREMPs)	CREMP - CREMP6
4	Enolases	Enolases 2 and 3
5	Heterogenous nuclear ribonucleoproteins	Heterogenous nuclear ribonucleoproteins A2/B1, A3, and D-like
6	Histones	Histones H1.11L, H1.11R, H2A, H2B, H3 family 3C, and H5
7	Motor proteins	Dyneins (axonemal heavy chain 1, 9, and 12), dynein (cytoplasmic heavy chain 1), and kinesin (21B and 26A).
8	Myeloid/lymphoid or mixed-lineage leukemia	Myeloid/lymphoid or mixed-lineage leukemia 2 and 3
9	Neuron navigator	Neuron navigators 2 and 3
10	Protein-coupled receptor kinase interactors	Protein-coupled receptor kinase interactors 1 and 2
11	Serpin peptidase inhibitors	Serpin peptidase inhibitors clade B (ovalbumin) members 1 and 5, and clade E (nexin, plasminogen activator inhibitor type 1) member 2
12	Transient receptor potential cation channel	Transient receptor potential cation channel subfamily M member 1 and Subfamily V member 2
13	Zinc finger proteins	Zinc finger proteins 185-like and 335

Source: Ahmed et al., 2017. In-depth comparative analysis of the chicken eggshell membrane proteome. *Journal of Proteomics*, 155, 49–62., with permission from *Journal of Proteomics*.

1.3 Multifunctional proteins

Largely composed of collagens and CREMPs, the ESM fibres serve as structural support for enzymes and proteins and a physical barrier that protects the embryo against invading microorganisms and external damage. Multifunctional proteins including antimicrobial, anti-inflammatory and antiviral proteins were directly identified in the ESM, such as lysyl oxidase (Akagawa et al., 1999), lysozyme (Hincke et al., 2000), ovotransferrin (Gautron, Hincke, Panheleux, et al., 2001), OCX-36 (Cordeiro et al., 2013), histones (Ahmed et al., 2017), Av β D 11 (Guyot et al., 2020), and so on. Other types of bioactivity proteins are identified in hen reproductive compartments or eggshell matrix suggesting the possibility of their existing in ESM, which includes OCX -32 (Gautron, Hincke, Mann, et al., 2001), OCX-36 and other bactericidal permeability-increasing protein/ lipopolysaccharide-binding protein/ palate, lung and nasal epithelial clone (BPI/LBP/PLUNC)-like proteins (Gautron et al., 2007), Av β D (type 1-5, and 7-12) (Mageed et al., 2008). These groups of proteins not only characterize the innate immune protection of the embryo but also inspire meaningful biomedical research and applications of the ESM as an attractive biomaterial (Baláž, 2014).

Collagen

Collagen is one of the structural proteins in ESM constituting 10% of its total protein content (Ahmed et al., 2017; Arias et al., 1991; Baláž, 2014). Similarly, collagen is the most abundant fibrous protein of the extracellular matrix (ECM) and makes up to 30% of the total protein mass of a multicellular animal (Frantz et al., 2010). This structural protein plays a critical role in various developmental events and tissue homeostasis, such as support tissue tensile strength, cell adhesion, chemotaxis, migration and tissue development, making them a potent

biomedical material for skin burn and cosmetic additive (Baláz, 2014; Frantz et al., 2010).

Noteworthy, skin substitutions that are commercially available contain collagen products including collagen engineered composites (TransCyte®, Biobrane®, Integra®) and collagen-based natural analogues like de-epithelialized allograft (Alloderm®) (Ruszczak, 2003).

Cysteine-rich eggshell membrane proteins (CREMPs)

The cysteine-rich eggshell membrane proteins (CREMPs) were first identified by Kodali et al. (2011) and verified by gene expression and proteomic analyses (Ahmed et al., 2017; Du et al., 2015). As a structural protein, the CREMPs share similar sequence motifs with spore coat protein SP75 of cellular slime molds. Proteomic analysis revealed the presence of 7 members of the CREMP family (CREMP, CREMP1, CREMP2, CREMP3, CREMP4, CREMP5, and CREMP6) (Ahmed et al., 2017). The CREMP family contains around 13.8% cysteine, in contrast to collagen X (α -1) which has only 0.2% cysteine, and is only detectable under the most intense extraction method by proteomic analysis due to repetition of the disulfide-containing modules and other cross-linkages, suggesting that the CREMP family is largely responsible for the relatively high cysteine content and the mechanical stability of the ESM (Ahmed et al., 2017; Du et al., 2015; Kodali et al., 2011).

Cysteine-rich peptides/proteins (CRPs) are highly divergent between groups and species but they all share some common features: (i) an N-terminal signal peptide, and (ii) a C-terminal cysteine-rich domain usually containing some cysteine residues (Marshall et al., 2011). Cysteine-rich proteins (CRPs) are found in many natural products, including the albumin family (e.g. serum albumin, ovalbumin and apo- α -lactalbumin), lysozyme, trypsin, ferritin and its derivatives (transferritin, apoferritin, lactoferrin), and keratin which possess multi-physicochemical

properties as well as biomedical potential (G. Yang et al., 2019). In the human body, members of the CRP family are associated with the processes of cell proliferation and differentiation, particularly cardiac and skeletal muscle development (Louis et al., 1997). Human secreted cysteine-rich mini-proteins are found to be ligands for G protein- and enzyme-coupled receptors, transporters, extracellular enzyme inhibitors, and antimicrobial peptides (Lavergne et al., 2012). Particularly, cysteine exhibited a comparable antioxidant activity to butylated hydroxyanisole (BHA), butylated hydroxytoluene (BHT), and α -tocopherol due to the redox ability of the sulfhydryl group (Taylor & Richardson, 1980). Moreover, a deficit in cysteine is one of the hallmarks of the ageing process, including the decrease in muscle and immune function, plasma albumin level as well as an increase in tumor necrosis factor- α (TNF- α) concentration, and has been considered as a major driving force for multiple aging-related degenerative processes (Dröge, 2005).

Disulfide bonds in CRPs play vital roles in a wide range of cellular processes – from the stabilization of secreted proteins to the regulation of cellular adhesion, migration and viral fusion (Hogg, 2003). Many mammalian secreted proteins that possess biological function and pharmaceutical potential contain disulfide bonds, including hormones, growth factors, immunoglobulins and integrins (Hogg, 2003; Salinas et al., 2011). More and more evidence shows that the cleavage of disulfide bonds in mature proteins contributes to significant consequences for protein function (Chiu & Hogg, 2019; Hogg, 2003). For instance, CD4, a receptor of the immunoglobulin (Ig) superfamily with extracellular disulfide bond domains that mediate cellular crosstalk in the immune response, is the primary receptor for human immunodeficiency virus type 1 (HIV-1) (Hogg, 2003; Matthias et al., 2002). However, conformational changes in CD4 by cleavage of the disulfide bond of the D2 domain can drive the

fusion of HIV-1 and cell membrane, thereby, increasing the chance of infection (Matthias et al., 2002).

Ovocalyxin-36 (OCX-36)

OCX-36 is an eggshell matrix protein of approximately 36 kDa molecular mass; it was first identified in the regions of the oviduct and uterine fluid where eggshell formation and the active growth phase of calcification take place (Ahmed et al., 2017; Gautron et al., 2011). OCX-36 is also present in the chicken calcified eggshell, vitelline membrane, intestine, and is particularly abundant in the ESM (Cordeiro et al., 2013; Gautron et al., 2007, 2011). OCX-36 shares a similar sequence region with the antibacterial protein superfamily BPI/LBP/PLUNC, with 20–27% identities (Gautron et al., 2007, 2011). This homology is further reinforced by the similarity of the exon/intron organization between the OCX-36 gene and mammalian LBP/BPI genes that have a major role in the innate immune response (Cordeiro et al., 2013; Gautron et al., 2007, 2011). Additionally, OCX-36 is a pattern recognition protein that recognizes bacterial endotoxins in innate immune response protection against bacterial invasion (Cordeiro et al., 2013). Specifically, ESM-purified OCX-36 demonstrated antimicrobial activity against *S. aureus* and binding activity to non-endotoxin pyrogen lipoteichoic acid (LTA) of *S. aureus* and endotoxin pyrogen LPS of *E. coli* during an inflammatory response. Furthermore, OCX-36 and enzymatically digested OCX-36 (dOCX-36) exhibited different immune-modulating activity on LPS-induced secretion of TNF- α and nitric oxide (NO) *in vitro* (Kovacs-Nolan et al., 2014). In their study, dOCX36 showed better efficiency in ameliorating LPS-induced inflammatory symptoms and inhibiting local production of proinflammatory mediators as compared to OCX-36 in the small intestine in an endotoxemia mouse model.

Avian Beta-Defensins (AvBDs)

In vertebrates, defensins are cysteine-rich antimicrobial peptides and classified as three main groups, α -, β - and θ -defensins, based on the position of disulfide bridge pairing and conserved six cysteine residues (Ahmed et al., 2017; Cuperus et al., 2013). β -defensins are found in all vertebrate species, while reptiles and birds only express type β -defensins, and mammals additionally produce α -defensins and θ -defensins (Ageitos et al., 2017). β -defensins are involved in the innate immune response, possessing a broad-spectrum antimicrobial activity against bacteria and fungi (Yacoub et al., 2015). The AvBDs are a family of small cationic antimicrobial peptides (AMPs) found in birds and characterized by a triple-stranded β -sheet structure that connects a loop of β -hairpin turn and is stabilized by three disulfide bridges (Ageitos et al., 2017). Most types of the AvBDs are expressed in the hen reproductive tract, whereas only 4 AvBDs were identified in the chicken egg by proteomics, namely AvBD-3, AvBD-10, AvBD-11 and AvBD-12 (Ahmed et al., 2017; Cuperus et al., 2013; Mann, 2008). Noteworthy, AvBD-11 was found in the egg vitelline membrane (VM) and ESM (Ahmed et al., 2017; Guyot et al., 2020; Hervé-Grépinet et al., 2010; Mageed et al., 2008) and its cationic N-terminal domain was shown to potentiate the antibacterial, antiviral, antiparasitic and anti-invasive activities *in vitro* (Guyot et al., 2020). Moreover, immunomodulatory and anti-inflammatory properties have also been identified in the AvBD family (van Dijk et al., 2008). For instance, AvBD-12 demonstrated a chemotactic activity on chicken macrophages, murine immature dendritic cells (DCs) and Chinese hamster ovary (CHO)-K1 cell line (M. Yang et al., 2016).

1.4 Biomedical applications of ESM

The hen eggshell membrane protects the chick embryo, just as the mammalian amniotic membrane protects the fetus. Centuries ago, ESM was mentioned as a remedy for injuries in the pharmacopeia of Chinese medicine by Bencao Gangmu (Sah & Pramanik, 2014). It was also widely used as a major ingredient, namely “phoenix cloth”, to treat decubitus ulcers, burns corneal ulcers and tympanic perforations (J. Jia et al., 2011). Furthermore, there is evidence showing that ESM has potential as a substratum for stroma cell adherence (Tavassoli, 1983); as creating an extracellular matrix (ECM) environment for human dermal fibroblast cells (HDF) adhesion (Ohto-Fujita et al., 2011); as a platform for molecular interaction analysis (Ohto-Fujita et al., 2011); as a dressing material for burns, ulcers and split-thickness skin graft (STSG) donor sites (J. Jia et al., 2011; Maeda & Sasaki, 1982; Mogoşanu & Grumezescu, 2014; Sah & Pramanik, 2014; Juiyung Yang et al., 2003; Zadik, 2007); as a treatment for pain and stiffness associated knee osteoarthritis (Ruff, DeVore, et al., 2009; Ruff, Winkler, et al., 2009); as a membrane for periodontal tissue regeneration (J. Jia et al., 2012; Kavarthapu & Malaiappan, 2019); as a nerve guide channel for peripheral nerve regeneration (Farjah et al., 2013); as a scaffold for bone tissue regeneration (cartilage and meniscal) (Pillai et al., 2015); as an eye model for vitreous surgery training (Hirata et al., 2013), etc.

In addition, ESM has received much attention from skin researchers. Hydrolyzed ESM fractions showed moisture protective effects on skin layers and exhibited anti-inflammatory, anti-wrinkle, and antimicrobial activities that were appropriate for cosmetic agents for skin health (Yoo et al., 2014). Moreover, Yoo et al. (2015) reported that ESM hydrolysate possesses functional potential for cosmetic applications, since it mitigated wrinkle formation in a UVB-radiation-induced SKH-1 hairless mice model. In addition, *in vitro* studies demonstrated stimulation of hyaluronan (HA) production, as well as inhibition of collagenase synthesis and

matrix metalloproteinase-I activity (MMP-1). More recently, a clinical pilot study of water-soluble egg membrane (WSEM)-containing facial cream reported reduction of facial wrinkle depth and increases in cellular collagen and elastin with antioxidant activity (Jensen et al., 2016).

ESM has applications for wound healing as well. Topical bonding of ESM to a full-thickness traumatic lip laceration appeared to relieve wound inflammation and pain with a positive healing outcome (Zadik, 2007). A combined application of hydrolyzed water-soluble egg membrane (WSEM) with *aloe vera*-based Nerium oleander extract (NAE-8i, oleandrin-free) was shown to enhance the immune-activating effect of NAE-8i *in vitro* by triggering the production of cytokines and chemokines during the wound healing process (Benson et al., 2016).

Therefore, ESM possesses a great potential for biomedical applications that include cell culture and tissue regeneration, as well as skin and bone health.

1.5 Skin immune system

The skin is a large architecturally and biologically heterogeneous organ of the human body. Anatomically, the skin is composed of epidermis, dermis and hypodermis from outer to inner layer with a geographically diverse distribution of densities of hair follicles, sebaceous glands and sweat glands, as well as regional variations in the thickness of the epidermal and dermal layers that compose the first line of defense of the human body (Figure 1-3) (Otberg et al., 2004; Turin et al., 2018). Moreover, the topographical and temporal diversity of skin microbiota residents in various skin areas help to shape the unique and precise skin immune defense (Grice et al., 2009; Grice & Segre, 2011).

The skin comprises microbiome, chemical, physical and immune barriers that interconnect to protect the body from external harm and to maintain homeostasis in response to

injury or assault (Figure 1-4). Microorganisms including viruses, bacteria, fungi, and mites reside on the skin surface, hairs and glands (Grice & Segre, 2011). Actinobacteria, Firmicutes, Bacteroidetes and Proteobacteria are four different phyla of most skin bacteria, of which Actinobacteria are the main members. Diversity of microbiota varies topographically due to regions of higher temperature and humidity that harbour more gram-negative bacilli, such as coryneform and *Staphylococcus aureus* (*S. aureus*) (Grice et al., 2009). On the skin surface, rod and round bacteria (e.g., *Proteobacteria* and *Staphylococcus* spp.) communities are deeply interwoven with each other and other microorganisms. *Propionibacterium acnes*, a common skin commensal bacterium, mainly grow in sebaceous glands and contribute to production of free fatty acids to maintain the acidic skin surface pH (~5), which inhibits the colonization by *S. aureus* and *Pseudomonas aeruginosa* (*P. aeruginosa*) and promote colonies of coagulase-negative staphylococci and corynebacterial (P. M. Elias, 2007; Gribbon et al., 1993; Grice & Segre, 2011).

The skin maintains its immunological functions by modulating colonization of commensal microbiota. For instance, pattern recognition receptors (PRRs) of keratinocytes, such as Toll-like receptors (TLRs), mannose receptors and the NOD-like receptors, are activated by pathogen-associated molecular patterns (PAMPs) and then initiate an innate immune response to produce AMPs, cytokines and chemokines which in return modulate microbiota homeostasis (de Koning et al., 2012; Nestle et al., 2009).

Moreover, the host-microbe symbiosis of the skin is tuned by host immunity that modulates sebaceous hyperplasia with altered levels of antimicrobial lipids that influence the composition of skin microbiota (T. Kobayashi, Naik, et al., 2019). For example, loss of skin-resident innate lymphoid cell (ILC) subsets can accelerate sebocyte growth via relaxing Notch

signaling from TNF/lymphotoxins restriction which then increases the production of antimicrobial lipids and suppresses Gram-positive bacteria commensalism (T. Kobayashi, Voisin, et al., 2019).

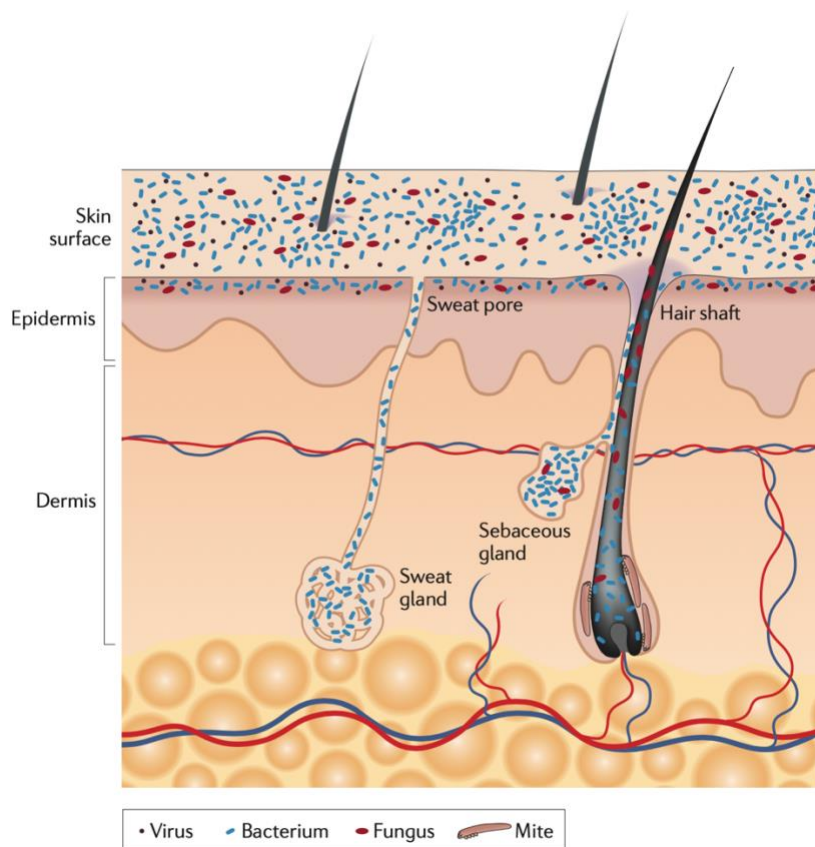


Figure 1-3 Schematic of skin histology viewed in cross-section with microorganisms and skin appendages

Microorganisms (viruses, bacteria and fungi) and mites cover the surface of the skin and reside deep in the hair and glands. On the skin surface, rod and round bacteria — such as Proteobacteria and Staphylococcus spp., respectively — form communities that are deeply intertwined among themselves and other microorganisms. Commensal fungi such as Malassezia spp. grow both as branching filamentous hypha and as individual cells. Virus particles live both freely and in bacterial cells. Skin mites, such as Demodex folliculorum and Demodex brevis, are some of the smallest arthropods and live in or near hair follicles. Skin appendages include hair follicles, sebaceous glands and sweat glands. Source: Grice & Segre, 2011. The skin microbiome. *Nature Reviews Microbiology*, 9(4), 244–253. With permission from Springer Nature.

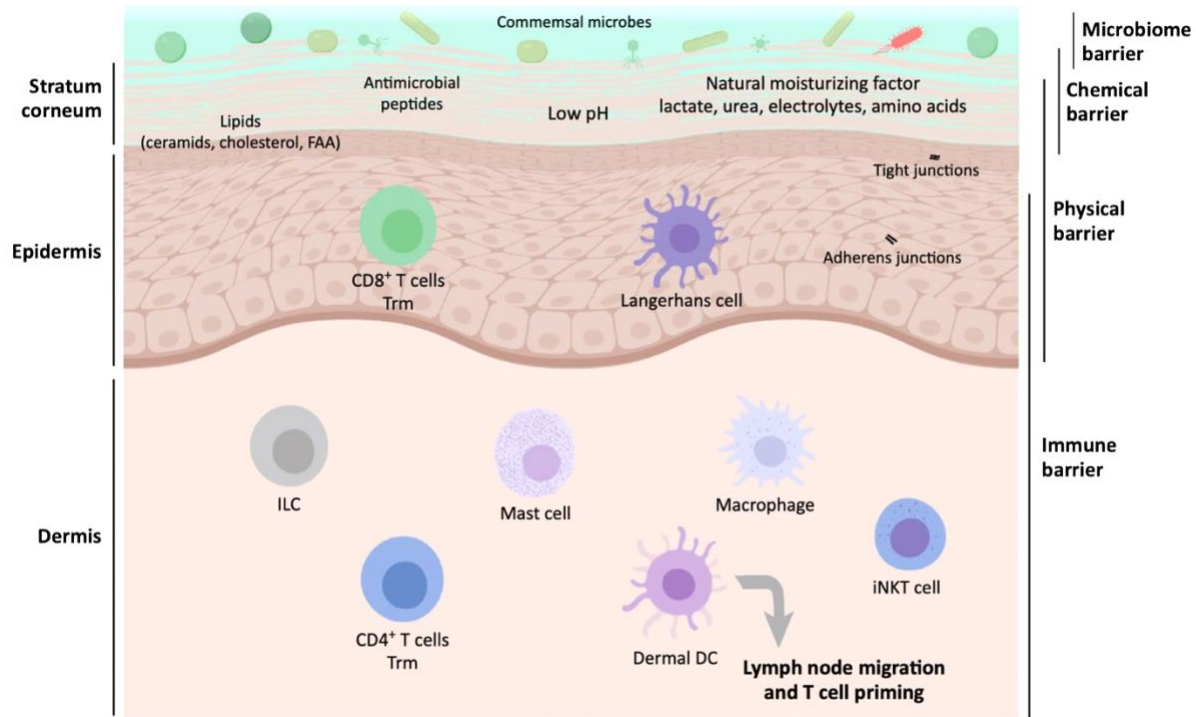


Figure 1-4 Levels and Components of the Cutaneous Barrier

Abbreviations: FAA, free fatty acids; ILC, innate lymphoid cell; iNKT, invariant natural killer cell; Trm, tissue-resident memory cell.

Source: Eyerich et al., 2018. Cutaneous Barriers and Skin Immunity: Differentiating A Connected Network. *Trends in Immunology*, 39(4), 315–327. With permission from *Trends in Immunology*.

1.6 Antimicrobial protein/peptides

Antimicrobial protein/peptides (AMPs) are the innate defense agents in many multicellular organisms that possess a broad-spectrum anti-infective capability against Gram-positive and/or -negative bacteria, fungi, viruses and even cancerous cells (Ageitos et al., 2017; Gordon et al., 2005). These small cationic peptides are multifunctional elements of the immune system that are primarily expressed by neutrophils, monocytes, and macrophages and also produced within the skin and mucosal surfaces by epithelial cells in the respiratory, gastrointestinal, and urinary tract (Battersby et al., 2016). AMPs are regarded as promising antibiotics to fight against pathogens with a low tendency for developing resistance. Specifically, the cationic nature of AMPs enables them to directly interact with the negatively charged bacterial cell membrane and their hydrophobic portions function to act on the other components of the membrane, at the same time, resulting in the structural arrangement of AMPs (Seo et al., 2012). Thereby, the antimicrobial effect can be achieved through membrane interaction (e.g., membrane penetration, pore formation, membrane disruption) or intracellular cytotoxicity [e.g., enzyme inhibition, gene material degradation, reactive oxygen species (ROS) generation, ATP leakage, macromolecular or cell wall synthesis inhibition] (Ageitos et al., 2017).

1.7 Antimicrobial resistance

The appearance of antimicrobial resistance (AMR) is a natural evolution for microorganisms that can be accelerated by the selective pressure of widespread use and misuse of antimicrobials (WHO, 2020a, 2020b). However, AMR is now threatening global health and the development of the antimicrobial drug. It is estimated by the World Health Organization (WHO) that AMR will exceed cancer to be the leading cause of death with 10 million cases by

the end of 2050 (WHO, 2016). Several antibiotic-resistant bacteria have been prioritized by the WHO as top pathogens that require the development of novel antibiotics, including *P.aeruginosa* (carbapenem-resistant), Enterobacteriaceae (e.g., carbapenem- and 3rd generation cephalosporin-resistant *Klebsiella pneumonia* and *E. coli*), and *S. aureus* (methicillin-resistant, vancomycin intermediate and resistant) (WHO, 2017).

Of note, as part of skin flora, *S. aureus* is a common cause of infections in the community and health-care facilities (WHO, 2020a). People infected with methicillin-resistant *S. aureus* (MRSA) are at higher risk of death (64%) than people with drug-sensitive infections. In the US and Canada, drug resistance between 1998 and 2004 showed a significant increase in methicillin resistance in *S. aureus*, vancomycin resistance in *Enterococcus*, and extended-spectrum β -lactamase production in *Klebsiella* spp. and *E. coli* that almost doubled to 47.4%, 16.3%, 12.8% and 14.8% respectively (May et al., 2009).

1.8 Skin inflammation

Inflammation is commonly triggered by infection or tissue injury that activates adaptive response (acute inflammation) for restoring homeostasis (Medzhitov, 2008). An effective acute inflammatory response is achieved by elimination of the invading pathogens, tissue repair, stress adaptation, and homeostatic restoration which is largely mediated by resident and recruited macrophages. Acute inflammation is a non-specific immune response that mainly functions through enhanced blood flow, vasodilatation, vascular permeability, leakage of plasma, and recruitment of phagocytic leukocyte to the inflamed site (Arulselvan et al., 2016).

A systemic inflammatory response is of benefit for the host to cleanse invaders. The innate inflammatory response relies on pathogen receptors as Toll-like receptor 4 (TLR4), which

is followed by a series of immune cascade signaling pathways, e.g. nuclear factor- κ B (NF- κ B), inflammasome, or other cytokine-activated signal transductions (Xu et al., 2018). For instance, exposure to pathogens or bacterial components, such as lipopolysaccharide (LPS) (Figure 1-5), can stimulate macrophages by neutrophil-generated cytokines or by differently activated macrophages (Vuong et al., 2017). Activated macrophages function to eliminate antigens and secrete growth factors, proinflammatory mediators (nitric oxide, NO) (Yarlagadda et al., 2017), as well as proinflammatory cytokines [e.g., interleukin-1 β (IL-1 β), IL-6, IL-8, and TNF- α], and then trigger the tissue proliferation and remodelling phase.

However, tissue stress and malfunction might lead to shifting in homeostatic balance, development of chronic inflammation or autoinflammatory diseases (Medzhitov, 2008). Chronic inflammation is a prolonged inflammatory response that involves detrimental changes at the inflammation site, including pathological tissue modelling, fibrosis, progressive cell infiltration, and leukocyte-mediated tissue damage (Andersen, 2015). It can follow acute inflammation or prolonged low-grade inflammation (Pahwa & Jialal, 2019). Chronic inflammation is one of the most significant causes of death in the world. It was reported that 3 out of 5 people would die due to chronic inflammatory diseases, such as stroke, chronic respiratory diseases, heart disorders, obesity, diabetes, and cancer (Pahwa & Jialal, 2019).

The skin is colonized by diverse bacterial species that live as commensals on its surface and in hair follicles. An imbalance of these bacteria or invasion of pathogenic strains can cause skin dysbiosis and even diseases (Pereira, 2014). Chronic skin inflammation states with dysregulation of cell extrinsic and intrinsic pathways, such as long-term exposure to NO, thereby, compromises cells to tumorigenesis through pre-transcriptional (e.g. DNA damage) or post-transcriptional regulations (e.g. apoptosis), or proliferative signaling pathway regulations

(P. Kim et al., 2001). Dysbiosis of skin is often accompanied by wound infections and inflammatory diseases, such as atopic dermatitis (AD), acne, psoriasis, seborrhoeic dermatitis, and chronic wounds (Grice & Segre, 2011)

Bacterial infection by Gram-positive bacteria *S. aureus*, and Gram-negative bacteria *P. aeruginosa* were responsible for more than 50% of human skin and tissue infections in North America from 1998 to 2004; *Enterococcus* spp. and *Escherichia coli* (*E.coli*) constitute 9.3% and 7.2% of bacterial infections and followed by *Enterobacter* spp., *Klebsiella* spp., β -hemolytic *Streptococcus* with about 4.5% for each pathogen infection (May et al., 2009). *S. aureus* and *Staphylococcus epidermidis* (*S. epidermidis*) were reported to be the main colonizers of AD lesions (Gonzalez et al., 2017).

AD is a chronic relapsing inflammation of the skin with eczematous lesions and intense itching (Gonzalez et al., 2017). AD can lead to epidermal barrier impairment, immune cell activation and alterations in the community of associated skin microorganisms. What's worse, in AD patients, a decreased microbial diversity can lead to colonization by *S. aureus* which is prone to cause apoptosis in keratinocytes, skin inflammation and excoriation that deteriorate the barrier function.

Psoriasis is an immune-mediated chronic inflammatory cutaneous disease mainly accompanied with red, flaky, and raised plaque area caused by hyperproliferative keratinocytes and misguided innate and adaptive immune response on the skin (Rendon & Schäkel, 2019; Q. Zhou et al., 2009). Inflamed site are continuously enriched by several proinflammatory mediators including IL-17, IL-21, IL-22, IL-6, IL-1 β , TNF- α , and IFN- γ (T. Kobayashi, Naik, et al., 2019; Rendon & Schäkel, 2019). Although there is no clear clue about how microbial species

lead to psoriasis, it is likely to be induced by complicated factors including trauma, stress, pathogens, drugs, or wounding (Q. Zhou et al., 2009).

As the most common dermatological inflammation worldwide, acne vulgaris is characterized by excessive sebum, pimples, pustules and scarring. Acne pathogenesis mainly consists of follicular hyper-keratinization, excess sebum, inflammation, and *Cutibacterium acnes* (*C. acnes*) dysfunction (Harper, 2020). *C. acnes* is a commensal skin microorganism but can become causative agent of acne by triggering cutaneous innate immune response, and also disturb keratinocyte differentiation and sebaceous glands function due to the miscommunication with skin microbial flora.

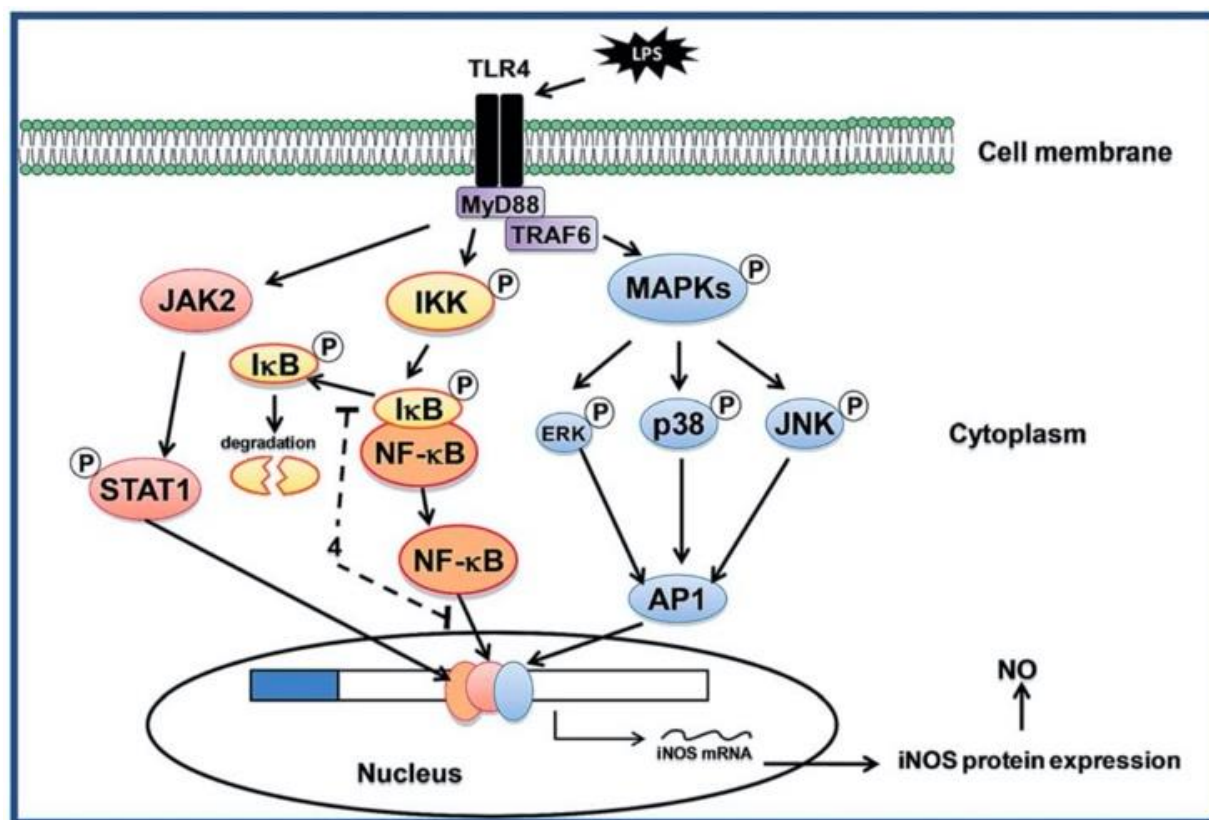


Figure 1-5 Inflammatory triggers (LPS) activate the expression of proinflammatory genes

Inducible nitric oxide synthetase (iNOS) signaling pathway activated by LPS binding the TLR4 and transduced via mitogen-activated protein kinases MAPKs (ERK, p38 and JNK), the nuclear factor NF- κ B as well as a Janus tyrosine kinase (JAK) and signal transducers and activators of transcription (STATs). Other shown protein components that participate in iNOS signaling and are shown include: ERK (extracellular-regulated kinase), JNK (NH₂-terminal kinase), AP-1 (activating protein-1), MyD88 (myeloid differentiation primary response gene 88), IKK (I κ B kinase) and I κ B (NF- κ B inhibitor protein). Solid lines represent signaling connections for LPS-induced NO production. Source: Hegazy et al., 2015. Anti-inflammatory sesquiterpenes from the medicinal herb *Tanacetum sinaicum*. *RSC Advances*, 5(56), 44895–44901. With permission from Royal Society of Chemistry.

1.9 Oxidative stress

Living organisms are exposed to various oxidative environments including exogenous stimuli that comprises air pollutants, atmospheric gases, ultraviolet (UV) radiation, heavy metal ions, microorganisms, viruses or xenobiotics, as well as endogenous radicals that are generated during normal cellular metabolism, immune response, or under pathological conditions (Birben et al., 2012; Trouba et al., 2002). Oxidative stress occurs when the balance between oxidants and antioxidants shifts to the excess formation and/or insufficient removal of highly reactive molecules such as ROS and reactive nitrogen species (RNS), or due to the depletion of antioxidants (Maritim et al., 2003).

The ROS is an integral part of normal metabolic systems, which includes superoxide anions (O_2^-), hydrogen peroxide (H_2O_2), hydroxyl radicals ($OH\cdot$), NO, and also can be derived from environment such as air pollutants, UV and microorganisms (Birben et al., 2012). ROS can react with nucleic acids, proteins, lipids, carbohydrates, and other biological macromolecules that related to hosting defense, inflammation, apoptosis, fibrosis, and cell proliferation in living organisms (Elmarakby et al., 2006). The endogenous ROS are produced by different intracellular organs such as mitochondria, peroxisomes and endoplasmic reticulum, where high oxygen consumption takes place (Phaniendra et al., 2015). The majority of intracellular ROS is derived from the mitochondria, and several different enzymes have been verified during the generation of ROS. For example, in animals, nicotinamide adenine dinucleotide phosphate (NADPH)-oxidase catalyzes the production of superoxide ($\bullet O_2^-$) by reducing one-electron of oxygen using NADPH as an electron donor (Apel & Hirt, 2004). Then the generated $\bullet O_2^-$ serves as a primary material for the production of various reactive oxidants, including oxidized halogens, free radicals, and singlet oxygen.

The intricate antioxidant defense system is categorized into enzymatic and non-enzymatic antioxidant groups. The enzymatic scavengers comprise SOD (superoxide dismutase), catalase (CAT) and glutathione peroxidase (GPx) that function to keep a redox balance through attenuating damaging effects of ROS, and impairing or reversing the events that contribute to toxicity and pathogenesis (Finkel & Holbrook, 2000). SOD accelerates the dismutation of superoxide to O₂ and H₂O₂ by combination with metal ions, which serves as the first line of antioxidant defense system (Apel & Hirt, 2004). On the other hand, CAT and GPx act as antioxidants by converting H₂O₂ to O₂ and H₂O in different ways. Furthermore, non-enzymatic scavengers, small molecules in the antioxidant system also play important roles in eliminating excessive ROS; these include ascorbate (vitamin C), α -tocopherol (vitamin E), carotenoids (β -carotene), glutathione pyruvate, and flavonoids (Ahmadinejad et al., 2017; Birben et al., 2012)

In skin oxidation, the accumulative oxidative stress can compromise skin and lead to the aging process, especially the UV exposure (Masaki, 2010; Rinnerthaler et al., 2015). Oxidative stress can trigger the expression of ROS (such as hydroxyl radicals and superoxide anions), resulting in skin erythema and inflammation (Wu et al., 2019); and activate the MAPK-mediated signal pathway that is involved in inflammatory response and skin aging (P. Wang et al., 2019). Moreover, free radicals and reactive oxygen metabolites can trigger and/or amplify inflammation via the upregulation of several genes, including NF- κ B (Conner & Grisham, 1996; Grimbble, 1999). Activation of NF- κ B, in turn, leads to the augmentation of inflammatory response by upregulating the production of several proinflammatory cytokines and enzymes, such as IL-1, IL-6, TNF- α , and iNOS that can regulate cell proliferation, apoptosis, morphogenesis and differentiation (T. Liu et al., 2017). Furthermore, the ROS pathway is involved in age-related processes such as dryness, roughness, wrinkle, contact dermatitis, psoriasis in human skin

(Bickers & Athar, 2006; Ishii et al., 2014; Trouba et al., 2002; Yoo et al., 2014; Q. Zhou et al., 2009).

CHAPTER 2 HYPOTHESIS AND OBJECTIVES

2.1 Hypothesis

We hypothesize that the positive effects of eggshell membrane on skin health maintenance, which are due to the bioactivity of functional components, could be improved by reducing the size of the eggshell membrane particles via micron-scaled particalization with enhanced solubility and increased bioactivity.

2.2 Objectives

- 1) Produce and characterize the Particalized Eggshell membrane (PEM);
- 2) Evaluate the antimicrobial activity of PEM against Gram +ve and Gram –ve bacteria strains;
- 3) Evaluate the *in vitro* anti-inflammatory activity of PEM using murine RAW 264.7 macrophage cell line;
- 4) Evaluate the antioxidant activity of PEM and PEM hydrolysates (PEM-H) using an antioxidant power kit.

CHAPTER 3 MATERIAL AND METHODS

3.1 Preparation of PEM

Eggs were obtained from Burnbrae Farms (BBF, Lyn, Ontario). Specifically, these graded white eggs laid by mid-lay Lohmann White Leghorn hens were used as a source of manually peeled eggshell membranes (flowchart shown in Figure 3-1) [details of this process are subject to an Invention Disclosure]. Eggs were inspected under a bright light to exclude cracked eggs (high eggshell contamination risk). Intact eggs were opened using an egg cutting tool and processed through emptying and washing steps in the presence of a Bunsen burner flame to minimize contamination. After three-times washing with 4 °C Milli-Q water, eggs were manually pulled from eggshell and stored at -20 °C before drying and grinding. Collected ESM from each sub-batch (30 eggs per sub-batch, 180 eggs per batch) were transferred to a sterile glass tray and dried at 50°C for 24 hours in an oven. Industrial processed ESM (I-ESM) (oven-dried) was provided by BBF as prepared by their proprietary process.

Moisture content

Manually peeled ESM was distributed in a glass tray and dried at 50 °C for 24 hours in an oven. The total moisture content was calculated using the following equation:

$$\text{Moisture content (\%)} = \frac{W_w - W_d}{W_w} \times 100$$

where W_w = wet weight of the sample, W_d = weight of the sample after drying

Cryo-Grinding (CG) of ESM

Dried ESM sub-batches were manually ground for 2 minutes before assessment of microbial contamination. After verifying zero contamination, ESM was ground for up to 10

minutes, using a mortar and pestle in the presence of liquid nitrogen, to produce PEM, which was stored at -20 °C before further evaluation. Additionally, I-ESM was ground for 10 min with liquid nitrogen and served as a control group.

Sieving and further processing

Cryo-ground sub-batches of PEM was sieved using a Keck Sieve Shaker Kit (Cole-Parmer, Montreal, QC) into five size ranges: <53 µm, 53-104 µm, 104-381 µm, 381-508 µm, and >508 µm. PEM<53 µm was homogenized using a lab-scale Emulsiflex instrument (C3 or D20, Avestin, Inc.) and freeze-dried (Labconco, Kansas City, MO) in order to produce smaller sized PEM (designated as <15 µm) (Kulshreshtha et al., 2020). PEM<53 µm (25 g) was thoroughly suspended in 500 ml of sterile water (pH 7.4) and circulated 4 times through Emulsiflex C3 or D20 at an increasing operating pressure range from 25,000 psi to 30,000 psi. The working temperature was maintained by refrigeration at 4°C. The processing rate for C3 was 3.0 L/h, and for D20 was 20 L/h. The freeze-dried material was stored at -80 °C before further experiments.

Assessment of microbial contamination

PEM was tested for microbial contamination (aerobic colony count, ACC) using broth dilution and agar plate assays. Briefly, 100 mg of the ESM powder from each sieving sub-batch (30 eggs per sub-batch, 180 eggs per batch) was added into a culture tube containing 3 ml of PBS or LB broth under sterile conditions. Sterile PBS was used as a negative control. The mixture was vortexed and incubated for 6 h at 37 °C with 250 rpm. Then, the suspension or solution was vortexed thoroughly and aliquots of 50 µl were spread-plated on LB agar and incubated for 72 h at 37°C with daily observation.

3.2 Characterization of PEM

Evaluation of surface morphology (Performed by G. Kulshreshtha)

The morphological features of PEM in various sizes were characterized using scanning electron microscopy (SEM; TeScan Vega-II XMU SEM, Brno, Czech Republic) at a voltage of 20.0 kV after gold sputter-coating (5 min, under vacuum) (Kulshreshtha et al., 2020). Elemental analysis was performed on samples after acquiring the SEM micrographs using EDS (INCA X-Act, Oxford Instruments, Abingdon-on-Thames, UK), following carbon coating at the Nano Imaging Facility, Carleton University, Ottawa, ON. Elemental weight percentages were calculated from the weight of the detected element relative to the weight of all elements in the sample using the manufacturers' software (INCA – The Microanalysis Suite Abingdon-on-Thames, UK).

PEM particle size analysis (Performed by G. Kulshreshtha)

The particle size distribution of PEM from manually grinding and EmulsiFlex®-C3 preparations was determined by laser diffraction particle size analysis (HORIBA-LA960, ATS Scientific, ON, Canada) at the National Research Council Laboratories, Ottawa (Kulshreshtha et al., 2020). PEM suspension was prepared by dispersing in isopropanol (50 mg/ml) and followed by ultrasonication for 1 min to obtain thorough dispersion.

Calcium content (Performed by T. Ahmed and L. Wu)

The eggshell surface can become contaminated by microorganisms at various stages of the food chain, from laying to the consumer table (De Reu et al., 2006). The calcium content of PEM (derived from eggshell CaCO_3) was evaluated using a calcium colorimeter kit after acid treatment followed by neutralization with base. Specifically, PEM (0.2 to 1 g) was suspended in 0.5 M HCl

and magnetically stirred for 24 h at room temperature at 300 rpm. The final pH of the mixture was verified as acidic to verify the complete dissolution of any contaminating eggshell CaCO_3 ; the mixture was then neutralized to pH 7.0 using 10 N NaOH. The soluble calcium content was measured using the calcium colorimeter kit (Hanna HI 758, ITM Instruments Inc., Canada) according to the manufacturer's instructions.

3.3 Evaluation of antimicrobial activity

Bacterial strains and growth conditions

The Gram-negative strain *Escherichia coli* K12 (ATCC® 29425) was obtained from the University of Ottawa Centre for Research on Environmental Microbiology (Ottawa, ON, Canada). Luria-Bertani (LB) agar and broth (BioShop, Canada) were used in bacterial cultures. Bacterial colonies from glycerol stocks were plated on LB agar plates and incubated overnight at 37 °C for revival. Single colonies from the plates were picked and grown in 3 mL LB broth overnight at 37 °C at 250 rpm. The inocula were diluted 1:50 in fresh LB broth, incubated at 37 °C at 250 rpm until exponential growth was reached ($\text{OD}_{600} = 0.2$, $\sim 10^8$ CFU/mL). The bacterial suspension was pelleted at $3000 \times g$, 4 °C for 10 min, washed with phosphate-buffered saline (PBS pH 7.4; ThermoFisher Scientific, Gibco™, Waltham, MA) twice and adjusted to five different cell concentrations in PBS by serial dilution: 10^5 - 10^6 , 10^4 - 10^5 , 10^3 - 10^4 , 10^2 - 10^3 , and 10 - 10^2 CFU/mL.

3.4 Evaluation of anti-inflammatory activity

Cell culture

A murine macrophage cell line, RAW 264.7 (ATCC® TIB-71™, Lot #70012232), was cultured in DMEM supplemented with 10% heat-inactivated fetal bovine serum (FBS; Millipore-Sigma, Burlington, MA), 100 U/mL penicillin and 100 µg/mL streptomycin (Life Technologies Gibco™), and 2 mM GlutaMAX (Gibco™) in a humidified 5% of CO₂ atmosphere. The cells were incubated in a 25 cm² flask (Corning™) and sub-cultured in a 75 cm² flask (Corning™) at approximately 90% confluency using an initial seeding density of 2×10^4 cells/mL. Attached cells were renewed using cell scrapers (Catalog NO. 541070; Greiner Bio-One™, Frickenhausen, Germany) and replace medium 3 times per week. In order to avoid a dramatic change in cell properties following prolonged periods in culture, RAW 264.7 cells were replaced by early frozen stock after 20 passages. All chemicals and supplies were purchased from Fisher Scientific and Sigma Aldrich, ON, Canada unless specifically indicated.

Preparation of LPS

Lipopolysaccharide from *Escherichia coli* 055: B5 was purchased from Sigma-Aldrich (Catalog NO. L6529-1MG) and dissolved with autoclaved PBS (1 mg/mL) to prepare stock at -20 °C. LPS stock was diluted with DMEM (1 µg/mL) to induce an inflammatory response in RAW 264.7 macrophage cells.

Cell viability assay

PEM was suspended in DMEM to produce the stock solution (0.1, 1.0, 2, 5 mg/mL) before use in experiments. After seeding the cells in a 48-well culture plate (Falcon; 25×10^4 cells/well; n = 3 per treatment), the adhesion and proliferation of cells were monitored. At 24 h, cells were washed with DMEM and incubated with various concentrations of PEM for an

additional 24 h. Then, an aliquot of alamarBlue[®] reagent (ThermoFisher Scientific, Invitrogen[™]) of 10% culture volume was added to each well and incubated for 1 h. At the end of this incubation, an aliquot of 150 μ L/well was removed and centrifuged (4 °C, 13,000 rpm) (ThermoFisher Scientific, Fisherbrand[™] accuSpin[™] Micro 17R Microcentrifuge) for 5 min and 100 μ L supernatant was added to a 96 well plate (Corning[™]; Clear Polystyrene 96-Well Microplates); fluorescence was measured at excitation/emission wavelengths of 560 nm/590 nm (BioTek Eon, BioTek). Cells cultured with media were served as a positive control. Culture media with PEM alone was used as an internal negative control. Normalized cell viability in each PEM preparation was determined using the following equations:

Normalized cell viability

$$= \frac{(\text{Fluorescence}_{PEM \text{ treatment}} - \text{Fluorescence}_{PEM \text{ negative control}})}{(\text{Fluorescence}_{\text{Positive control}} - \text{Fluorescence}_{\text{Negative control}})} \times 100\%$$

Nitric oxide assay

RAW 264.7 cells were seeded in a 48-well culture plate (Falcon; 25×10^4 cells/well; n = 3 per treatment) 24 h to facilitate adherence and proliferation. Next, the culture media was replaced with fresh media containing various concentrations of PEM (0, 0.1, 1, 2 or 5 mg/mL), with or without LPS, and incubated for an additional 18 and 24 h. Then, an aliquot of 150 μ L/well of culture media was removed and centrifuged (4 °C, 13,000 rpm) (ThermoFisher Scientific, Fisherbrand[™] accuSpin[™] Micro 17R Microcentrifuge) for 5 min and 150 μ L supernatant was added to a 96 well plate. The accumulation of NO in the culture supernatant was detected using a Griess Reagent System (Promega, Madison, WI) following the manufacturer's instructions. Briefly, the absorbance of culture supernatant was measured at 540 nm using the EON microplate spectrophotometer and Gen5 data analysis software (BioTek, Winooski, VT,

USA). Cells cultured with LPS were served as a positive control for stimulation of inflammatory response. Cells in culture media with PEM alone was used as an internal negative control. A standard curve of NO production was generated by serial dilution (two-fold) of 100 μ M Nitrite Standard (NaNO_2). Accumulation of NO level was determined from the standard curve. The relative production of NO compared to the non-treatment group was determined using the following equation:

$$\text{Relative Production of NO} = \frac{(NO_{PEM \text{ treatment}} - NO_{PEM \text{ negative control}})}{(NO_{Positive \text{ control}} - NO_{Negative \text{ control}})} \times 100\%$$

3.5 Evaluation of antioxidant activity

PEM Hydrolysis

In order to enhance the bioactivity of PEM, I evaluated an alkaline hydrolysis process to obtain PEM-H. The optimum conditions to modify the antioxidant activity of PEM-H was conducted by single-factor experiments with a stepwise screening method. Specifically, five sizes of PEM (5 mg/mL and or 10 mg/mL) were digested in 1.25 N NaOH (ratio 1:1, v/v) for 24 h at 37°C. Then, a selected size of PEM was digested by various concentrations of NaOH (0.1, 0.3 or 1.25 N) at 37°C or 50°C for 0, 0.5, 6, 16 or 24 h (Table 3-1). The alkaline-treated PEM suspension was sampled at five-time points for each group and centrifuged at 13,000 rpm for 10 min (ThermoFisher Scientific, Fisherbrand™ accuSpin™ Micro 17R Microcentrifuge). The supernatant was termed as PEM-H and stored frozen at -20°C before analysis. All the reaction stocks were prepared with sterile deionized water.

Total antioxidant assay

The Trolox equivalent antioxidant capacity (TEAC) of various sizes of PEM was measured using the Total Antioxidant Power Kit (Oxford Biomedical Research, Product Number: TA02), which is based on cupric (Cu^{2+}) reducing antioxidant capacity (CUPRAC). Trolox, a water-soluble vitamin E analog, served as an antioxidant standard. Briefly, Trolox standards were reconstituted from 2mM Trolox standard stock by serial dilution using sterile deionized water. Both PEM-H and Trolox standards were diluted 1:40 in the provided dilution buffer (e.g., 10 μL sample + 390 μL dilution buffer), PEM suspensions were diluted at a ratio of 1:8 due to high turbidity. An aliquot of 100 μL PEM suspensions or alkaline digested PEM and Trolox standards were added to a 96 well plate prior to a reference dual-wavelength measurement at 450 and 600 nm. Then 25 μL copper solution was added to each well and incubated for 10min at room temperature. Next, 25 μL stop solution was added to each well and the absorbance at 450 and 600 nm was measured a second time. The net absorbance was calculated by subtracting the reference absorbance readings. The dilution buffer served as a reagent blank. Dilution buffer instead of the copper solution was used as a negative control for each undigested PEM sample.

Protein quantification

The protein content of various sizes of PEM and their soluble supernatants produced by alkaline hydrolysis (PEM-H) was quantified with bicinchoninic acid (BCA) using the Pierce™ BCA Protein Assay Kit (Thermo Scientific, Rockford, USA), with bovine serum albumin (BSA) as standard. Briefly, the stock BSA standard (2mg/mL) was serially diluted in sterile Milli-Q water according to the manufacturer's instructions. BSA standards (25 μL) or PEM suspensions were added to a 96 well plate. Then 200 μL working reagent was added to each well. The plate

was mixed thoroughly and incubated in the dark at 37 °C for 30 min before the measurement of the absorbance at 562 nm. Protein concentration (g BSA equivalent protein / mL material) was determined from the BSA standard curve and expressed as gram BSA equivalent protein per gram material (g protein/g material).

3.6 Statistical analysis

Results are expressed as mean \pm SEM of triplicate measurements unless specified otherwise. Statistical analyses were carried out using GraphPad Prism software (San Diego, CA, USA). The statistical significance of the data was determined by student's t test, one-way or two-way analysis of variance (ANOVA) followed by Tukey's multiple comparison test, with a $P \leq 0.05$ taken as a value of significance.

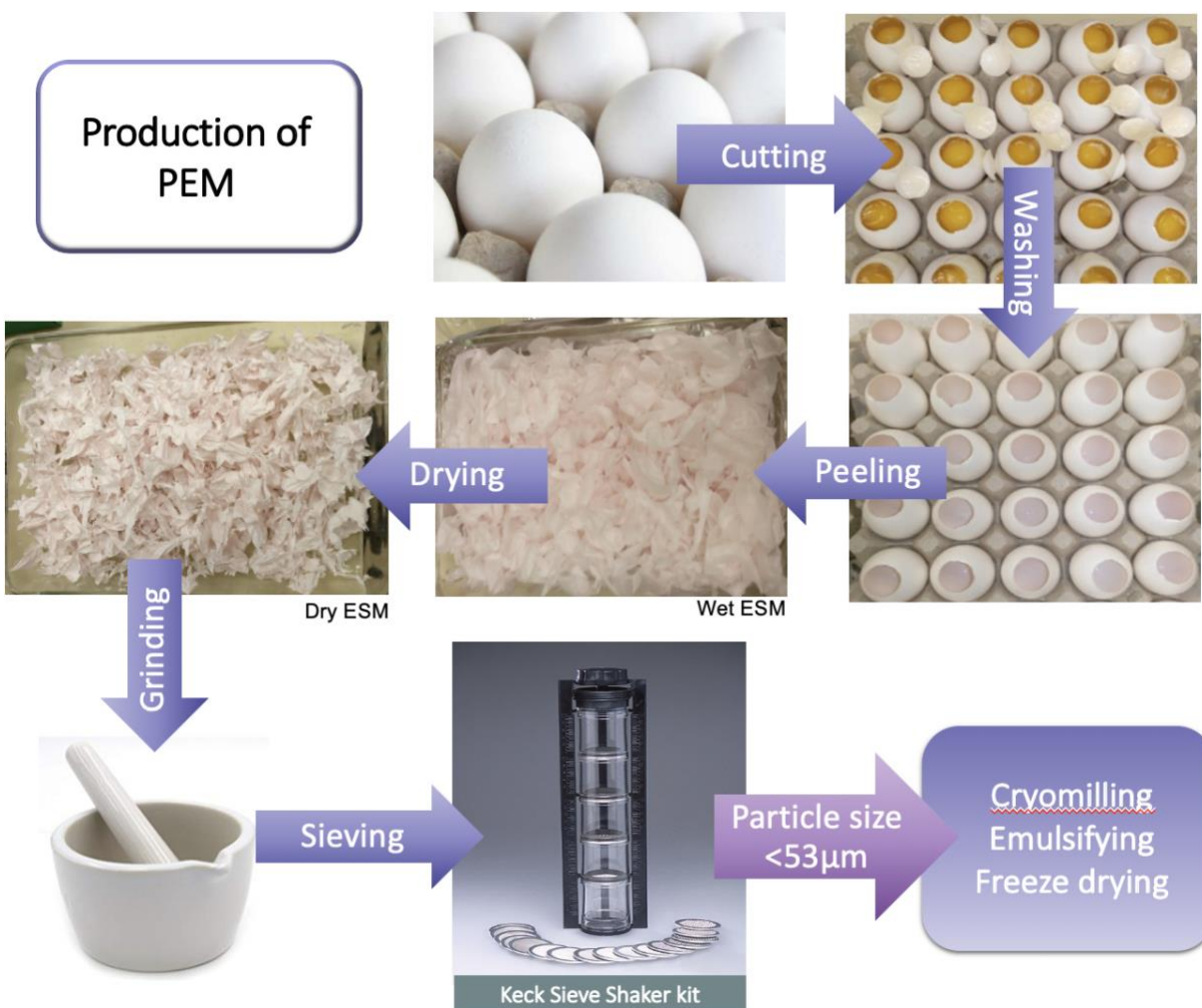


Figure 3-1 Flowchart of production of PEM

Fresh and intact eggs were opened at the sharp end, using a cutting tool. After emptying egg contents, eggshell was washed with 4 °C sterile water for three times. Then, manually peeled ESM went through oven-dry, grinding and sieving process to obtain 5 size ranges of PEM (<math>< 53</math>, $53-104$, $104-381$, $381-508$, and $> 508\ \mu\text{m}$). Collected PEM<math>< 53\ \mu\text{m}</math> was continuously processed by cryomilling, emulsifying and freeze drying to produce PEM<math>< 15\ \mu\text{m}</math>. Flowchart generated from: Kulshreshtha et al., 2020.

Table 3-1 Hydrolysis conditions of PEM-H (permutations and combinations are described in the text)

PEM dose	NaOH concentration	Temperature	Time
5 or 10 mg/mL	0.1, 0.3, or 1.25N	37 or 50 °C	0, 0.5, 6, 16, or 24h

CHAPTER 4 PRODUCTION AND CHARACTERIZATION OF PEM

4.1 Introduction

In 2019, the Canadian egg industry produced about 774 million dozen eggs, with a value of approximately \$1.3 billion (Egg Farmers of Canada, 2020a, 2020b); however, about 30% of eggs are processed at breaking plants for liquid egg products, generating eggshell (ES) and eggshell membrane (ESM) waste that has low commercial value (Cordeiro & Hincke, 2011). It is estimated that the global demand for eggs will increase by 50% in the next two decades that will generate greater production of eggshell and eggshell membrane waste (Shahbandeh, 2017). Although there are a few recycling methods for eggshell and eggshell membrane waste such as fertilizer and animal feed, about 26% of the waste are discarded in municipal dumps annually wasting high-value calcium carbonate and bioactive proteins (Daengprok et al., 2002). Therefore, more research is necessary to develop value-added applications for ES and ESM waste to achieve 100% reuse and reduce environment burden.

ESM is a highly insoluble material that is intractable to utilize as a proteinaceous source in biomedical applications. The solubility and bioavailability of ESM are restricted due to considerable amounts of cross-linkages as lysine-derived desmosine and isodesmosine that reinforce multiple disulfide bonds (Ahmed et al., 2017; Sah & Rath, 2016). These limitations can be overcome by chemical hydrolysis or enzymatic digestion to produce Soluble ESM Protein (SEP) (Kovacs-Nolan et al., 2014; Ohto-Fujita et al., 2011; Sah & Rath, 2016; Vuong et al., 2017; Yi et al., 2003; Zhao et al., 2019); or physically micronizing ESM with the retained structure of raw ESM to produce Processed ESM Powder (PEP, <100 μm) (Ahmed, Suso, Maqbool, et al., 2019; Amundsen et al., 2016; Vuong et al., 2018). For instance, Li (1995) obtained a cosmetic additive aqueous ESM solution by solving raw ESM in a 3:1 mixture of 1.5

mol/L NaOH/ethanol; Yi et al. (2003) isolated soluble eggshell membrane protein by treating ESM with aqueous 3-mercaptopropionic acid (3-MPA, $C_3H_6O_2S$) in the presence of acetic acid; Agroplas AS (Norway) invented a mechanical method (Amundsen et al., 2016) to separate ES and ESM through a gas-driven low temperature and high-speed cyclone, followed by milling, which reduces ESM particle size to under 100 μm (Vuong et al., 2017).

To some extent, physical partialization is more beneficial than a chemical method to achieve the target that preserves intact constituents of the raw material while increasing the surface area to promote bioavailability of the ESM (Hasebe, 2013). For instance, Haesebe (2013) employed a jet pulverizer to grind ESM into $<20 \mu m$ particles by ultrahigh-speed and high-pressure streams without heating and chemicals. This ESM powder showed enhanced digestion and absorption rate compared to that of natural ESM due to preservation of original ESM component, as well as accelerated recovery from carbon tetrachloride (CCl_4)-induced liver damage by dampening hepatic stellate cells (HSCs) activation that eventually prevent liver fibrosis in rat feeding studies (Hasebe, 2013; H. Jia et al., 2013, 2014). Therefore, the aim of this present study was to establish an eco-friendly and cost-effective physical method to improve and preserve the bioactivity of the natural proteinaceous resource ESM for biomedical applications, and simultaneously, pave a new avenue for the repurposing of a low-value industrial waste.

4.2 Results

4.2.1 Production of PEM

Eggshell and eggshell membranes are natural calcium and protein-rich raw material that have been utilized as soil conditioner or animal fodder, or disposed in landfills (Daengprok et al., 2002). More and more researchers investigate potential recycling pathways for ES and ESM

waste for pharmaceutical applications, in order to increase the environmental and economic value of a natural waste. The objective of our experimental approach was to develop a chemical-free and mechanical approach to process particalized ESM, while maximizing the valuable components of the ESM.

In this study, we established an eco-friendly approach to produce particalized ESM (PEM). Five size ranges of PEM ($>508 \mu\text{m}$, $381\text{-}508 \mu\text{m}$, $104\text{-}381 \mu\text{m}$, $53\text{-}104 \mu\text{m}$, and $<53 \mu\text{m}$) were obtained by sieving process and preserved for further experiments (Figure 4-1). Sub-batches of 30 shell eggs were processed at a time. Graded white eggs were mechanically opened using a cutting tool. Eggshell membrane was harvested from the eggshell after emptying the egg yolk and egg white contents and flushing with $4 \text{ }^\circ\text{C}$ sterile Milli-Q water. Fresh ESM was processed with chemical-free drying, cryo-grinding, sieving, homogenization and freeze-drying to produce size-reduced PEM while preserving bioactivity.

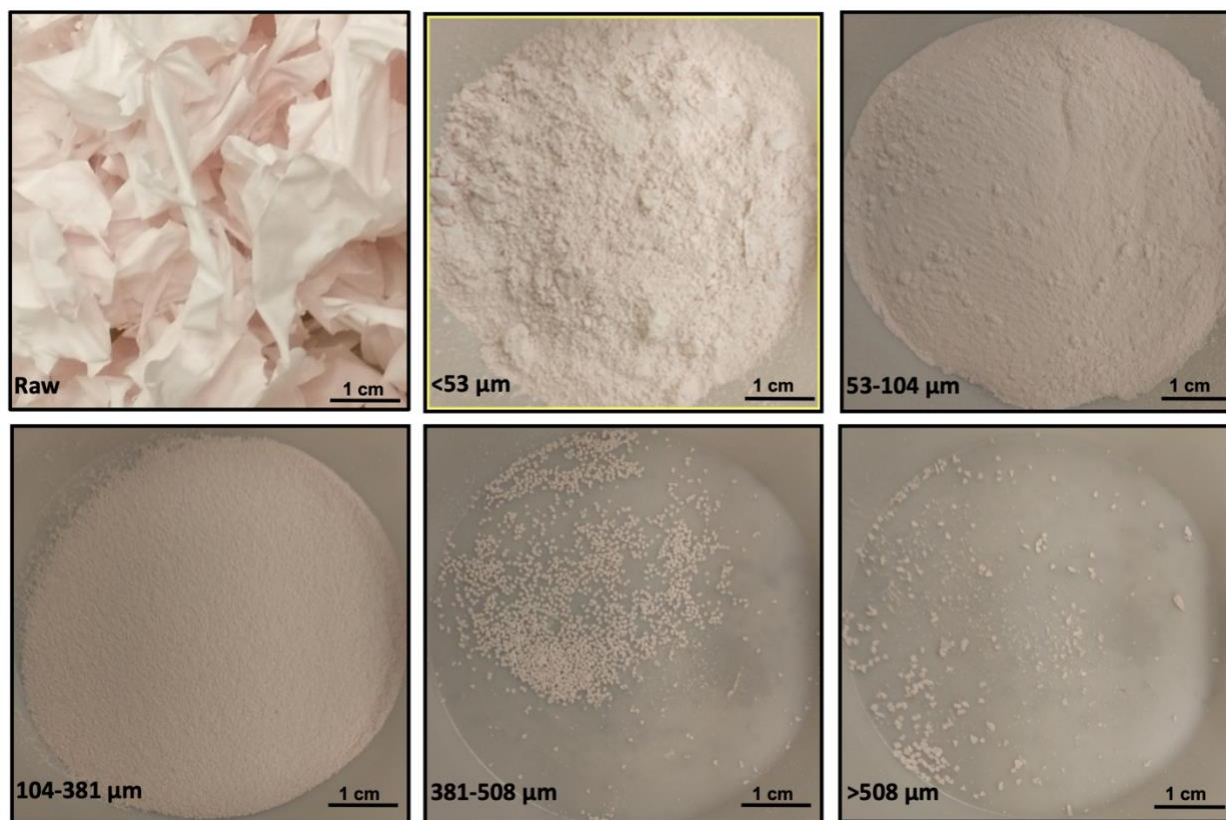


Figure 4-1 Macroscopic appearance of dried ESM and the resultant PEM after grinding and sieving

Source: Kulshreshtha et al., 2020. A novel eco-friendly green approach to produce particalized eggshell membrane (PEM) for skin health applications. *Biomaterials Science*, 2020;8(19):5346–61. With permission from Royal Society of Chemistry.

Moisture content

The moisture content of fresh ESM was evaluated during the drying process for each sub-batch in order to control the quality of the drying process (Table 4-1). The average loss of water content during the drying process corresponded to $81.4 \pm 2.02\%$.

Table 4-1 Moisture loss of ESM during drying

ESM processing*	Moisture loss (%)
pre CG-1	78.8
pre CG-2	80.3
pre CG-3	81.2
pre CG-4	82.8

* Moisture loss was evaluated before each CG process, which was designated as pre CG.

(Kulshreshtha et al., 2020, with permission)

Cryo-Grinding and further process

Sterile dried ESM was used for four cryo-grinding processing approaches (CG-1, CG-2, CG-3, CG-4) in order to obtain sufficient amounts of PEM of different sizes. After cryo-grinding for different times (CG-1, 10 min; CG-2, 2 min; CG-3, 30 sec; CG-4, 10 sec) and sieving process, ESM was obtained in 5 size ranges (<53, 53-104, 104-381, 381-508, and >508 μm) (Table 4-2; Figure 4-2). The size distribution is proportional to CG time. For instance, 10 min procedure (CG-1) yielded most PEM in <53 μm (40.1%) and 104-381 μm (39.7%), while minimum amount of PEM (0.1%) was in the largest size range >508 μm . In order to collect a sufficient amount of each size particle for characterization and bioactivity assays, CG time was adjusted to 2 minutes (CG-2), 30 (CG-3) and 10 (CG-4) seconds. As a result, CG-2 and CG-3 yielded more PEM at the range of 104-381 μm with 55.7% and 65.9% of all sizes respectively; whilst reducing the total production of <53 and 53-104 μm PEM to 39.6% and 13%. The shortest cryo-grinding time (CG-4) allowed accumulation of larger size PEM resulting in 12.1% of 381-508 μm and 58.8% of >508 μm particles, with zero yield of size less than 104 μm . Further homogenization procedures by emulsifying were employed on PEM <53 μm from CG-1 and CG-2 processing in order to obtain <15 μm particles. The I-ESM material went through 10 minutes of CG processing to produce <53, 53-104, and 104-381 μm particles with a percentage of 57%, 28%, and 15%, respectively.

Table 4-2 Summary of the yield of PEM obtained after cryo-grinding and sieving

ESM processing	Number of eggs/sub-batches	Processing Time	The yield of ESM particles in various size ranges (dry weight %)				
			<53 μm	53-104 μm	104-381 μm	381-508 μm	>508 μm
CG-1	690 eggs	10 min	40.1	19.3	39.7	0.7	0.1
CG -2	750 eggs/ 25 sub-batches	2 min	24.7	14.9	55.7	3.4	1.4
CG -3	150 eggs/ 5 sub-batches	30 sec	6.7	7.0	65.9	9.2	11.3
CG-4	450 eggs/ 15 sub-batches	10 sec	0.0	0.0	29.1	12.1	58.8

(Kulshreshtha et al., 2020, with permission)

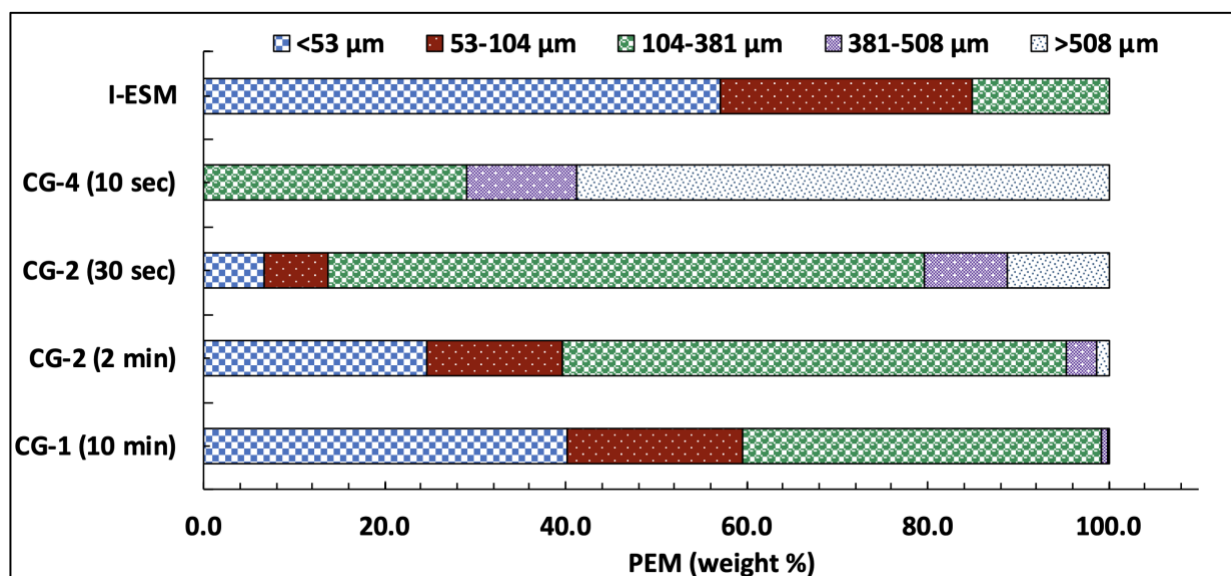


Figure 4-2 Particle size distribution of industrial ESM (I-ESM) and PEM obtained from top-down processing, including cryo-grinding for different times followed by sieving.

Different batches collected from cryo-grinding were sieved separately to determine the size range of resulting ESM particles. I-ESM went through 10 min CG.

(Kulshreshtha et al., 2020, with permission)

Assessment of microbial contamination

Microbiological screening identified 28% contaminated PEM sub-batches (n=17 contaminated sub-batches out of 62 total sub-batches) with an average ACC of 3.5 ± 1.2 Log CFU/gm.

Significant microbial contamination (ACC= 5.6 ± 0.1 Log CFU/ gm) was detected in batch-1 of I-ESM, while reduction in microbial counts was observed in batch-2 of I-ESM (3.6 ± 0.2 Log CFU/gm). All contaminated sub-batches were excluded in further study, only growth negative PEM (0 CFU/gm) was used for bioactivity evaluation. The characteristics and bioactive functionality of PEM was evaluated in subsequent experiments.

4.2.2 Characterization of PEM

Morphology and particle size

In our previous studies, the surface morphology of PEM in various size ranges was visualized by SEM (Figure 4-3). Dried ESM flakes (Figure 4-3, A) presented a cross-linked fibrous meshwork structure at high magnification. The cryo-grinding process physically broke down the fibrous structure leaving a variety of irregular particles with different morphologies and yielding various size ranges of particalized ESM with mean size of $374 \pm 390 \mu\text{m}$ (Figure 4-3, B; Table 4-3). Further processing, including sieving and emulsifying, generated much finer PEM particles (Figure 4-3, C-G). The morphology of PEM was significantly changed from ESM flakes to finer particles $<15 \mu\text{m}$. Homogenization processing from PEM $<53 \mu\text{m}$ to PEM $<15 \mu\text{m}$ resulted in an increased number of spherical particles and exposure of particle surface area with a mean size of $5 \pm 3 \mu\text{m}$ (Table 4-3).

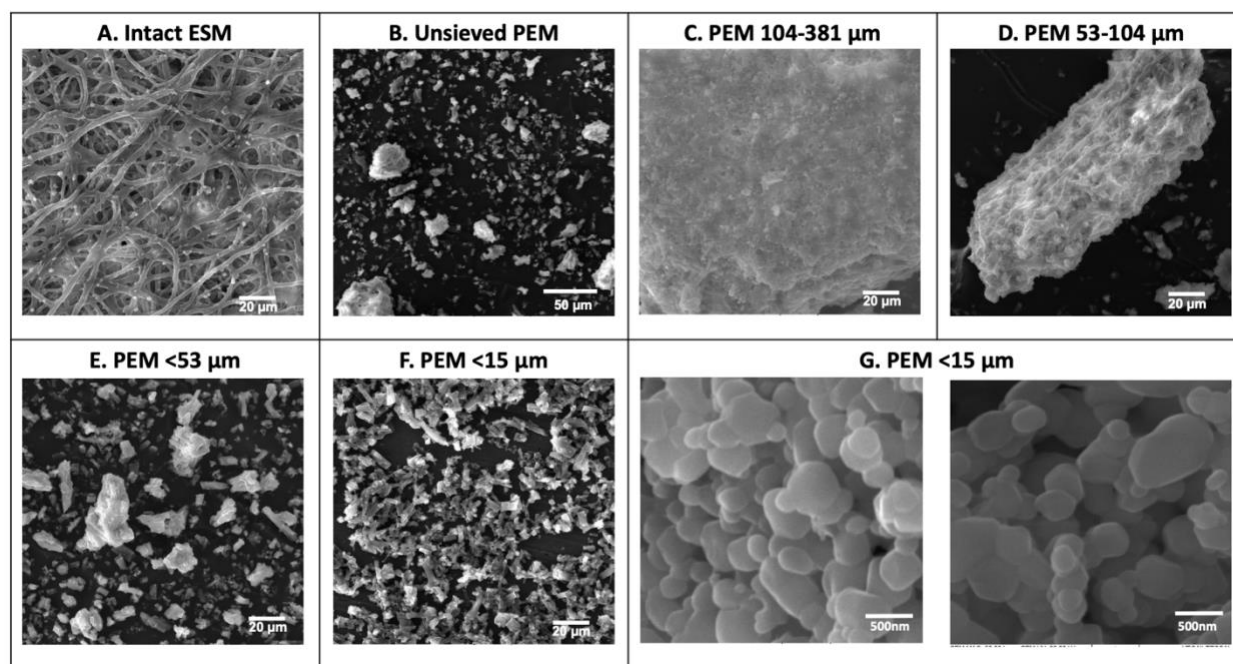


Figure 4-3 Scanning electron microscopy (SEM) of ESM in various size ranges

SEM images of ESM at 1000X from A. Randomly selected ESM flake (dried); B. Unsieved PEM; C-D. Various size range PEM processed by sieving 104-381 μm , PEM 53-104 μm , and PEM <53 μm ; F. PEM <15 μm , homogenized from PEM <53 μm using Emulsiflex D-20; G. Some particles of PEM <15 μm approaching nanoscale [Microscopy was carried out using the Tescan Vega-II XMU SEM (Dr. J. Wang, Nano-imaging facility, Carleton University, Ottawa)].

(Kulshreshtha et al., 2020, with permission)

Table 4-3 Impact of top-down approach on PEM particle size

Raw material	Top-down approach/ Particle size reduction techniques	*Mean particle size (Average \pm SD)
Water washed ESM flakes	Manually grinding using liquid nitrogen	374 \pm 390 μ m
Manually ground and sieved ESM (<53 μ m)	EmulsiFlex®-C3	5 \pm 3 μ m

*Mean particle size evaluated using HORIBA LA960 in collaboration with Dr. David Kingston and Toll Floyd, National Research Council, Ottawa; Eggshell membranes concentration: 12.5 mg; Solvent: isopropanol. (Kulshreshtha et al., 2020, with permission)

Calcium content

A colorimetric assay was employed to evaluate the calcium content of size reduced ESM particles, in order to establish the degree of contamination by eggshell. The calcium content of five sizes of PEM ranged between 0.37 % (w/w, g of CaCO_3 per 100 g of PEM) and 1.55%, while higher levels were detected in I-ESM with 2.64% calcium (Table 4-4). In general, PEM showed minimum calcium contamination with less than 1% compared to the I-ESM. Manual separation of ESM from eggshell significantly ($P < 0.0001$) reduced the eggshell contamination, showing higher purity of ESM component of PEM and more optimized processing than the industrial material.

Table 4-4 Calcium content of PEP and I-ESM

Type of ESM processing	CaCO₃ (ES) content (wt %)
PEM 381-504µm	0.39 ± 0.16
PEM 104-381µm	0.42 ± 0.22
PEM 53-104µm	1.55 ± 1.15
PEM 53 µm	0.49 ± 0.29
PEM <15 µm	0.37 ± 0.20
I-ESM	2.64 ± 0.12

*Values represent Mean ± SD from 2 independent samples of manually processed and 3 independent samples of industrially processed, each done in triplicate (Colorimetric kit: Hanna HI 758, ITM Instruments Inc., Canada). (Kulshreshtha et al., 2020, with permission)

Table 4-5 Elemental analysis of PEM in various preparations analyzed by energy-dispersive x-ray spectroscopy (EDS)

Element	PEM, Weight (%) (Average±SD)				
	<15µm	<53µm	53-104µm	104-381µm	Intact membranes
Carbon	68.30±9.25 ^a	60.72±4.55 ^{ab}	55.09±3.96 ^b	70.36±4.65 ^a	64.13±5.74 ^{ab}
Nitrogen	12.61±8.45 ^{ab}	18.65±3.42 ^{ab}	21.36±2.82 ^a	9.17±3.34 ^b	13.82±6.07 ^{ab}
Oxygen	16.67±1.72 ^{ab}	18.29±3.47 ^{ab}	21.13±2.98 ^a	13.36±3.64 ^b	19.87±1.29 ^a
Magnesium	0.01±0.02	0	0	0	0
Sulfur	2.21±0.06 ^b	2.25±0.55 ^b	2.34±0.87 ^b	6.88±2.58 ^a	2.15±1.07 ^b
Calcium	0.08±0.11 ^{ab}	0.07±0.05 ^b	0.06±0.06 ^b	0.22±0.06 ^a	0.01±0.03 ^b

Values with different superscript letters (Tukey multiple means comparison) are significantly different (ANOVA; P < 0.05). Values represent Mean ± SD from 3 independent samples each done in triplicate (n = 3).

(Kulshreshtha et al., 2020, with permission)

Table 4-6 Amino acid composition of PEM in various sizes as compared to literature values for ESM

No.	Amino acid	mole%	
		PEM % (mean ± SD) ^a	ESM % (mean ± SD) ^b
1	Asx (Asp+Asn)	7.6±0.1	7.9±0.4
2	Glx (Glu+Gln)	10.1±0.1	10.5±0.5
3	OH-Pro	0.9±0.0	1.1±0.2
4	Ser	6.6±0.1	6.7±0.5
5	Gly	9.9±0.1	10.4±0.5
6	His	3.2±0.0	3.1±0.3
7	Arg	5.1±0.1	5.2±0.2
8	Thr	6.0±0.1	6.1±0.3
9	Ala	3.5±0.0	4.0±0.1
10	Pro	9.7±0.1	10.6±0.8
11	Tyr	1.3±0.0	1.3±0.2
12	Val	7.7±0.1	7.5±1.1
13	Met	3.3±0.0	3.2±0.4
14	Ile	3.1±0.0	3.2±0.4
15	Leu	4.4±0.1	4.7±0.2
16	OH-Lys	0.4±0.0	0.2±0.2
17	Phe	1.7±0.0	1.4±0.3
18	Lys	3.1±0.0	3.2±0.2
19	Cys A	12.2±0.9	9.9±0.7

a. Data from four sizes of PEM (<53, 53-104, 104-381 µm, Emulsiflex), plus unsieved. (Hospital for Sick Children, Peter Gilgan Centre for Research & Learning, SPARC Biocentre, Toronto, ON).

b. Average of 5 references: 1. Leach RM, Jr., Rucker RB, Van Dyke GP (1981) Egg shell membrane protein: a nonelastin desmosine/isodesmosine-containing protein. Arch Biochem Biophys 207: 353-359; 2. Baumgartner S, Brown DJ, Salevsky E, Jr., Leach RM, Jr. (1978) Copper deficiency in the laying hen. J Nutr 108: 804-811; 3. Salevsky E, Leach RM (1980) Studies on the Organic-Components of Shell Gland Fluid and the Hens Eggshell. Poultry Science

59: 438-443; 4. Crombie G, Snider R, Faris B, Franzblau C (1981) Lysine-Derived Cross-Links in the Eggshell Membrane. *Biochimica et Biophysica Acta* 640: 365-367; 5. Ahmed TAE, Suso HP, Maqbool A, Hincke MT (2019) Processed eggshell membrane powder: Bioinspiration for an innovative wound healing product. *Mater Sci Eng C Mater Biol Appl*; 95:192-203

Data from: Kulshreshtha et al., 2020, with permission.

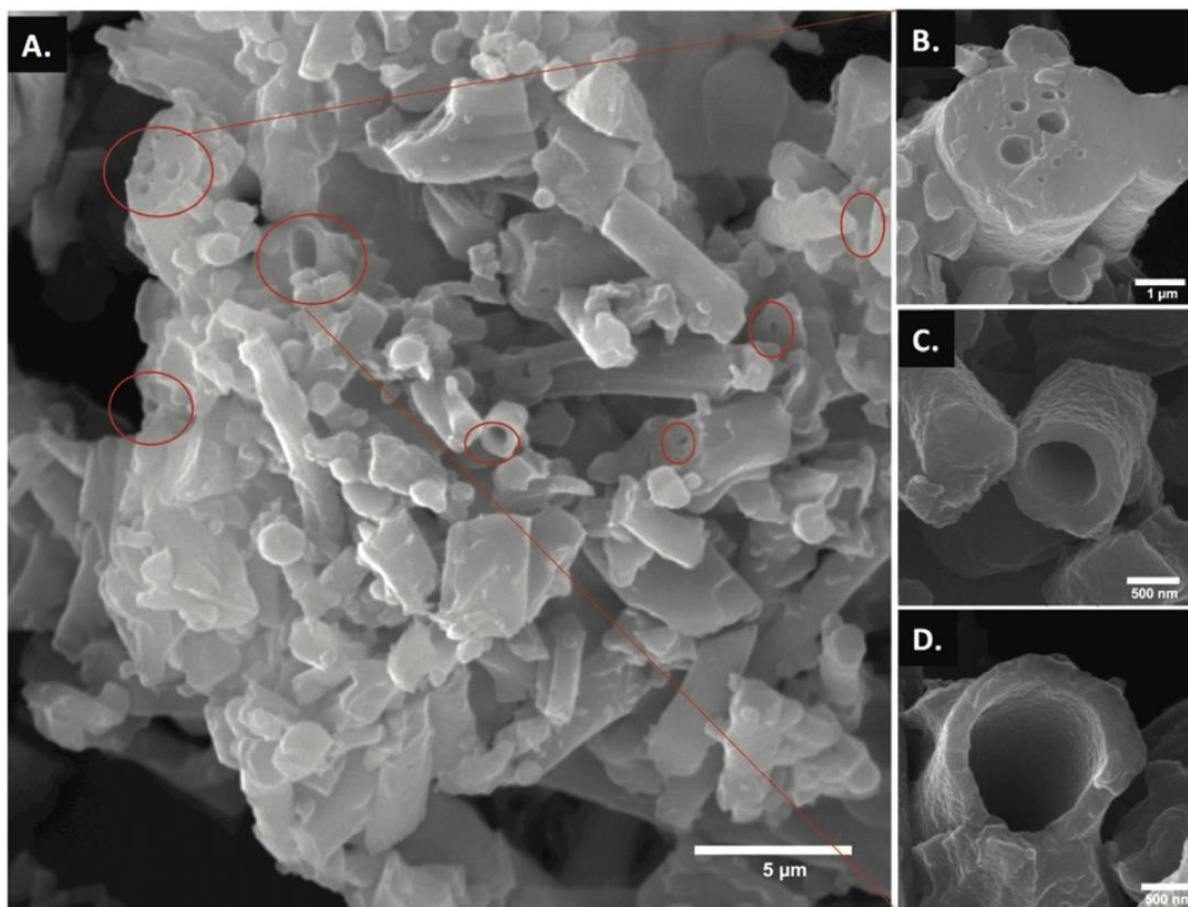


Figure 4-4 *Cross-sectional views homogenized PEM hollow fibers*

Cross-sectional views of A. homogenized PEM fibers demonstrating two novel morphologies in approximately 10% of them; either B. fibers with holes of different diameter, or C. and D. completely hollow fibers indicating separation of central ESM core from the outer mantle layer. Microscopy was carried out using the Tescan Vega-II XMU SEM (Dr. J. Wang, Nano-imaging facility, Carleton University, Ottawa). (Kulshreshtha et al., 2020, with permission)

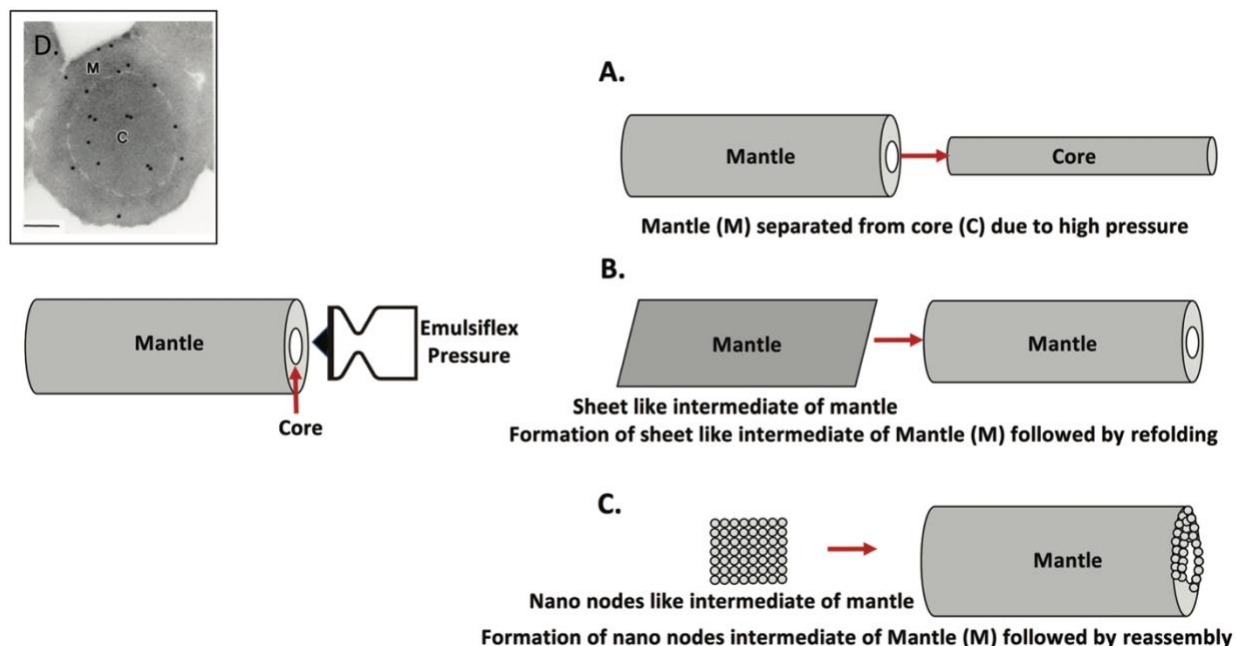


Figure 4-5 Hypothetical mechanisms for the formation of PEM hollow fibers after Emulsiflex homogenization

The generation of hollow fibers by Emulsiflex treatment could arise by at least three different possible mechanisms: A. Release of mantle from core due to two cycles of high/low pressure resulting in compression/decompression, or B. formation of sheet like intermediate of mantle followed by refolding into hollow structure, or C. formation of globular nano-node subunits of the mantle, followed by re-assembly into hollow fibers. Antimicrobial proteins such as lysozyme are present in both mantle and core of the fibers as previously shown by Hincke et al. 2000. D. Electron micrograph of colloidal-gold immunocyto-chemical localization of lysozyme in the shell membrane cross-section Scale bars: 200 nm. (Kulshreshtha et al., 2020, with permission)

4.3 Discussion

Eggshell and eggshell membranes are waste material from breaking plants, hatcheries, and fast food industries that are accessible and ready to collect in large amounts (King`ori, 2011). Traditional disposal streams for ES and ESM waste are feedstuffs, fertilizer and landfills. Setting aside the valuable nutrient component of these waste materials, the problems associated with waste handling are big challenges for industry, which includes the cost of disposal, selection of disposal sites, odour, contamination, vermin, high water use (facilitate separation shell and liquid content), vacuum system blockages, disinfection, etc. (Glatz & Miao, 2009). Moreover, when directly applied into the soil, high levels of protein waste can lead to high nitrogen contamination of the ecosystem; resulting in eutrophication by nitrates in groundwater, lakes or streams, pathogen transmission, production of phytotoxic substances, air pollution and greenhouse gas emission (Williams et al., 1999). Excessive application of organic waste as fertilizer for cropping system can increase the risk of groundwater contamination by nitrates, resulting in a high levels in drinking water that can leads to methemoglobinemia, respiratory disease, and cancer in human and fetal abortions in livestock (Glatz & Miao, 2009; Kelleher et al., 2002; Williams et al., 1999). Alternatively, an environmentally acceptable recycle route for ESM and ES waste with potential health and financial benefits provides a better choice to handle these poultry industry by-products. Hence, the strategy of sustainable development for eggshell waste recycling will support the ecosystem and economy.

In this study, we established a novel eco-friendly approach to transfer eggshell membrane waste into multifunctional bioactivity material while maximizing original components of raw ESM. Compared with the aforementioned chemical and physical method (4.1 Introduction), the extraction of ESM in this study is a chemical-free process. Only water was used as a solvent to

clean the egg content and three times wash consumed approximately 2 L water per 30 eggs. During the cryogenic grinding process, liquid nitrogen was employed as a thermal stabilizer functioning to reduce the working temperature and protect bioactive ingredients. PEM was also suspended in sterile water during the emulsification procedure (20 ml H₂O per gram PEM). Although chemical demineralization treatment with 5% ethylenediaminetetraacetic acid (EDTA) was used for eggshell to facilitate extraction of shell membranes and preserve protein quality, the risk of EDTA residues in ESM cannot be ignored (Fernandez et al., 2001; Sah & Rath, 2016). Comparing with the dish-shaped bottom stirred tank (Chi et al., 2019) which was recently employed to separate ESM from ES by feeding fresh eggshell into the water, our method reduced water consumption and electricity usage, as well as carbon emissions. Therefore, in our process, the exclusion of chemical solvent is conducive to eliminate the usage and removal of toxic and pungent chemicals, reduce energy consumption, meanwhile, lessen the emission of pollutants to the environment.

We established a new method to physically breakdown the ESM structure while maintaining its proteinaceous components. Generally, both chemical and physical methods preserved similar amino-acid composition and biodegradability of ESM that is comparable to that of natural (Ahmed et al., 2017; Hasebe, 2013; Sah & Rath, 2016; Yi et al., 2007). Likewise, PEP preserves fibrous structures of native ESM while exposes more cross-linked collagens and thicker fibres; and maintains collagen, and carbohydrate components such as hyaluronic acid, sulfated glycosaminoglycans (GAGs), N-glycans, mostly with uncharged structures (Vuong et al., 2017). However, in the chemical process, the denaturation of the valuable protein collagen and loss of acid-soluble collagen of ESM due to disulfide bond cleavage during strong acid/alkali and high-temperature treatment can undermine the bioactivity of ESM components (Sah & Rath,

2016). Traditional methods were designed to heat eggshells to the range of 80 to 100 °C for the purpose of separation and dehydration of collected ESM at 88 °C (Sah & Rath, 2016; Thoroski, 2003), but we limited the drying temperature to 50 °C to preserve as much component as possible. Moreover, Yi et al. (2007) reported a loss of antibacterial activity of SEP against *E. coli* compared to the natural ESM which is due to structural and componential changes after aqueous 3-MPA treatment. Consequently, physical partialization is more favourable than the chemical method when the target is to increase the solubility and successive bioactivity of the ESM.

The integrity of ESM components is a vital criterion to evaluate the effect of PEM processing. The twenty-four-hour drying process was controlled under 50 °C in order to prevent the deterioration of ESM proteins. Elemental and amino acid analysis of various preparation of PEM illustrated the stability of PEM components after processing (Table 4-5; Table 4-6). No significant changes were measured between intact ESM and PEM less than 104 µm in terms of carbon, nitrogen, oxygen, sulfur, and calcium. The average amino acid composition of various sizes PEM was comparable to that of ESM as summarized in Table 4-6. Thereby, we can conclude that the size reducing process has a minute effect on the integrity of the ESM component.

Additionally, of particular note is that PEM showed minimum calcium contamination with less than 1% compared to the industrial material (2.64%) in the present study. Minimum eggshell residues imply reduced bacterial contamination of PEM, as eggshell cuticle composition and maturity are the determinants of egg contamination by salmonellae and genus *Pseudomonas* (De Reu et al., 2006; Muñoz et al., 2015). On the other hand, calcium ion (Ca²⁺) is a universal and ubiquitous signaling molecule in the cell cycle, metabolism, structural integrity, motility, etc., which can be regulated by channels, pumps, sensors, binding proteins, hormones, and

receptors on the plasma membrane and intracellular organelles (Berridge et al., 2000; Mascia et al., 2012). Ca^{2+} concentration gradient is essential in the epidermis regulating keratinocyte differentiation, skin barrier formation, and permeability barrier homeostasis (S. E. Lee & Lee, 2018). Calcium-mediated disturbance of keratinocyte differentiation and proliferation are involved in human skin disease, such as psoriasis, atopic dermatitis, basal and squamous skin cancer, and genetic skin diseases such as Darier's disease and Olmsted syndrome (Elsholz et al., 2014; Leuner et al., 2011). Lin et al. (2012) reported a gene-mediated high intracellular calcium concentration caused high levels of apoptosis in keratinocytes in Olmsted syndrome patients. Additionally, as a potential topical ingredient, the negative bacterial growth PEM possess acceptable levels of total aerobic and pathogenic microbes which is above the cosmetic jurisdiction standard in the European Union and the United States (Kulshreshtha et al., 2020). Herein, minimum eggshell and pathogen contamination could be an important characteristic of PEM for biomedical applications.

PEM size was reduced to the submicron dimension approaching 200 nm after emulsifying homogenization. Scanning electron microscopy of $\text{PEM} \leq 508 \mu\text{m}$ showed the absence of fibres (Figure 4-3, B-G) after cryo-grinding, which is consistent with a previous study of PEP (average: 40 μm) from Biovotec AS (Ahmed, Suso, & Hincke, 2019). Size-reduced natural products approaching nanoscale can significantly increase the solubility and bioavailability of both *in vitro* and *in vivo* (Celia et al., 2013; Hasebe, 2013; Pund et al., 2014). As mentioned before (4.1 Introduction), pulverized ESM less than 20 μm exhibited an enhanced digestion and absorption rate compared to raw ESM, and increased bioactivity in rat liver fibrogenesis prevention through downregulation of peroxisome proliferator-activated receptor gamma ($\text{PPAR}\gamma$)-Endothelin 1 interaction signaling pathway (Hasebe, 2013; H. Jia et al., 2013,

2014). Later, the same group also verified the anti-inflammatory activity of fine eggshell membrane powder against inflammatory bowel disease (IBD) that significantly ameliorated gene expression of inflammatory mediators, intestinal epithelial cell proliferation, restitution-related factors and antimicrobial peptides (H. Jia et al., 2017).

The significant improvement of ESM bioactivity could be attributed to the increased relative surface area of ESM particles that would help to expose ESM components to the environment. For instance, lysozyme is present in both the mantle and core regions of ESM fibres (Hincke et al., 2000). In our published study (Kulshreshtha et al., 2020), lysozyme specific activity of PEM<15 μm ($9.6 \pm 0.5 \times 10^2$ U/mg) was significantly ($P = 0.013$) increased during size reduction as compared to the PEM 104–381 μm with $4.1 \pm 0.9 \times 10^2$ U/mg. This improvement could be because of the separation of ESM fibre core from the mantle. Cross-section SEM of hollow fibres of Emulsiflex homogenized PEM indicates the separation of central ESM core from the outer mantle layer as shown in Figure 4-4. This generation of hollow fibres could be due to one of the following mechanisms: (a) release of the mantle from core due to Emulsiflex compression/decompression pressure, or (b) formation of sheet-like intermediates of mantle followed by refolding, or (c) formation of nano ball substructure of the mantle, followed by hollow fibers re-assembly (Figure 4-5).

The same effect of size-reduced natural products was echoed by other studies in nanomedicine. For instance, the nano-bergamot essential oil was formulated as high water solubility material and exhibited enhanced anticancer activity *in vitro* against human SH-SY5Y neuroblastoma cells (Celia et al., 2013). Self-nano emulsifying drug delivery system (SNEDDS) of berberine was studied both *in vivo* inflammatory (acetic acid-induced inflammatory bowel model in rats) and *in vitro* anti-inflammatory and anti-angiogenic (chick chorioallantoic

membrane assay) that exhibited an improvement on therapeutic result compared to free berberine (Pund et al., 2014). Another study of nano emulsifying technique demonstrated a significant increase in permeability parameters, steady-state flux and permeability coefficient for transdermal delivery of caffeine (X. Zhou et al., 2018).

Collectively, we established a novel technique to upcycle eggshell membrane waste as a multifunctional bioactivity material while preserving original components of raw ESM. The efficacy of this innovative technique on the bioactivity of proteinaceous PEM needs to be further evaluated for antimicrobial, anti-inflammatory and antioxidant studies (see following chapters).

CHAPTER 5 EVALUATION OF THE ANTIMICROBIAL ACTIVITY OF PEM

5.1 Introduction

As the most efficient treatment for bacterial infections, antibiotics have greatly changed global health since the first discovery of penicillin. However, overuse and misuse of antibiotics in agriculture and medicine has led to the emergence of antibiotic-resistant and even multi-drug resistant bacterial pathogens (WHO, 2016, 2020b). AMR is a major problem worldwide that threatens human health and treatment of infectious diseases, leading to a prolonged illness, disability and fatality and increased health care cost (WHO, 2020b). Therefore, it is necessary to search for novel antimicrobial alternatives, thereby overcoming the threat of AMR.

On the other hand, as the largest organ of the human body, skin is colonized by beneficial microbiota that collaborate with physical, chemical and immune barriers to prevent the invasion of pathogens and also to stabilize and restore cutaneous homeostasis. Thereby, dysbiosis in each component of the skin barrier can cause pathogenic conditions, such as skin infections, sterile skin inflammation, allergic sensitization, or cutaneous tumorigenesis (Eyerich et al., 2018). Of note, commensal bacteria of the skin microbiota are dominated by Actinobacteria with plentiful Gram-positive bacteria which can be potentially involved in skin pathogenesis, especially *Staphylococcus* (e.g., *S. aureus* in atopic dermatitis, carbuncles, furuncles, cellulitis, impetigo, boils, hair follicle infection), *Propionibacterium* (e.g., *Propionibacterium acnes* in acne), and *Corynebacterium* species (in pitted keratolysis, erythrasma, and trichobacteriosis) (Geoghegan et al., 2018; Grice & Segre, 2011; Pinto et al., 2016; Stulberg et al., 2002). In addition, Gram-negative pathogens are responsible for a number of skin dysfunctions, particularly *P. aeruginosa* (folliculitis, erythematous, ecthyma, cellulitis), *Brevibacterium* spp (foot odour), *E. coli* (surgical site or wound infection, otitis media, cellulitis), and *Klebsiella pneumoniae* (*K. pneumoniae*) and

Serratia marcescens (skin rashes and blisters) (Afolabi et al., 2012; Chiller et al., 2001; Petkovšek et al., 2009; Stulberg et al., 2002). Thereby, the development and search for new antimicrobials are always the key point for public health.

Possessing multiple bioactive proteins, such as histones, defensins, lysozyme, cysteine-rich proteins, gallin, OCX-36, the ESM possesses natural immune defenses ability to prevent pathogen invasion of the egg and thereby protect the propagation of avian species (Ahlborn & Sheldon, 2005; Hincke et al., 2000; Makkar et al., 2015; Rath et al., 2016). In fact, ESM has been evaluated as a potential antimicrobial ingredient in several studies. The fresh eggshell membrane was used as an antimicrobial tissue adhesive for certain skin wound healing including lip lacerations (Cordeiro & Hincke, 2011; Zadik, 2007). ESM was reported to decrease the viability and heat resistance of *Salmonella* Enteritidis, *Salmonella* Typhimurium, *E. coli* (O157:H7), *Listeria monocytogenes* Scott A (*L. monocytogenes*), and *S. aureus* (Poland & Sheldon, 2001). Soluble eggshell matrix (cuticle and shell proteins) inhibited the growth of *P. aeruginosa*, *Bacillus cereus* (*B. cereus*), and *S. aureus*, and was observed by micrograph to disrupt the membrane integrity of bacteria (Mine et al., 2003). Synthesized silver-ESM nanoparticles showed a wide inhibitory effect against *L. monocytogenes*, *S. aureus*, *B. cereus*, *E. coli*, *P. aeruginosa*, and *Salmonella* typhimurium (Baláž et al., 2017). Furthermore, purified OCX-36 from ESM exhibited inhibitory activity against the growth of *S. aureus* and affinity for bacterial endotoxin (*E. coli* O111: B4 LPS) and non-endotoxin pyrogen [(*S. aureus* lipoteichoic acid (LTA)] suggesting interventional ability in bacterial infection (Cordeiro et al., 2013). Moreover, in our recent study, the PEM demonstrated a bactericidal activity against skin associated pathogens *S. aureus* and a bacteriostatic activity against *P. aeruginosa* with enhanced lysozyme

specific activity (Kulshreshtha et al., 2020). Therefore, the antimicrobial spectrum of PEM worth full exploration for skin health, and I investigated its antimicrobial activity against *E. coli*.

5.2 Results

5.2.1 Dose-dependent antimicrobial activity of PEM versus *E. coli*

In my work, PEM<53 μm exhibited a significant ($P=0.0021$) bacteriostatic activity against Gram-negative *E. coli* in a dose-dependent manner with IC_{50} (half maximal inhibitory concentration) = 32.57 ± 5.49 mg/mL (Figure 5-1). The results presented are based on 10^{5-6} CFU/mL for skin associated pathogen *E. coli* K12. The absorbance reduction at the end of the incubation observed in growth curves (Figure 5-1a) was reflected by bacterial logarithm reduction as shown in (Figure 5-1b).

The *E. coli* was most susceptible to the highest concentration of PEM<53 μm (50 mg/mL) which showed a significant inhibitory effect against (\log_{10} reduction = 2.20 ± 0.47) as compared to untreated bacteria ($P=0.0011$). Although 30 mg/mL (\log_{10} reduction = 1.12 ± 0.21) was not statistically different from 50 mg/mL ($P=0.0932$), no significant difference was observed between untreated, 1, 10 and 30 mg/mL PEM<53 μm . Thereby, the PEM at 50 mg/mL was selected for following evaluation.

5.2.2 Size-dependent antimicrobial activity of PEM versus *E. coli*

The PEM exhibited a size-dependent bacteriostatic activity against *E. coli*. The absorbance reduction at the end of the incubation that observed in growth curves (Figure 5-2 A) was reflected by bacterial logarithm reduction as shown in (Figure 5-2 B). The PEM<53 μm showed a significant ($P<0.05$) and strongest inhibitory effect against *E. coli* (\log_{10} reduction =

2.24 ± 0.20) as compared to the PEM preparations containing larger particle sizes, namely PEM 53-104µm, 104-381 µm, and 381-508 µm. The PEM<15 µm (log₁₀ reduction = 1.72 ± 0.38) demonstrated the second-highest antimicrobial activity as compared to control (P=0.0025), but not significantly different from PEM<53 µm (P=0.6408). Additionally, *E. coli*. demonstrated similar sensitivity (P>0.05) to PEM<15 µm, 53-104 µm, and 104-381 µm preparations. No significant difference in bacterial inhibitory effect was observed between PEM 53-104 µm, 104-381 µm, 381-508 µm and nontreatment (control).

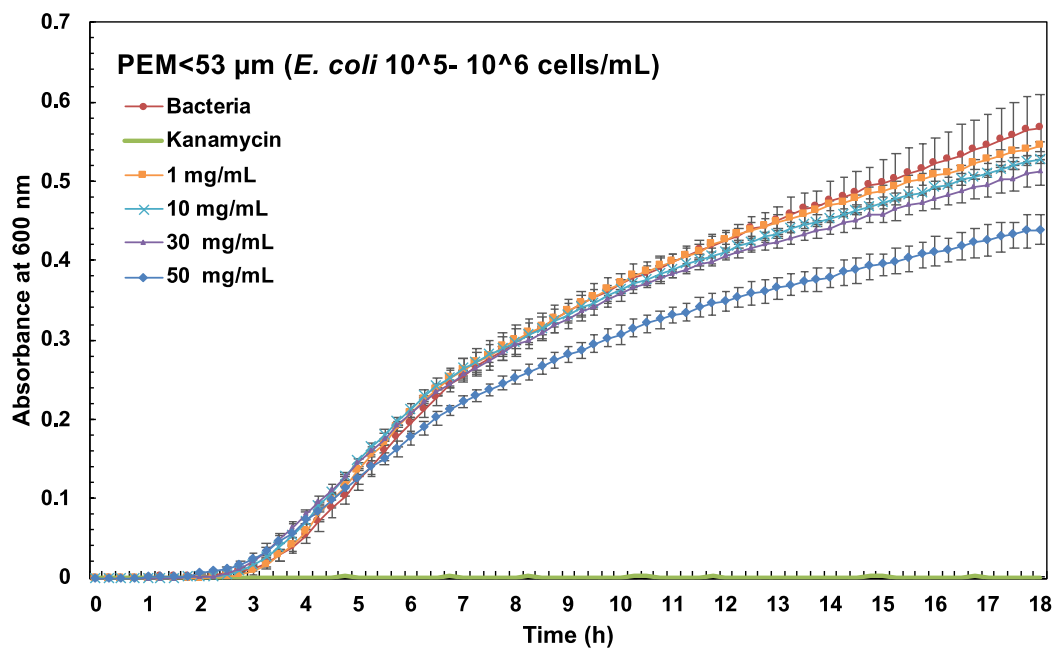
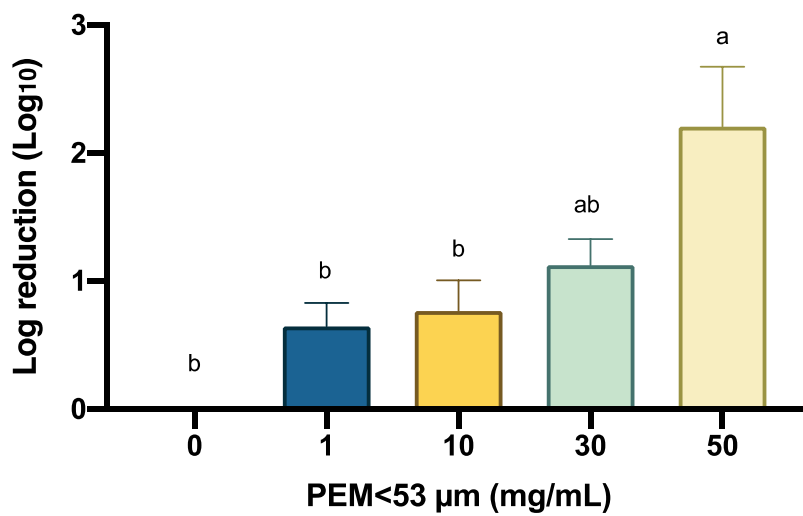
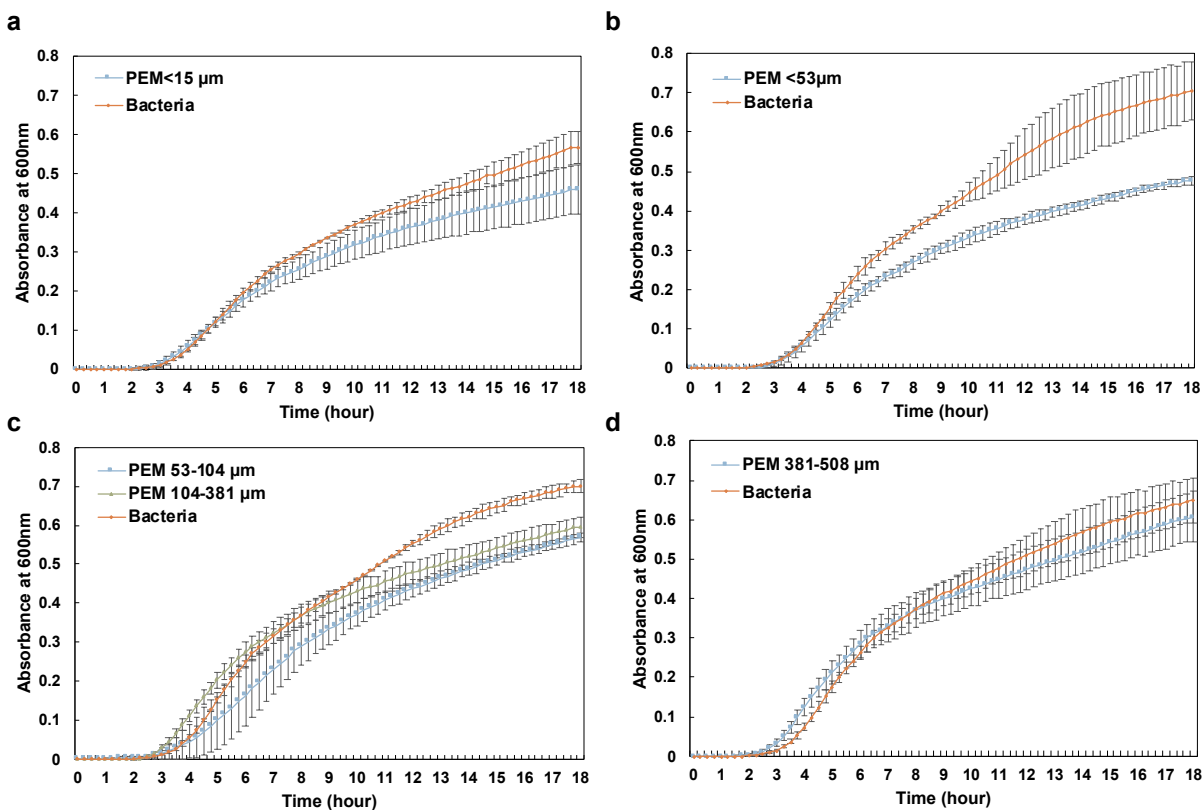
a Growth curves:**b Bacterial growth reduction**

Figure 5-1 Dose-dependent antimicrobial activity of PEM<53 μm against *E. coli*

a) Growth curves of gram-negative *E. coli* (K12) (10^{5-6} CFU/mL). *E. coli* was incubated with various concentrations of PEM<53 μm for 18 h after 3 h pre-inoculation (broth microdilution assays; turbidity was measured at 600nm). **b)** Dose-dependent antimicrobial activity of PEM<53 μm was reflected by the logarithm reduction of cell count at the end of incubation as compared to control ($P=0.0021$) with $\text{IC}_{50} = 32.57 \pm 5.49$ mg/mL. Bacterial cell count was determined by standard curves generated from the number of viable bacteria in the associated control group. Sterile H_2O , pH 7.4, was the negative control for inhibition. Kanamycin (1 mg/mL) served as a positive control. Data are presented as Mean \pm SEM of triplicate independent experiments, each performed in triplicate. Values with different superscript letters indicate statistical significance ($P<0.05$; one-way ANOVA; Post-hoc Tukey).

A. Growth curves



B. Bacterial growth reduction

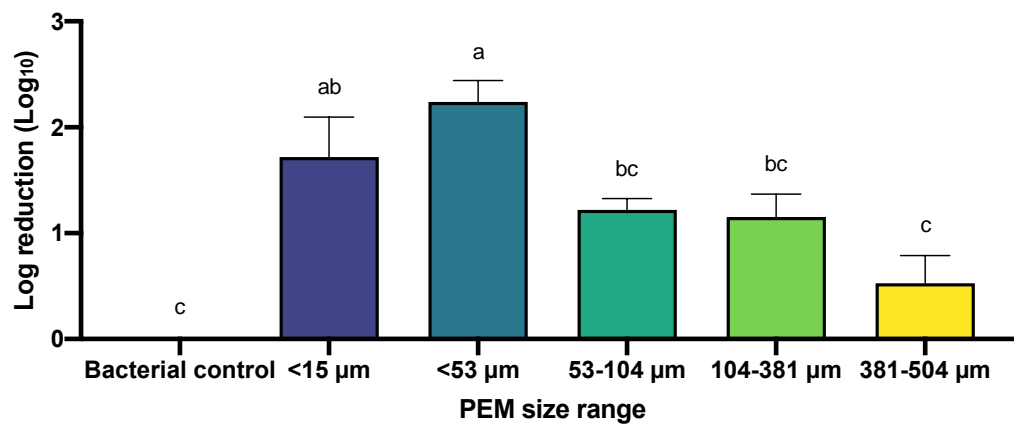


Figure 5-2 Size-dependent antimicrobial activity of various sizes PEM against *E. coli*

A. Growth curves of gram-negative *E. coli* (10^{5-6} CFU/mL) which was incubated with 50 mg/mL PEM **a)** <15 μm , **b)** <53 μm , **c)** 53-104 μm , 104-381 μm , and **d)** 381-508 μm for 18 h after 3 h pre-inoculation (broth microdilution assays; turbidity was measured at 600nm). **B.** Size-dependent antimicrobial activity of various sizes PEM was reflected by the difference of bacterial logarithm count at the end of incubation as compared to control ($P < 0.0001$). Bacterial cell count was determined by standard curves generated from the number of viable bacteria in the associated control group. Sterile H_2O , pH 7.4, was the negative control for inhibition. Kanamycin (1 mg/mL) served as a positive control (data not shown). Data are presented as Mean \pm SEM of triplicate independent experiments, each performed in triplicate. Values with different superscript letters indicate statistical significance ($P < 0.05$; one-way ANOVA; Post-hoc Tukey).

5.4 Discussion

In the present work, I evaluated the antimicrobial activity of PEM on the skin associated pathogen *E. coli* that complements our recently published study of PEM against *S. aureus* and *P. aeruginosa* (Kulshreshtha et al., 2020). In general, PEM<15 μm and <53 μm exhibited a dose-dependent inhibitory activity against both Gram-positive and negative pathogens on *S. aureus* and *E. coli*, with maximum efficacy at 50 mg/mL. The smaller sizes of PEM exhibited a significant bactericidal effect on Gram-positive pathogens *S. aureus* (10^{2-3} CFU/mL) with 4.5 log reduction of PEM<15 μm and 4.3 log reduction for PEM<53 μm as compared to the untreated group. Bacteriostatic activity of PEM was observed against Gram-negative pathogens *P. aeruginosa* (10^{2-3} CFU/mL) with approximately 3-fold reduction, and *E. coli* with 2-fold reduction. However, *S. aureus*, *P. aeruginosa* and *E. coli* demonstrated similar susceptibilities to 50 mg/mL PEM<15 μm and <53 μm . No significant difference was observed between the bacterial inhibitory effect of PEM 53-104 μm , 104-381 μm , 381-508 μm versus the untreated control when incubated with any of these pathogens.

These findings proved our hypothesis that the bioactivity of ESM could be enhanced through partialization. Moreover, finer particles in submicron scale of PEM<15 μm and <53 μm might contribute to the significantly improved antimicrobial activity due to the increased solubility and bioactivity as compared to larger particles (>53 μm), ESM flakes, or intact ESM. With preserved constituents from raw ESM and increased surface area, PEM might possess higher affinity and accessibility to bacterial pyrogens which can be demonstrated by the high affinity to LPS and LTA of ESM purified OCX-36 (Cordeiro et al., 2013), as well as the enhanced exposure of other antimicrobial proteins in ESM (Ahmed et al., 2017; Du et al., 2015; Hasebe, 2013; Makkar et al., 2015).

The innate immunity of avian egg against pathogens depends upon the physical barrier of the eggshell and the chemical defense system that is characterized by antimicrobial egg proteins and peptides incorporated into the egg yolk, egg white, ESM and shell during its assembly within the reproductive tract (R  hault-Godbert et al., 2011). Proteomics and transcriptomics technologies identified plenty of ESM proteins including lysozyme, histones, AvBDs, ovalbumin, gallin (ovotransferrin), ovocalyxin, keratin peptides that have been shown to possess antimicrobial and immune-modulating activities (Ahmed et al., 2017; Du et al., 2015; Gong et al., 2010; Makkar et al., 2015; Rose-Martel & Hincke, 2017). Some minor constituents of protease inhibitors and antiproteases such as ovalbumin Y, ovomacroglobulin, and ovomucoid are also potential antimicrobial compounds in ESM (Andersen, 2015; Makkar et al., 2015). Glycoproteins such as ovomucin and mucin possess antibacterial and antiviral capabilities (Liegel et al., 2012; Makkar et al., 2015; Omana et al., 2010). Serine proteases, present in methanol and guanidine hydrochloride (GuHCl) extracts of ESM, are also potential microbicide compounds (Makkar et al., 2015).

The potent antimicrobial activity of PEM could be credited to various preserved antimicrobial protein/peptides (AMPs). For example, lysozyme is a powerful AMP that is enriched in ESM and can enzymatically hydrolyze cell membrane peptidoglycan (especially Gram-positive pathogens) and thereby result in their cell lysis (Rose-Martel & Hincke, 2017). Of note, lysozyme also exert a broad antimicrobial activity against Gram-negative bacteria (e.g., *E. coli*) through proteolytic digestion to release its nonenzymatic bacteriostatic domains from the primary sequence (Mine et al., 2004). In our study, the size reduction process for PEM exhibited a significant increase in lysozyme specific activity which could contribute to the improved antimicrobial capability of PEM (Kulshreshtha et al., 2020). Related to the antibacterial protein

superfamily BPI/LBP/PLUNC, OCX-36 is an abundant AMP in ESM that exhibited a bacteriostatic inhibition on the growth of *S. aureus* (Cordeiro et al., 2013; Gautron et al., 2007, 2011). Also, histones are positively charged hydrophobic cationic antimicrobial peptides (CAMPs) that possess wide-spectrum bactericidal activity against both Gram-positive and -negative bacteria including *Staphylococcus*, *Escherichia*, *Salmonella*, *Pseudomonas*, *Listeria*, *Shigella*, *Bacillus* and *Klebsiella* (Hirsch, 1958; Jodoin & Hincke, 2018). Noteworthy, histones that were purified from avian erythrocytes exhibited antibiofilm activity against VRE, MRSA and MSSA (Jodoin & Hincke, 2018; Rose-Martel et al., 2017). Likewise, the AvBDs are small cationic non-glycosylated AMPs which exhibit a wide range of antimicrobial activity against Gram-positive and Gram-negative bacteria, such as *S. aureus*, *L. monocytogenes*, *E. coli*, *Salmonella* Enteritidis, and *Salmonella* Typhimurium, *Campylobacter jejuni*, and *Clostridium perfringens* (Hervé-Grépinet et al., 2010; van Dijk et al., 2007, 2008). Gallin (7 kDa) is an AMP related to the AvBDs family containing six cysteine motifs which were initially identified in the chicken egg white proteome (Gong et al., 2010; Mann, 2007). Recombinant gallin displayed a significant antimicrobial activity versus *E. coli* but failed to inhibit the growth of *Salmonella* Enteritidis, *Salmonella* Typhimurium, *S. aureus*, and *L. monocytogenes* (Gong et al., 2010; Hervé et al., 2014). Thus, the combination of multiple proteins in PEM contributes to its wide-spectrum antimicrobial capability.

With the increasing trend of AMR and accumulating drug-resistant strains, there is an urgent worldwide need for novel therapy and antimicrobial drugs. The promising antimicrobial activity of PEM against Gram-positive and -negative pathogens enables it to be considered as a possible AMP to treat skin and soft tissue infections (SSTIs). In addition to the prevalence of *S. aureus* and *P. aeruginosa* in SSTIs, MRSA, VRE, methicillin-resistant *S. epidermidis* (MRSE)

and resistant Gram-negative bacilli are major causes of nosocomial and chronic infections (May et al., 2009). Also, the *Streptococcus* spp. and *Clostridium* spp. are frequently identified in necrotizing soft tissue infections, while the streptococci are the most common invasive pathogen isolated from the patient organisms. As the fourth leading pathogen in SSTIs, *E. coli* has been found to be the causative agent of urinary tract infections, otitis media, bacteremia, neonatal omphalitis, cellulitis in limbs, necrotizing fasciitis, surgical site or burn injury infections, and others (Denamur et al., 2020; Petkovšek et al., 2009).

Moreover, respiratory, gastrointestinal, urinary and vaginal are common site of bacterial infections. The human respiratory tract can be infected or colonized by pathogens including *Streptococcus pneumoniae* (pneumococcus), *Haemophilus influenzae*, *Moraxella catarrhalis*, *S. aureus*, and *K. pneumoniae* (Bosch et al., 2013; Paczosa & Meccas, 2016). The human gastrointestinal tract can be affected by imbalance of microbial flora (dysbiosis) and infected by pathogens such as *Salmonella*, *E. coli*, *Clostridium difficile*, *Mycobacterium* spp., *Campylobacter*, *Klebsiella*, and *Helicobacter pylori* (*H. pylori*) (Sekirov et al., 2010). On the other side, urinary tract infections (UTIs) are most commonly caused by uropathogenic *E. coli* (UPEC), *K. pneumoniae*, *Proteus mirabilis*, *Enterococcus faecalis* (*E. faecalis*) and *Staphylococcus saprophyticus* (Flores-Mireles et al., 2015). And vaginal infections are commonly caused by the overgrowth of anaerobic and microaerophilic bacteria, including *Gardnerella*, *Atopobium*, *Prevotella*, *Leptotrichia*, etc; or aerobic bacteria of intestinal origin, such as *E. coli*, *S. aureus*, *S. epidermidis*, *Streptococcus agalactiae*, *E. faecalis*, which can lead to tissue inflammation (Łaniewski & Herbst-Kralovetz, 2018). Additionally, *Candida albicans* is the most common pathogen of vulvovaginal candidiasis.

Few studies were carried out to explore the therapeutic effect of ESM on bacterial infections. Oral administration of ESM powder was reported to ameliorate intestinal inflammation by facilitating the restitution of epithelial injury and improving microbial dysbiosis in an *in vivo* mouse model (H. Jia et al., 2017), which represents a potential impact of ESM on gastrointestinal health. Likewise, ESM hydrolysates exhibited an antimicrobial activity against *S. aureus*, *Bacillus subtilis*, *K. pneumoniae*, *Serratia marcescens*, and *E. coli*, and were proposed as a constituent of topical acne formulations (Yoo et al., 2014). Hence, more research is required to explore the feasibility of PEM as an alternative treatment for infections including skin, respiratory tract, gastrointestinal tract, urinary tract, vagina, etc.

In addition, published studies and commercially available ESM-derived skincare products pave the way to consider cosmetic topical applications of PEM. For example, Ovoderm® is an ESM-derived oral supplement reported to improve cutaneous aging by ameliorating skin elasticity (Aguirre et al., 2017). Nutrient supplements of BiovaBio™ (hydrolyzed water-soluble eggshell membrane, WSEM) showed an improvement in facial skin and hair appearance (Kalman & Hewlings, 2020). Their Biovaderm® (a WSEM facial cream) was confirmed to reduce skin wrinkles, free radicals and oxidative damage by topical application (Jensen et al., 2016). Thereby, it is highly plausible that PEM has potential applications as an ingredient for cosmetic and nutraceutical products to maintain skin and hair health.

CHAPTER 6 *IN VITRO* EVALUATION OF THE ANTI-INFLAMMATORY ACTIVITY OF PEM

6.1 Introduction

The inflammatory process is vital for host defense system and is involved in many disease, including dermatitis, asthma, diabetes, arthritis, obesity, atherosclerosis and cancer (J. Liu et al., 2019). Cutaneous homeostasis is largely shaped by colonized microbiota which communicate with resident antigen-presenting cells (innate lymphoid cells, innate-like cells, keratinocytes, etc.) and regulate their secretion of AMPs, cytokines and chemokines (de Koning et al., 2012; Eyerich et al., 2018; Nestle et al., 2009). Dysbiosis of skin is found in wound infections and certain inflammatory diseases, such as AD, acne, psoriasis, seborrhoeic dermatitis, and chronic wounds (Grice & Segre, 2011). To restore barrier integrity, the cutaneous barrier triggers inflammatory responses to protect body from external disturbances and restore immune homeostasis, but is almost always accompanied by tissue damage and temporary loss of functionality (Eyerich et al., 2018).

Macrophage plays an important role in the inflammatory process which functions through polarization, antigen presentation, phagocytosis, and immunomodulation (Shapouri-Moghaddam et al., 2018; Yeom, Kim, et al., 2015). LPS is a major component of the Gram-negative bacteria cell wall that is usually recognized by TLR4 on the macrophages cell membrane and then induce inflammatory cascades of enzymes and transcription factors. However, superfluous proinflammatory mediators from activated macrophages can increase the incidence of chronic inflammation, severe tissue damage, and disease (Yeom, Kim, et al., 2015). Thereby, therapeutic methods were developed to suppress the excessive anti-inflammatory response and restore skin homeostasis (Ko et al., 2017; Kovacs-Nolan et al., 2014; Yeom, Kim, et al., 2015).

Innate immune defense of avian egg is also armed with proteins possessing immune-modulatory and anti-inflammatory activities to support the development of the embryo (Ahmed et al., 2017), such as OCX-36 (Cordeiro et al., 2013; Kovacs-Nolan et al., 2014), ovotransferrin (Y. Kobayashi et al., 2015), lysozyme (M. Lee et al., 2009), defensins (van Dijk et al., 2008), glycoprotein, collagen, glucosamine, chondroitin sulfate and hyaluronic acid (Cordeiro & Hincke, 2011; DeVore & Long, 2013). For example, PEP and the ESM-derived carbohydrate fraction exhibited a diverse immunomodulatory effect in monocytes and macrophage-like cells (Vuong et al., 2017). ESM hydrolysate was reported to ameliorate inflammation in some *in vitro* and *in vivo* studies (Shi, Kovacs-Nolan, et al., 2014a; Shi, Rupa, et al., 2014; Yoo et al., 2014), suggesting a potential anti-inflammatory effect of ESM for human health. Therefore, it is necessary to evaluate the potential benefits of PEM as a novel treatment for inflammation.

6.2 Results

6.2.1 The effect of PEM on LPS-activated murine macrophages

Cell viability

In this study, I evaluated the anti-inflammatory activity of PEM by measuring its effect on the LPS-stimulated accumulation of nitric oxide in culture media of RAW 264.7 cells. Various concentrations of PEM were tested on RAW 264.7 macrophages to determine the range of PEM concentration that were not cytotoxic and had minimum effect on cell viability. Cells were treated with various concentrations of PEM (0, 0.1, 1, 2 and 5 mg/mL) with two size ranges (<15 and <53 μm) for 24 h.

Figure 6-1 illustrates the cell viability of RAW 264.7 cells after treatment with PEM (<15 and <53 μm) for 24 h. Both sizes of PEM at 0, 0.1, 1, and 2 mg/mL did not have any significant

effect on cell viability. PEM<15 μm and <53 μm had a similar effect on cell viability, at $78.80 \pm 9.58\%$ and $81.83 \pm 8.86\%$ respectively. However, cell viability of PEM<15 μm and <53 μm at the 5 mg/mL significantly dropped to $39.90 \pm 6.24\%$ ($P < 0.0001$) and $21.72 \pm 4.76\%$ ($P < 0.0001$). There was no significant difference between PEM<15 μm and <53 μm on cell viability in each treatment. In general, a dose-dependent decrease in cell viability was observed when RAW 264.7 macrophages were incubated with an increased concentration of PEM. Thereby, for further investigation of anti-inflammatory activities of PEM, the 5 mg/mL treatment was excluded due to high cytotoxicity.

Proinflammatory mediator NO level

The anti-inflammatory activity of PEM was evaluated by measuring its effect on the *E. coli* LPS-stimulated accumulation of NO in culture media of RAW 264.7 macrophages (Figure 6-2). A dose-dependent reduction in proinflammatory mediator NO level was observed when LPS-induced macrophages were treated with increasing concentrations of PEM<15 μm ($P < 0.0001$) and <53 μm ($P < 0.0001$), over the range of 0.1-2 mg/mL. The maximum inhibitory effect on NO levels was observed with treatment of 2 mg/mL ($56.89 \pm 7.39\%$, $P < 0.0001$) of PEM<53 μm as compared to 0 mg/mL and followed by 1 mg/mL with $66.49 \pm 7.33\%$ ($P = 0.0009$), and 0.1 mg/mL with $86.77 \pm 5.19\%$ ($P = 0.4448$). Furthermore, NO production levels of PEM<15 μm at 2 mg/mL significantly dropped to $57.93 \pm 8.36\%$ ($P = 0.0002$) after 24 hours accumulation as compared to 0 mg/mL. However, no significant difference of anti-inflammatory activity was observed between PEM<15 μm and <53 μm . In addition, PEM<15 μm and <53 μm had no significant effect on the NO production between 0 to 1 mg/mL. Besides, we confirmed that the incubation with complete growth media of either LPS only, or PEM only, or LPS with

PEM did not produce NO to the culture media. Also, different concentrations of LPS (0.1, 0.5, and 1 $\mu\text{g/mL}$) were tested for stimulatory activity by comparing NO production level in macrophages. These preliminary experiments showed that 1 $\mu\text{g/mL}$ of LPS triggered the most intense inflammation response with good cell survival (>80% viability). And no significant difference of NO accumulation between treatments after 18 h incubation was observed (data not shown).

To summarize, we observed a dose-dependent decline of NO production when LPS-induced RAW 264.7 macrophages were treated with increasing concentrations of PEM. The 2 mg/mL PEM of both <15 μm and <53 μm showed a significant decrease of NO compared to the non-treatment group.

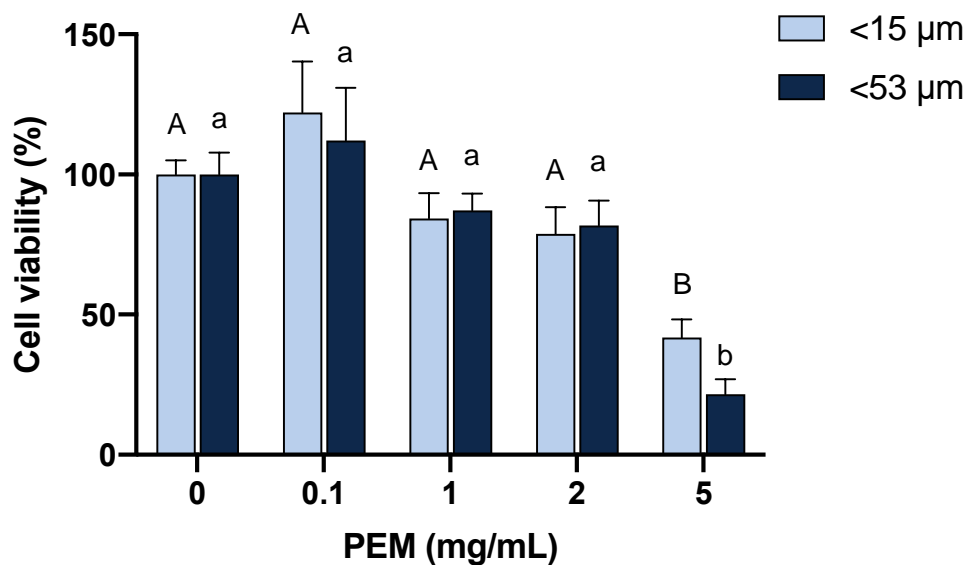


Figure 6-1 Effect of PEM on cell viability of RAW 264.7 macrophages

Macrophages were treated with 0, 0.1, 1, 2 or 5 mg/mL PEM<15 μm or <53 μm for 24 h. Cell viability was measured by alamarBlue® assay (PEM<15 μm: $P < 0.0001$; PEM<53 μm: $P < 0.0001$). Data are presented as Mean \pm SEM of triplicate independent experiments, each performed in triplicate. Values with different superscript letters indicate statistical significance ($P < 0.05$; ANOVA; Post-hoc Tukey).

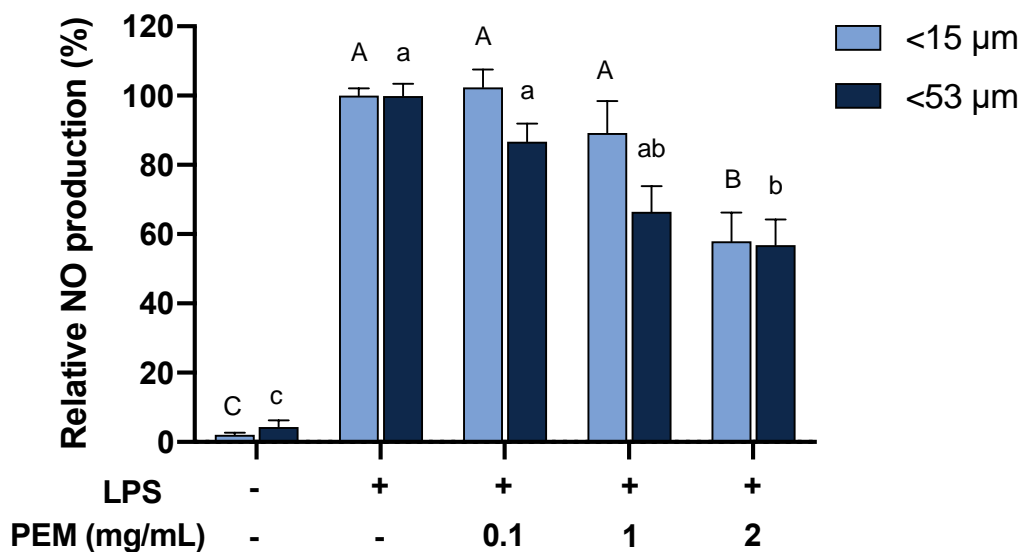


Figure 6-2 Effect of PEM on NO production in LPS-stimulated RAW 264.7

Cells were treated with 0, 0.1, 1, or 2 mg/mL PEM (<15 μm or <53 μm) in the presence or absence of 1 μg/mL *E. coli* LPS for 24 h. Dose-dependent anti-inflammatory activity of PEM was reflected as relative NO production as compared to the positive control cells (0 mg/mL PEM, normalized as 100%) (PEM<15μm: $P<0.0001$, <53 μm: $P<0.0001$). NO concentration was measured by the Griess Reagent System. Cells alone were served as a negative control. Data are presented as Mean \pm SEM of triplicate independent experiments, each performed in triplicate. Values with different superscript letters indicate statistical significance ($P<0.05$; ANOVA; Post-hoc Tukey).

6.3 Discussion

In this study, we evaluated the effect of PEM on NO production using the well-defined proinflammatory model of LPS-induced inflammation. The RAW 264.7 macrophage has been one of the most commonly used myeloid cell lines for *in vitro* assessment of anti-inflammatory activity for 40 years with stable phenotype and functional characteristics during the consecutive passages (Denlinger et al., 1996; Mosser & Edwards, 2008; Ralph & Nakoinz, 1977; Taciak et al., 2018). LPS is the major component of the outer membrane of Gram-negative bacteria, which is frequently utilized for *in vitro* studies on the inflammatory response (Boscá et al., 2005; Chen & Tsao, 2013; Ko et al., 2017; Vuong et al., 2017; Yeom, Park, et al., 2015; Zhai et al., 2016). The extent of an inflammatory response is controlled by complicated cellular pathways. For instance, LPS is a well-known stimulator of Mitogen-activated protein kinases (MAPKs) (Ko et al., 2017). Signals in MAPKs-regulated inflammatory responses, such as extracellular signal-regulated kinase (ERK), c-Jun N-terminal kinases (JNK), p38, and I κ B α , can be phosphorylated after cell membrane receptor TLR4 activated by LPS (Hambleton et al., 1996; Hommes et al., 2003; Ko et al., 2017). NF- κ B is also an important molecule exists in the cytoplasm as an inactivated form with the inhibitory protein I κ B α . Once the I κ B α is phosphorylated by inflammatory stimuli, NF- κ B can become activated for inflammatory downstream regulation (Baker et al., 2011).

Based on the size-dependent antimicrobial activity of PEM, we selected the PEM <15 μ m and <53 μ m (highest activities) for the present study. To determine the cytotoxicity concentration of PEM <15 μ m and <53 μ m, RAW 264.7 macrophages were treated with PEM at various concentrations ranging from 0 mg/mL to 5 mg/mL up to 24 h and the alamarBlue[®] assays were conducted for quantitative measurements (Figure 6-1). Cell viability above 80% is

regarded as non-cytotoxic, pursuant to ISO 10993-5, 60%–40% moderate and below 40% strongly cytotoxic respectively (López-García et al., 2014). We observed that PEM<15 μm and <53 μm did not demonstrate cytotoxicity up to 2 mg/mL showing its safety on murine macrophages.

After this, we evaluated the anti-inflammatory efficacy of PEM<15 μm and <53 μm on *E. coli* LPS-induced macrophages by measuring proinflammatory mediator NO. PEM<53 μm demonstrated the most powerful inhibitory effect at 2 mg/mL with $56.89 \pm 7.39\%$ NO levels as compared to PEM<15 μm at 2 mg/mL with $57.93 \pm 8.36\%$ after 24 hours accumulation. Similar to the antimicrobial study, both smaller sizes PEP exhibited similar effects on stimulated RAW cells.

NO is an important molecule in the human body. Biologically, NO is enzymatically synthesized from the amino acid L-arginine and molecular oxygen by NO synthases (NOS) with the by-product of L-citrulline (Wilson & Garthwaite, 2009). Three isoforms of NOS are identified as endothelial, neuronal, and inducible NOS (eNOS, nNOS, and iNOS, respectively) subserving the important role of NO in smooth muscle relaxation, neural communication, and immune defense. Hence, NO is a multifunctional molecule in a biological system that possesses numerous interactions with other molecules such as reactive oxygen species (ROS), metal ions, and proteins (P. Kim et al., 2001). The activation of NO production in macrophage begins with the response to inflammatory stimuli such as IFN- γ , TNF- α , IL-1 β or LPS (McSorley & Liew, 1998). NO produced by macrophages and related cells plays a pathophysiological role in causing cell damage, in a cytostatic or cytotoxic manner, on invading bacteria, fungi, viruses, as well as cancer cells (Ignarro, 2014). For instance, NO was able to impede apoptosis by inhibiting the main mediators of cell death, the caspase-3 like proteases in hepatocytes (Y. Kim et al., 1999).

Furthermore, intrinsic and extrinsic NO modulation can be dose-dependent and cell-type specific (P. Kim et al., 2001).

Other mechanisms of signaling pathways also take part in anti-inflammatory response activation, such as NF- κ B, MAPK (e.g., ERK, JNK, p38), PI3K/AKT, ROS, JAK-STAT, NO-induced mitochondrial dysfunction and apoptosis, etc. (Boscá et al., 2005; P. Kim et al., 2001). For instance, post-translational modification of pro-apoptotic compounds in mitochondria, such as cytochrome c and apoptosis induced factor (AIF) can regulate downstream caspase activity that further modifies different cell fates. The Bcl-2 family (especially Bax) and NO are involved in the release of proteins such as cytochrome c from mitochondria, while NO also upregulates the expression of tumor suppressor p53 during apoptosis (Boscá et al., 2005; Kuwana et al., 2002). Also, I κ B kinase (IKK) is the main regulator of the NF- κ B pathway that once activated can prompt expression of NF- κ B and change relevant cell fate, such as mitochondria-mediated apoptosis in melanoma cells (Yahfoufi et al., 2018; Jinming Yang et al., 2006). Thereby, the action mechanism of PEM on LPS-induced macrophages should be studied based on the above signaling pathways as well.

In this study, the PEM $<15\ \mu\text{m}$ and $<53\ \mu\text{m}$ possessed a more powerful inhibitory effect on NO production than the purified OCX-36 (no reduction) and its hydrolysates ($<10\%$ reduction) in LPS-induced RAW cells (Kovacs-Nolan et al., 2014). Additionally, when incubated with macrophages in the absence of LPS, the PEM did not induce the secretion of NO, indicating inflammatory response of macrophages was not inherent to PEM but was mediated by the LPS. The plausible enhancement of the anti-inflammatory activity of PEM could be ascribed to increased surface area and exposure of multiple immunomodulating constituents of ESM. For example, ESM-purified OCX-36 exhibited LPS and LTA binding activity that was able to

interfere with bacterial infection (Cordeiro et al., 2013). Furthermore, enzymatically digested OCX-36 downregulated *in vitro* expression of NF- κ B and *in vivo* mediators, such as IL-10, IL-1 β , CCL2 (monocyte chemoattractant protein-1, MCP-1), chemokine receptor 4 (CXCR4), myeloid differentiation primary response gene 88 (MyD88) and Proteoglycan 2 (Prg2), which are involved in LPS signaling and inflammatory responses (Kovacs-Nolan et al., 2014). Also, the ESM hydrolysates produced via fermentation, enzymatic, or chemical processing were reported to activate the NF- κ B in unstimulated human leukemic monocyte (THP-1) cells (Ruff et al., 2015). Processed ESM particles maintain bioactivity similar to that of native membranes, and both PEP and the ESM-derived carbohydrate fraction downregulate immune response differently in monocytes and macrophage-like cells by reducing the activity of transcription factor NF- κ B and expression of TLR-4, intercellular adhesion molecule1 (ICAM-1), and cell surface glycoprotein (CD44) (Vuong et al., 2017). PEP regulated cytokines in inflammation by increasing the anti-inflammatory cytokine IL-10, while the ESM-derived carbohydrate fraction decreased the proinflammatory cytokines IL-1 β and IL-6. In addition, previous research carried out in our lab demonstrated that the topical application of ESM powder accelerated the wound healing process in a mouse excisional wound splinting model; these observations paved the way for the development of the innovative DermaRep® wound dressing material (Biovotec) (Ahmed, Suso, Maqbool, et al., 2019). All in all, these findings and applications validate the PEM as a prospective immunomodulating and anti-inflammatory ingredient for treatment of skin inflammation.

CHAPTER 7 *IN VITRO* EVALUATION OF ANTIOXIDANT ACTIVITY OF PEM

7.1 Introduction

Aerobic organisms have evolved an integrated antioxidant defense system that recruits enzymatic and non-enzymatic antioxidants to block the detrimental effects of ROS/RNS. Long-term exposure to various exogenous and endogenous stimuli can lead to oxidative stress where abnormally high ROS/RNS level damages cell structures and alters their functions. Oxidative stress is involved in many pathological progressions, including aging (Rinnerthaler et al., 2015), dermatological diseases (Q. Zhou et al., 2009), gastrointestinal diseases (Thomson et al., 1998), diabetes mellitus (Maritim et al., 2003), neurodegenerative disorders (Uttara et al., 2009), cardiovascular diseases (Madamanchi et al., 2005) and cancer (Cannavò et al., 2018).

Hence, antioxidant compounds received much attention to ameliorate oxidative stress. For example, vitamin C and vitamin E are essential diet-dependent nutrients and antioxidants which cannot be synthesised by human body. As an antioxidant, vitamin C is found out to get involved in many biological events including oxidative stress, collagen synthesis, connect tissue regeneration, infections, inflammation, and tumor progression. Vitamin E functions as a lipid hydroperoxyl radical scavenger in human body that is able to protect erythrocyte membranes and nervous tissues from oxidative stress (Traber & Stevens, 2011).

Increasingly, natural proteins or peptides derived from food have been verified as potential antioxidants to inhibit oxidative stress, such as dairy, soybean, gelatin, egg yolk (R. J. Elias et al., 2008) and ESM (Huang et al., 2010). Proteins and peptides are unique antioxidants that can prevent oxidation through different pathways including inactivation of ROS, scavenging free radicals, chelation of prooxidative transition metals, reduction of hydroperoxides, as well as adduction of aldehyde (R. J. Elias et al., 2008). Peptides or protein hydrolysates possess better

antioxidant activity compared to intact proteins due to the exposure of proline, histidine, methionine, or threonine in the amino acid sequence, or hydrophobic amino acid residues valine or leucine at the N-terminus, and / or tryptophan, tyrosine at the C-terminus (R. J. Elias et al., 2008; Shahidi & Zhong, 2010). The total antioxidant activity of a protein can be increased by disruption of its secondary and tertiary structure, such as reductive cleavage of disulfide bonds, which can increase solvent accessibility to free radical scavenging and prooxidative metal chelating amino acid residues (R. J. Elias et al., 2008; Yi et al., 2004).

Proteinaceous ESM comprises amino acids that have been shown to exhibit antioxidant activities (Nimalaratne et al., 2015; Uchida & Kawakishi, 1992), including cysteine, histidine, tryptophan, lysine, arginine, leucine, valine, glutamic acid, proline, and β -hydroxyl tryptophan (Huang et al., 2010; Yi et al., 2004). For instance, dietary ESM ameliorated hepatic fibrogenesis in a mouse model by suppressing oxidative stress and promoted collagen degradation by deactivating the hepatic stellate cell (HSC) transformation (H. Jia et al., 2014). In another study, a fraction from alcalase hydrolyzed soluble eggshell membrane (SEP) with an average molecular weight of 619 Da was reported to exhibit strong free radical scavenging activity and protective effect against DNA damage *in vitro* after 3-MPA treatment (Huang et al., 2010). Likewise, enzymatic hydrolysates of ESM, especially the peptides obtained from Na₂SO₃-assisted protease digestion, displayed high water-solubility and antioxidant activities (Zhao et al., 2019). Furthermore, fish skin-derived collagen hydrolysates, particularly the peptide sequence of His-Gly-Pro-Leu-Gly-Pro-Leu (797 Da), possess high free radical scavenging activity (Mendis et al., 2005). Overall, these findings underline the necessity to evaluate potential antioxidant activity of PEM and PEM-H in our study.

7.2 Results

7.2.1 Specific antioxidant activity of PEM

In this study, the Trolox equivalent antioxidant capacity (TEAC) of PEM was evaluated by the Total Antioxidant Power Kit, and the protein concentration was determined by the Pierce™ BCA Protein Assay Kit. The total antioxidant activity is expressed as μmol of Trolox equivalents (TE) per gram of protein ($\mu\text{M TE/g protein}$) as shown in Figure 7-1.

The PEM exhibited a significant ($P < 0.001$) dose-dependent antioxidant activity across five size ranges. Particularly, PEM 104-381 μm showed the strongest specific antioxidant activity compared to other four sizes with $311.30 \pm 38.47 \mu\text{M TE/g protein}$. PEM 381-508 μm presented the second highest specific antioxidant activity with $132.93 \pm 64.77 \mu\text{M TE/g protein}$, followed by PEM 53-104 μm with $98 \pm 20.11 \mu\text{M TE/g protein}$. The two smallest sizes of PEM exhibited the lowest level of antioxidant potency with only $19.40 \pm 1.84 (<15 \mu\text{m})$ and $50.53 \pm 14.93 (<53 \mu\text{m}) \mu\text{M TE/g protein}$. In general, PEM showed a size-dependent total antioxidant activity with the highest level around 311 $\mu\text{M TE/g protein}$ for PEM 104-381 μm .

7.2.2 Effect of NaOH hydrolysis on the specific antioxidant activity of PEM

In order to evaluate and enhance the antioxidant potential of the PEM, an alkaline digestion process was performed to modify the antioxidant activity associated with PEM. The optimum hydrolysis conditions including alkali concentration, PEM dose, time and temperature were screened by a stepwise screening method.

Firstly, the concentration of PEM was compared by 24 hrs reaction for 5 and 10 mg/mL PEM < 53 μm with 1.25 N NaOH (ratio 1:1, v/v) at 37 °C. As shown in Figure 7-2 **a**, the lower dose of PEM-H (5 mg/mL) contributed to higher specific antioxidant activity as compared to the

higher reaction dose (10 mg/mL). The specific antioxidant activity of the 5 mg/mL reaction system was significantly ($P < 0.0001$) increased to $630.13 \pm 11.60 \mu\text{M TE/g protein}$, compared to the 10 mg/mL reaction which was $289.84 \pm 8.13 \mu\text{M TE/g protein}$. Thus, we selected the 5 mg/mL reaction system for further study.

Then the specific antioxidant activities of PEM-H from 1.25 N NaOH digested various sizes PEM was evaluated after 24 h incubation at 37°C . As illustrated in Figure 7-2 **b**, PEM-H obtained from five sizes of PEM exhibited a significant size-dependent antioxidant activity ($P < 0.0001$). Notably, PEM-H $<15 \mu\text{m}$ and $<53 \mu\text{m}$ showed the highest activities than the other three sizes of PEM-H with 609.33 ± 11.21 and $651.42 \pm 17.66 \mu\text{M TE/g protein}$. But no significant difference was observed between PEM-H $<15 \mu\text{m}$ and $<53 \mu\text{m}$, so PEM-H $<53 \mu\text{m}$ was selected for further analysis. Nevertheless, the specific antioxidant activities among the PEM-H 53-104 μm , 104-381 μm and 381-508 μm were not significantly different from each other, with 454.91 ± 8.98 , 449.25 ± 11.04 , and $422.75 \pm 25.48 \mu\text{M TE/g protein}$, respectively.

As compared to each size of PEM (Figure 7-1), the alkaline digestion process contributed to a higher level of cupric reducing antioxidant capacity for PEM-H (Figure 7-2). Particularly, the antioxidant capacity of PEM-H obtained from PEM <15 and $<53 \mu\text{m}$ digestion increased more than 30- and 10- folds, respectively. In summary, the overall specific antioxidant activity of PEM (five sizes) was considerably increased from 19.40-311.30 $\mu\text{M TE/g protein}$ to 422.75-651.42 $\mu\text{M TE/g protein}$ after NaOH hydrolysis.

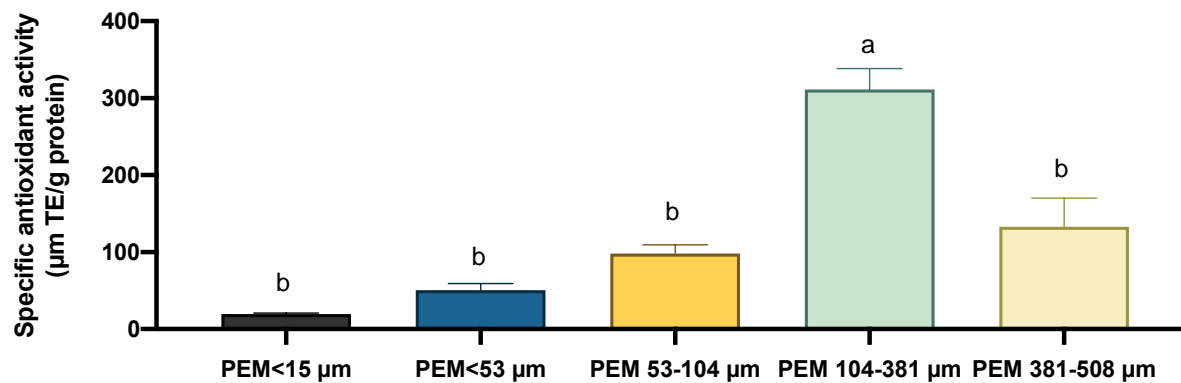


Figure 7-1 Specific antioxidant activity of various sizes of PEM

Specific antioxidant activity of five size ranges of PEM was determined by the Total Antioxidant Power Kit and the Pierce™ BCA Protein Assay Kit ($P < 0.001$). Data are presented as Mean \pm SEM for three independent experiments, each performed in triplicate. Values with different superscript letters indicate statistical significance ($P < 0.05$; one-way ANOVA; Post-hoc Tukey).

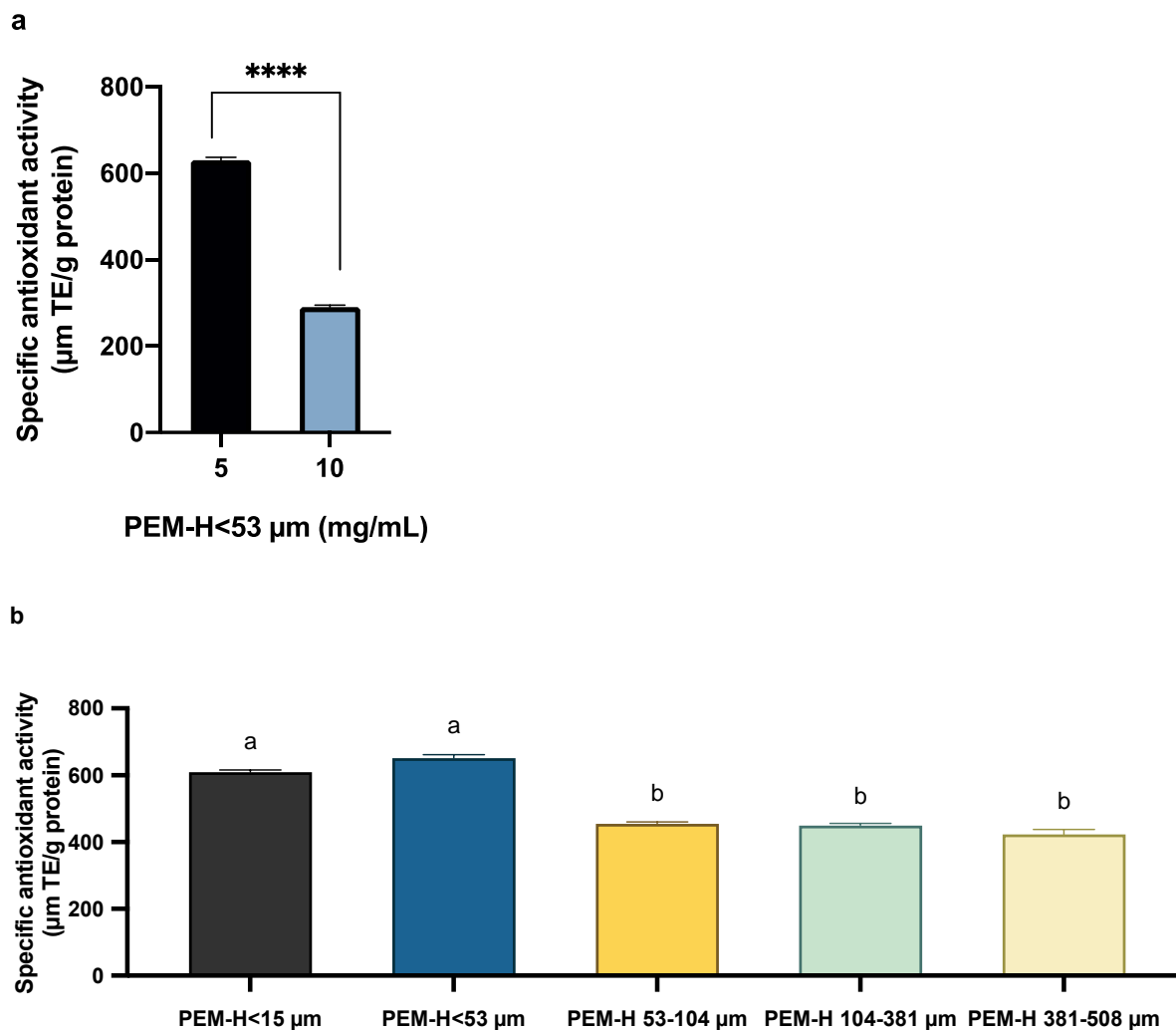


Figure 7-2 Effect of PEM dose and PEM size on specific antioxidant activity of PEM-H

a) Two concentrations of PEM < 53 μm (5 and 10 mg/mL) were digested by 1.25 N NaOH at 37 °C for 24 h (student's t-test; **** P<0.0001); **b)** Five sizes of PEM at 5mg/mL were digested by 1.25 N NaOH at 37 °C for 24 h (P<0.05; one-way ANOVA; Post-hoc Tukey). Specific antioxidant activity of PEM-H was determined by the Total Antioxidant Power Kit and the Pierce™ BCA Protein Assay Kit. Data are presented as Mean ± SEM from three independent experiments, each performed in triplicate. Values with different superscript letters indicate statistical significance.

7.2.3 Effect of hydrolysis parameters on the antioxidant activity of PEM-H

The antioxidant activity of protein hydrolysates is determined by the amino acid sequences of peptides that are produced by hydrolyzing agent (type and concentration), temperature, pH, reaction time and reaction ratio (Shahidi & Zhong, 2008). In my work, parameters containing base concentration, reaction temperature and time were evaluated for the effect on total antioxidant activity exhibited by PEM-H.

Macroscopic appearance changes in response to different hydrolysis conditions

Macroscopic appearance changes in response to different hydrolysis conditions are shown in Figure 7-3 **a** (37 °C) and **b** (50 °C). The turbidity of PEM in each tube varies according to the concentration of NaOH and reaction time which indicates distinctive differences in the hydrolysis impact on PEM < 53 µm. For instance, all the tubes remained opaque after 0.5 h reaction at both 37 and 50 °C. By 6 h, the tube at 50 °C were clearer than other tubes suggesting a harsher disruption of the insoluble constituents of PEM. Over the next 10 hours, the PEM suspensions became less opaque than before, and particularly, the 0.3 N NaOH tube at 50 °C was visibly clearer than that at 37 °C. The maximum solubility of PEM of each tube was achieved after 24 h hydrolysis with the least turbidity in tubes for the 1.25 N NaOH digestion (37 and 50 °C). Hydrolysates from these 30 types of reaction conditions were processed by centrifugation (13,000 rpm for 10 min) to collect the supernatants (designated PEM-H) for CUPRAC assay, protein concentration measurement and calculation of specific antioxidant activity.

TEAC levels and protein concentrations in the PEM-H samples

The effect of different NaOH concentration, reaction temperature and time on the TEAC levels and protein concentrations in the supernatants following hydrolysis are shown in Figure 7-3. In general, these three parameters contribute to similar trends for TEAC level and protein concentration for the same incubation temperature, such as Figure 7-3 **a** and **c** (37 °C), Figure 7-3 **b** and **d** (50 °C).

As reaction time was extended, PEM-H<53 μm exhibited an overall increase in TEAC levels, as well as protein concentration, as compared to the initial time zero point, but with fluctuations under some conditions (1.25 N NaOH at 37 °C and 50 °C). In terms of lower NaOH concentration, namely 0.1 and 0.3 N, both TEAC levels and protein concentrations for PEM-H<53 μm showed a slight increase after 6 h of hydrolysis, and finally reached a plateau in the following 18 hours. The 1.25 N NaOH contributed to the highest TEAC levels and protein concentration at each time point suggesting the strongest hydrolysis process that was consistent with the turbidity appearance as the suspensions, as discussed before. My results demonstrated that hydrolysis temperature plays an important role in generating PEM-H bioactivity. When treated with the same NaOH concentration, PEM-H<53 μm showed higher TEAC levels and protein concentration at 50 °C than that at 37 °C, for each time point. Notably, the TEAC levels and protein concentrations kept increasing until 24 h at 37 °C (TEAC= 499.66 ± 59.33 μM TE, protein concentration = 1.14 ± 0.04 g protein/g material), while the highest levels were reached after 6 hours of reaction at 50 °C (TEAC= 575.68 ± 24.26 μM TE, protein concentration = 1.11 ± 0.04 g protein/g material), and then started to decrease towards the end of the incubation period. Thus, in terms of the CUPRAC assay, the PEM-H<53 μm that was hydrolyzed by 1.25 N NaOH for 24 h at 37 °C (P<0.0001) and 1.25 N NaOH for 6 h at 50 °C (P<0.0001) significantly increased the TEAC level of PEM-H<53 μm as compared to the control (time = 0 h) group and

were considered to be the best conditions for enhancing the antioxidant activity of PEM in this study.

Specific antioxidant activity

In order to select the potential antioxidants, the specific antioxidant activity of PEM-H<53 μm from different dose-, temperature- and time-dependent preparations were calculated from the TEAC values using the associated protein concentration of the hydrolysate, as shown in Figure 7-4.

The PEM-H<53 μm obtained from 37 and 50 °C presented a different and fluctuating trend of specific antioxidant activity compared to specific values as shown in Figure 7-3. The highest specific activity for hydrolysates obtained from 37 °C was $807.30 \pm 62.58 \mu\text{M TE/g}$ protein for the 0.5 h reaction with 1.25 N NaOH ($P=0.0089$ as compared to control), and for 50 °C was $783.93 \pm 67.54 \mu\text{M TE/g}$ protein for the 24 h reaction with 0.1 N NaOH ($P<0.0001$, as compared to control).

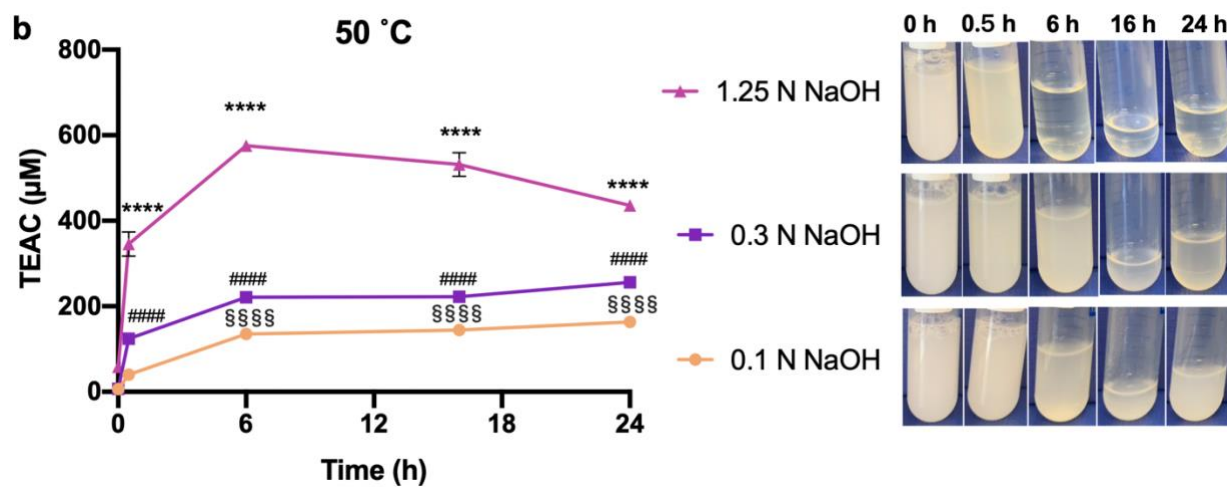
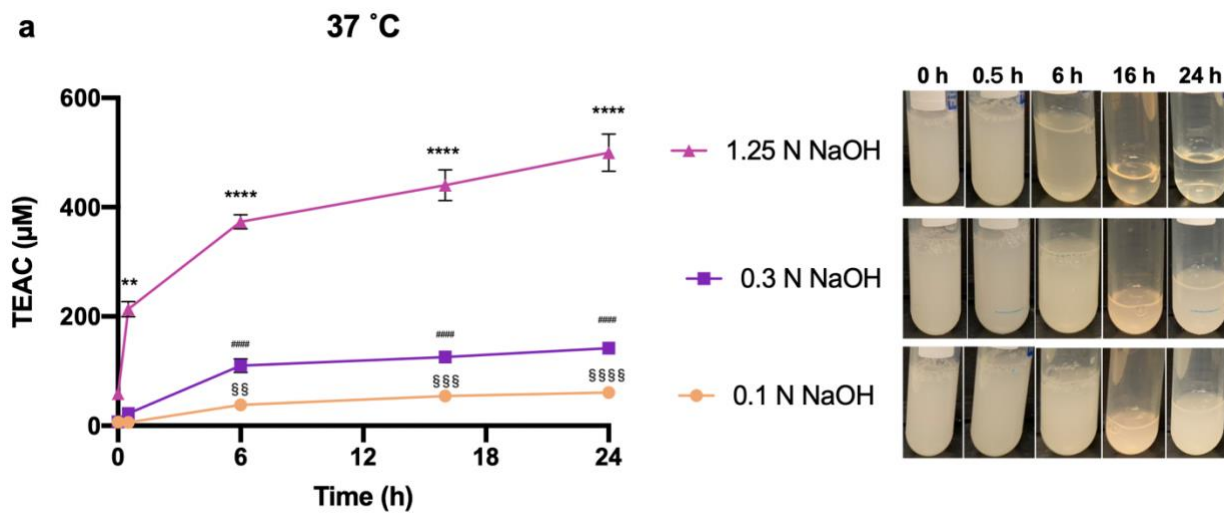
Under 37 and 50 °C incubations, PEM-H<53 μm obtained from 0.3 N NaOH showed a similar escalating trend that reached 548.01 ± 107.79 and $676.40 \pm 67.25 \mu\text{M TE/g}$ protein, respectively, at the end of 24 hours. Dissimilarly, PEM-H<53 μm exhibited a declining specific antioxidant activity when hydrolyzed with 0.1 and 1.25 N NaOH. For instance, the hydrolysates produced by 0.1 N NaOH from 50 °C showed two peaks of antioxidant activity at 6 and 24 h during the incubation which finally increased by 95.2% as compared to that of 0.5 h ($401.60 \pm 21.30 \mu\text{M TE/g}$ protein). As for PEM-H<53 μm , obtained from 0.1 N NaOH at 37 °C, the highest specific antioxidant activity appeared at 6 h with $516.01 \pm 78.75 \mu\text{M TE/g}$ protein but decreased continuously in the following 18 hours. It is noteworthy that the higher concentration of NaOH

and higher temperatures contributed to a lower specific antioxidant activity with long-term reaction of PEM-H<53 μm . For instance, the specific antioxidant activity of 1.25 N NaOH at 50 °C started to descend after 0.5 h ($588.17 \pm 26.15 \mu\text{M TE/g protein}$) and finally was reduced to $559.77 \pm 22.76 \mu\text{M TE/g protein}$ at 24 h. But no significant difference was observed among five time points of PEM-H<53 μm hydrolyzed by 1.25 N NaOH at 50 °C. Particularly, the specific antioxidant activity of PEM-H<53 μm from 1.25 N NaOH at 37 °C sharply dropped after 0.5 h by 45.9% to $436.67 \pm 38.07 \mu\text{M TE/g protein}$. Moreover, the strongest specific antioxidant activity obtained from 1.25 N NaOH at 37 °C ($807.30 \pm 62.58 \mu\text{M TE/g protein}$) was higher than that at 50 °C ($559.77 \pm 22.76 \mu\text{M TE/g protein}$). Thus, the specific antioxidant activity indicated a high prospect for the PEM-H<53 μm , which was hydrolyzed by 1.25 N NaOH for 0.5 h at 37 °C and 0.1 N NaOH for 24 h at 50 °C, as potential antioxidants for biomedical applications.

Summary of the correlation between three parameters and antioxidant activity index

As shown in Table 7-1, the TEAC of PEM-H<53 μm showed a high positive correlation with NaOH concentration ($R^2 = 0.725$; $P < 0.0001$) and low positive correlation with incubation time ($R^2 = 0.423$; $P < 0.0332$), while there was no significant correlation between TEAC and hydrolysis temperature. And there was no significant correlation between hydrolysate protein concentration and hydrolysis time, dose and temperature. The specific antioxidant activity of PEM-H<53 μm showed a weak positive correlation with NaOH concentration ($R^2 = 0.375$; $P < 0.0332$) and incubation time ($R^2 = 0.390$; $P < 0.0332$), but was not significantly correlated with temperature. In my study, the incubation temperature was not significantly correlated with the TEAC total activity, protein concentration or specific antioxidant activity of PEM-H<53 μm . To

summarize, PEM-H<53 μm exhibited a time- and NaOH dose-correlated total and specific antioxidant activity.



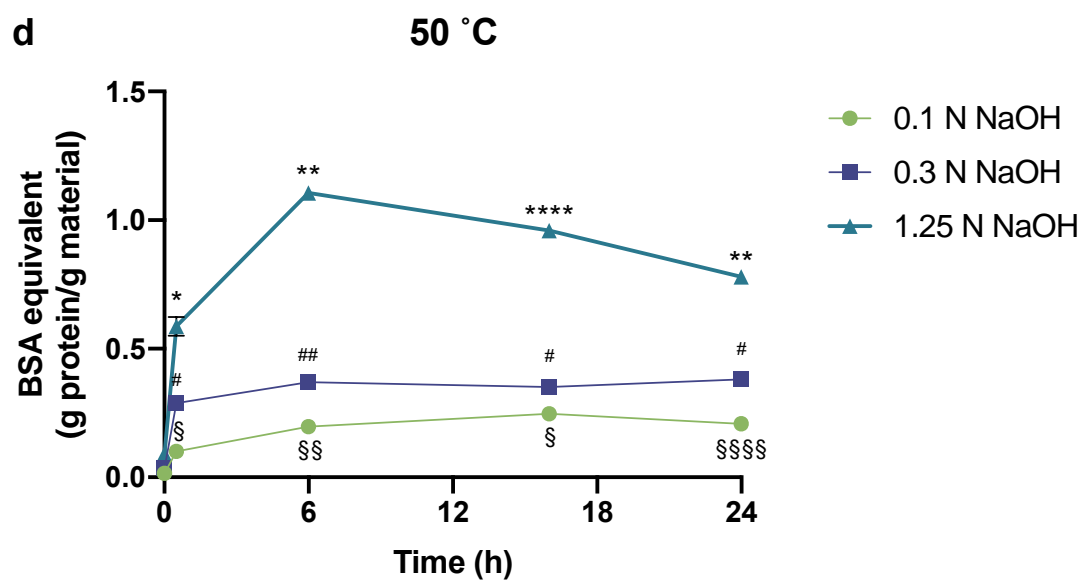
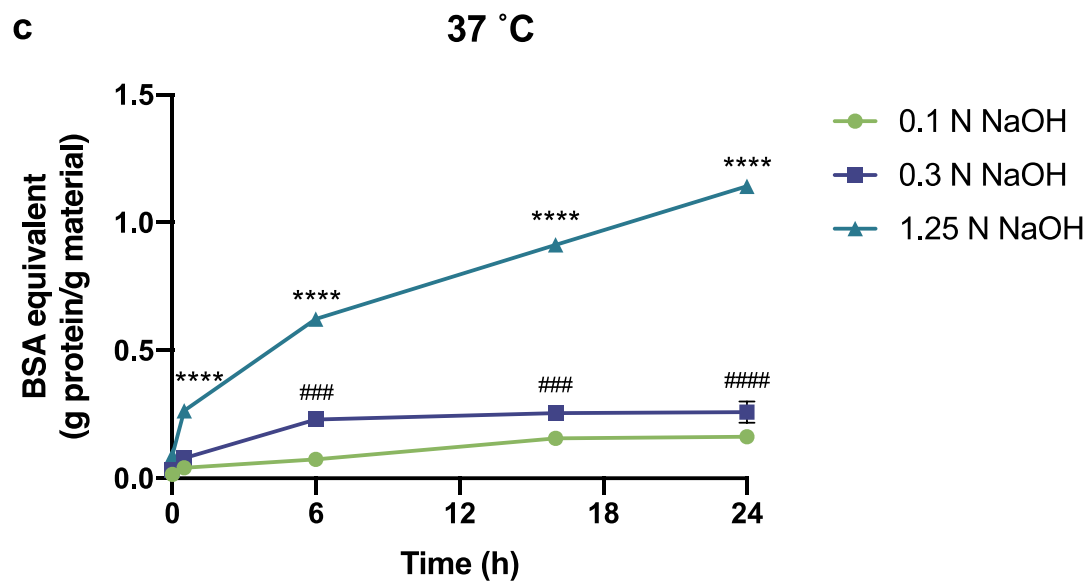


Figure 7-3 Effects of time-, dose- and temperature-dependent NaOH hydrolysis on TEAC level and protein concentration of PEM-H<53 μm

PEM<53 μm was digested by 0.1, 0.3 and 1.25 N NaOH at 37° or 50 °C for up to 24 h and centrifuged to obtain a soluble supernatant for further evaluation as PEM-H<53 μm.

a) and **c)**. The macroscopic appearance of PEM-H<53 μm after various hydrolysis conditions.

Total Trolox equivalent antioxidant activity (TEAC) of PEM-H<53 μm was measured by the Total Antioxidant Power Kit for **a)** 37 °C (0.1 N: P<0.0001; 0.3 N: P<0.0001; 1.25 N: P<0.0001) and **c)** 50 °C (0.1 N: P<0.0001; 0.3 N: P<0.0001; 1.25 N: P<0.000).

b) and **d)**. The protein concentration of supernatants from hydrolysis of PEM-H<53 μm was measured by the Pierce™ BCA Protein Assay Kit with BSA as standard for **b)** 37 °C (0.1 N: P=0.2680; 0.3 N: P<0.0001; 1.25 N: P<0.0001) and **d)** 50 °C (0.1 N: P<0.0001; 0.3 N: P<0.0001; 1.25 N: P<0.0001).

Data are presented as Mean ± SEM of three independent experiments, each performed in triplicate. Values with different superscript letters indicate statistical significance (P<0.05; one-way ANOVA; Post-hoc Dunnett). For all symbols conferring statistical significance compared to each control (0h): single symbol P<0.05, double symbol P<0.01, triple symbol P<0.001, quadruple symbol P<0.0001. TEAC: Trolox equivalent antioxidant activity.

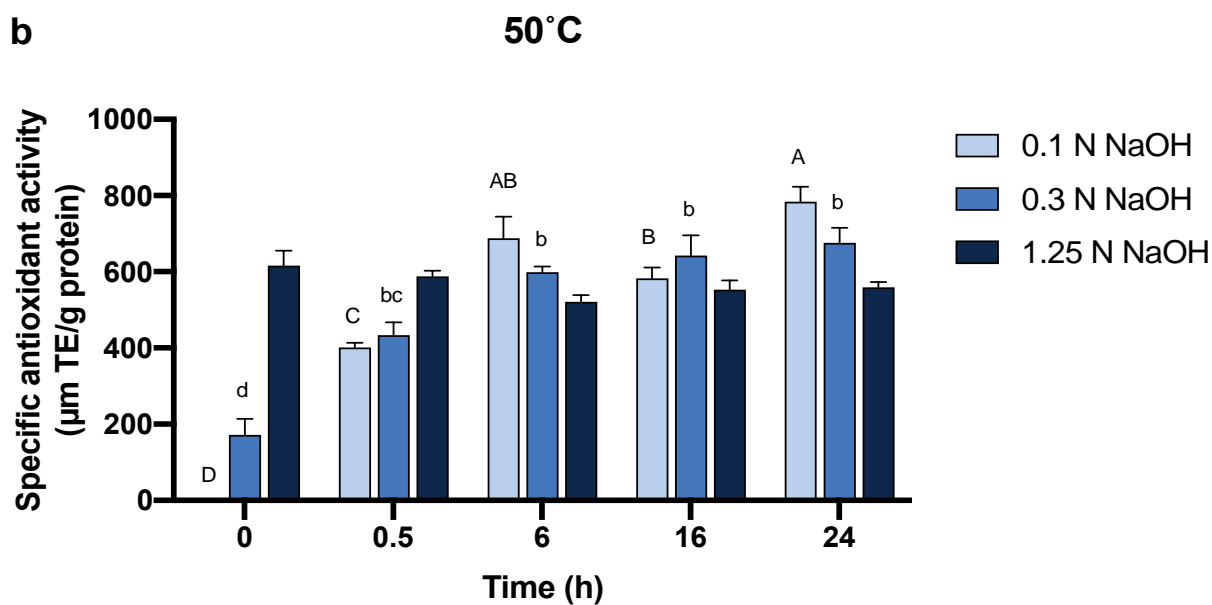
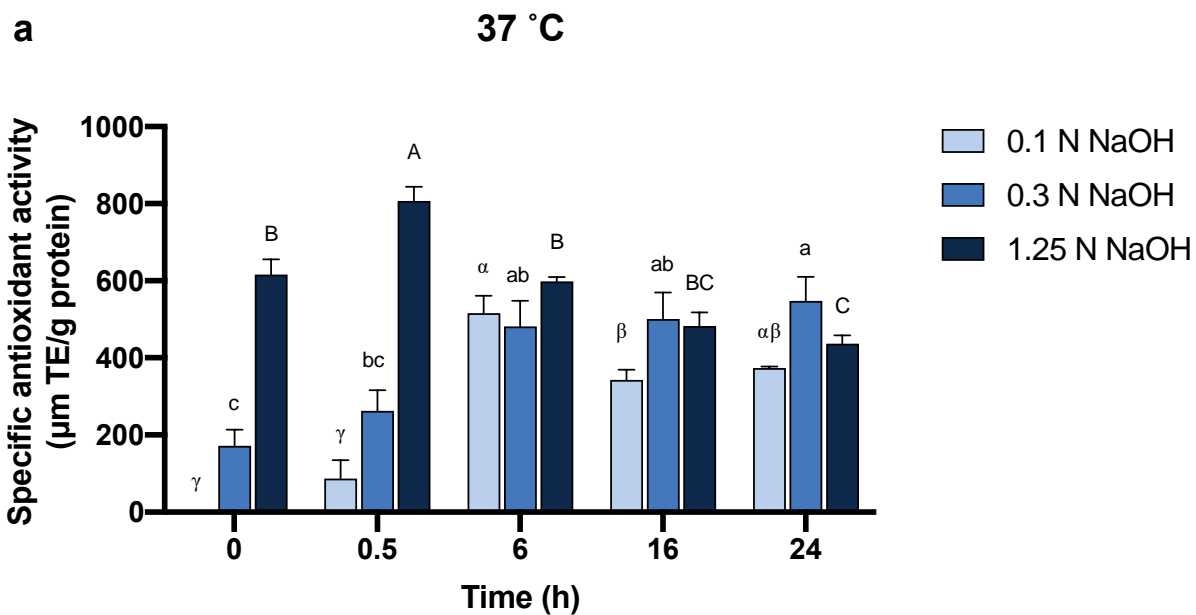


Figure 7-4 Effects of time-, dose- and temperature-dependent NaOH hydrolysis on specific antioxidant activity of PEM-H<53 μm

Specific antioxidant activity of PEM-H<53 μm that was digested at **a)** 37 °C (0.1 N: P<0.0001; 0.3 N: P=0.0039; 1.25 N: P<0.0001); and **b)** 50 °C (0.1 N: P<0.0001; 0.3 N: P<0.0001; 1.25 N: P=0.1320). The specific antioxidant activity of soluble supernatants from hydrolysis of PEM-H <53 μm was calculated from total TEAC values and protein concentration. Data are presented as Mean ± SEM of three independent experiments, each performed in triplicate. Values with different superscript letters indicate statistical significance (P<0.05; one-way ANOVA; Post-hoc Tukey).

Table 7-1 Analysis of the correlation between three parameters and specific antioxidant activity

Pearson's r	Time	Dose	Temperature
TEAC (Total antioxidant activity)	0.423 *	0.725 ****	0.216 ^{ns}
Protein concentration	0.332 ^{ns}	-0.224 ^{ns}	0.310 ^{ns}
Specific antioxidant activity	0.375 *	0.390 *	0.254 ^{ns}

ns indicates not significant ($p > 0.1234$); * $p < 0.0332$; ** $P < 0.0021$; *** $P < 0.0002$; **** $P < 0.0001$

(Pearson correlation; significance: two-tailed). TEAC: Trolox equivalent antioxidant activity.

7.3 Discussion

The living body is exposed to multiple external and intrinsic oxidative stimuli. Under normal conditions, ROS play a critical role as signaling molecules and take part in vital cellular processes, including cell proliferation, apoptosis, differentiation and immune responses (Trouba et al., 2002). For instance, ROS produced by activated leukocytes and macrophages play an important role in immunological defense against invading pathogens (Dröge, 2002). Moreover, the macrophage produced-ROS function to amplify antigen receptor-mediated signal cascades and decrease the activation threshold of T cells. Also, ROS is tightly linked to the regulation of transcription factor HIF-1 (hypoxia-inducible factor 1), as a sensor for redox homeostasis involving in the degradation of HIF-1 α , which are essential for angiogenesis, energy metabolism, erythropoiesis, cell proliferation and viability, vascular remodelling, vasomotor responses, and in addition to hypoxia-regulated hormones and proteins. Thereby, increased or prolonged free radical action can counteract ROS protective functions leading to oxidative stress that is involved in the development of many disorders and diseases such as psoriasis (Q. Zhou et al., 2009), intestinal bowel disease (Thomson et al., 1998), diabetes (Maritim et al., 2003), Alzheimer's disease, Parkinson's disease (Uttara et al., 2009), atherosclerosis, hypertension (Madamanchi et al., 2005) and cancer (Cannavò et al., 2018).

Antioxidants are able to counteract oxidative stress and restore the redox equilibrium. Regarding the safety of its natural source and accessibility, the search for natural antioxidants as alternatives has attracted wide interest among researchers. A variety of protein-rich natural products, such as milk, whey, soybean, and egg were verified with antioxidant activities (Sarmadi & Ismail, 2010; P. Wang et al., 2019).

In reality, protein hydrolysates exhibit better antioxidant activity than their intact form due to the structural changes of the secondary and tertiary structure including reductive cleavage of disulfide bonds that increase the free radical scavenging and prooxidative metal chelating capacity (R. J. Elias et al., 2008; Yi et al., 2004). A majority of peptides derived from natural sources and industrial by-products presented potential radical scavenging activity, inhibition of liposome oxidation or inhibition of thiobarbituric acid reactive substances (TBARS, degradation products of fats) (Shahidi & Zhong, 2008). For instance, soy peptides, a potential source of antioxidants, obtained from different enzymes, such as pepsin, papain, chymotrypsin, Alcalase, Protamex, and Flavourzyme, inhibited 28 to 65% of the formation of TBARS in a liposome-oxidizing system (Peña - Ramos & Xiong, 2002). The protein-rich feature of egg aroused many antioxidant types of research as well. Interestingly, Dávalos et al. (2004) found that the hydrolysate of treatment of egg white with pepsin exhibited strong angiotensin I-converting enzyme (ACE) inhibitory activity *in vitro* and oxygen radical absorbance capacity (ORAC) which could provide combined bioactivity against cardiovascular disease. Egg yolk protein enzymatic hydrolysates was reported to present superoxide, hydroxyl, and 1,1-diphenyl-2-picrylhydrazyl (DPPH) radical scavenging activities that inhibited the formation of TBARS in beef and tuna homogenates (Sakanaka & Tachibana, 2006). Another study on egg yolk protein showed an enhanced ORAC after bacterial proteases or trypsin hydrolyzing and ultrafiltration, especially the peptides of phosphoproteins that were separated from delipidated egg yolk protein with molecular weight lower than 5 kDa (Ting et al., 2011). Additionally, ultrafiltered ESM enzymatic hydrolysate fractions demonstrated a range of antioxidant activity including iron (Fe^{3+}) reducing, DPPH, hydroxyl radical scavenging, and Fe^{2+} chelating activity which were further verified to reduce proinflammatory cytokine IL-8 secretion in oxidative stress-

induced human intestinal epithelial Caco-2 cells (Shi, Kovacs-Nolan, et al., 2014a). Similarly, ESM enzymatic hydrolysates and corresponding identified synthetic peptides showed strong ability to quench ABTS, inhibit TBARS and high total antioxidant activity in a study by Zhao and coworkers (2019). In addition, cysteine was shown to possess a high antioxidant activity in hemoglobin oxidized linoleate emulsion owing to the presence of the sulfhydryl group (Taylor & Richardson, 1980). Likewise, cysteine-rich peptides derived from *Spirulina fusiformis* exhibited free radical scavenging capability and inhibited the ROS-induced DNA damage *in vitro* (Madhyastha & Vatsala, 2010). These arouse our interest to evaluate the antioxidant activity of CREMP-enriched PEM for biomedical applications.

Therefore, based on the above evidence and our proteomic results (Ahmed et al., 2017), we propose that the proteinaceous PEM and its hydrolysates have the potential to be an alternative antioxidant for biomedical applications. In this study, we firstly established an innovative eco-friendly method to produce multifunctional bioactive PEM for biomedical applications. Different sizes of PEM exhibited a significant antibacterial and anti-inflammatory activity for potential skin health applications. Then, in this chapter, we evaluated the antioxidant activity of PEM and established a new method to enhance its antioxidant potency by alkaline hydrolysis.

The CUPRAC method is an electron-transfer-based antioxidant capacity assay utilizing the copper(II)-neocuproine [Cu(II)-Nc] reagent as a chromogenic oxidizing agent that was first established by Apak and colleagues in 2004. Since then, the CUPRAC method has been improved and widely applied in many antioxidant assays, which is comparable with other antioxidant measurements such as ABTS and DPPH methods using Trolox equivalent (TEAC) as a reference (Apak et al., 2008; Bursal & Gülçin, 2011; Özyürek et al., 2011; Usal & Sahan,

2020). Among other electron-transfer-based assays [e.g., Folin-Ciocalteu (FCR), ferric reducing antioxidant potency (FRAP), 2,2'-azino-bis(3-ethylbenzothiazoline-6-sulfonic acid) (ABTS), DPPH], CUPRAC is superior because of its physiological pH, favourable redox capability, accessibility and stability of reagents, and applicability to lipophilic/ hydrophilic antioxidants (Apak et al., 2008; Özyürek et al., 2011).

Firstly, we evaluated the total antioxidant activity of five size ranges PEM and found out that PEM exhibited a dose-dependent activity, and particularly, PEM 104-381 μ m showed the strongest specific antioxidant activity approximately 311 μ M TE/g protein (Figure 7-1.). However, due to the presence of insoluble components in PEM, we had to modify the assay to subtract the background turbidity in the cupric reducing assay solution. But after a prolonged reaction study, we observed that a majority of the yellow colour (high reducing reaction) came from insoluble particles rather than the supernatant. Thereby, this explained the impaired total antioxidant activity of PEM especially for smaller sizes (<15 and <53 μ m) which used to exhibit significant antibacterial and anti-inflammatory activities among five sizes.

Thus, we recognized that the intractable structural proteins in PEM such as CREMPs and the disulfide bonds hindered the multifunctional application of PEM due to its low solubility. Therefore, we established a top-down method to produce soluble bioactive hydrolysates/ peptides from PEM, namely PEM-H.

Many hydrolysis conditions for ESM have been evaluated by researchers, which can be classified as chemical, enzymatic or combined hydrolysis. Acidic hydrolysis was first reported in 1994 when Arai patented a method to solubilize ESM with 3-MPA at 80 °C (Arai, 1994). After this, acid hydrolysis conditions have been evaluated to hydrolyze ESM, including aqueous 3-MPA in the presence of acetic acid (Ahmed, Suso, & Hincke, 2019; Yi et al., 2003), methanol in

the presence of acetic acid, and guanidine hydrochloride (GuHCl) / EDTA / sodium acetate, pH 5.8 (Makkar et al., 2015). Alkaline hydrolysis conditions have also been explored (Ahmed, Suso, & Hincke, 2019; Y. Liu et al., 2014). An alkaline water-containing organic solvent [NaOH or potassium hydroxide (KOH) mixed with one of isopropanol, methanol, ethanol, acetone, n-propanol] was applied to solubilized-ESM at 30-60 °C for 8-11 hours (Giry et al., 1989). Similarly, Li (1995) reported a method to extract ESM by 5% (1.25 N) NaOH and ethanol at 50-60 °C for 2-3 hours. A company, Biova LLC (Johnston, IA, USA), patented a process to digest ESM by 5 % NaOH between 35-65 °C for 3-24 h which was then oxidized using H₂O₂ after molecular membrane filtration (Strohbehn et al., 2010). They also produced a product called water-soluble eggshell membrane (WSEM) by dissolving ESM in an alkaline solution (pH 10.5-11.5, NaOH, KOH, or calcium hydroxide) at 50 °C (Jensen et al., 2016; Strohbehn & Figgins, 2012). Kewpie Cooperation (Tokyo) patented a method to digest the heat sterilized (90 °C) ESM powder with an alkaline solution (preferably NaOH) at 90 °C (Hasebe et al., 2018; Matsuoka et al., 2019; Ohto-Fujita et al., 2011). Other chemical methods have been adopted to dissolve processed ESM powder, such as lithium dodecyl sulfate/dithiothreitol (LDS/DTT) (Ahmed, Suso, & Hincke, 2019) or digesting ESM through H₂O₂ oxidation (Y. Liu et al., 2014).

Enzymatic hydrolysis of ESM also attracted plenty of interest to produce bioactive peptides. Various types of enzymes have been utilized to digest ESM including Alcalase, trypsin, neutrase, caroid and pepsin (Huang et al., 2010), serine endopeptidase (Tanaka, 2013), alkali protease (Y. Liu et al., 2014), protease S (Shi, Kovacs-Nolan, et al., 2014b), and papain (Ürgeová & Vulganová, 2016). With slight modification, Kewpie Cooperation digested ESM powder using alkaline protease (Matsuoka et al., 2019). In addition, ESM protein hydrolysates were produced following fermentation with *Lactobacillus plantarum* by Jain and Anal (2018).

Researchers also combined physical, chemical and enzymatic methods to hydrolyze insoluble ESM. Takahashi et al. (1996) obtained SEP from pulverized ESM using performic acid (PFA) to oxidative cleave the disulfide bonds, followed by pepsin digestion (Ino et al., 2006; Takahashi et al., 1996). Functional ESM hydrolysates could be produced by ultrasonic-assisted extraction using Alcalase and papain (Jain & Anal, 2016), NaOH (Marcet et al., 2018), or urea/ammonium bicarbonate (Ahmed, Suso, & Hincke, 2019) hydrolysis. Solubilized by 3-MPA in the presence of acetic acid, the extracted ESM proteins were hydrolyzed by Alcalase, viscozyme L and protease (from *Bacillus amyloliquefaciens*) (Santana et al., 2016). ESM hydrolysates were extracted with acidified methanol and GuHCl (containing EDTA) and then subjected to reduction/alkylation followed by a final trypsin digestion (Rath et al., 2016). Na₂SO₃-assisted ESM protease hydrolysis was also practiced using alkaline protease, pepsin, chymotrypsin, neutral protease, and papain by Zhao and colleague (2019).

Regarding the above bioprocesses, we propose that the NaOH is a suitable solvent to directly hydrolyze the PEP under 50 °C with low cost and less impairment of the ESM component. Because the removal of sulfur odour (sulfur group) using oxidizing agent H₂O₂ might compromise the cysteine disulfide bonds component (Strohbehn et al., 2010). And it has been pointed out that high digestion temperature (>43 °C), especially approaching 90 °C, can lead to irreversible denaturation and loss of ESM protein (Mackay & Chilkoti, 2008; Schön et al., 2017). What is more, limitations of enzymatic hydrolysis including the regulation of enzyme denaturation, access of enzyme to substrate, functional parameter of temperature and pH, can be hard to overcome at an industrial scale (Khueychai et al., 2019). On the other hand, acid hydrolysis may destroy tryptophan, and partially degrade cystine, serine, and threonine, or convert asparagine and glutamine residues to their acid versions.

Thus, in my study, I employed NaOH solution as hydrolyzing solvent to evaluate the effect on five size ranges of PEM under 50 °C. The reaction ratio between PEM and NaOH was optimized by comparing specific antioxidant activity of PEM-H<53 µm from 5 and 10 mg/mL (PEM<53 µm + 1.25 N NaOH, 1:1 v/v) reaction settings. As shown in Figure 7-2 **a**, the specific antioxidant activity of the 5 mg/mL reaction system was significantly increased to 630.13 µM TE/g protein, greater than the PEM<53 µm control (50.53 µM TE/g protein), and also higher than the PEM-H<53 µm from 10mg/mL reaction group which was 289.84 µM TE/g protein.

The massive increase in antioxidant activity from PEM<53 µm to PEM-H<53 µm could be attributed to the breakage of peptide bonds, cross-linkages and disulfide bonds in PEM, as well as the generation of small molecular weight soluble peptides which ultimately enhance the solvent accessibility of free radical scavenging and prooxidative metal-chelating amino acid residues (R. J. Elias et al., 2008). In fact, the most oxidatively reactive amino acids are favourably containing either nucleophilic sulfur-containing side chains (e.g., cysteine, methionine) or aromatic side chains (e.g., tryptophan, tyrosine, and phenylalanine), and or imidazole-containing side chain (e.g., histidine) where hydrogen is easily abstracted (R. J. Elias et al., 2008). This indicates that proteins/peptides could protect lipids from oxidation if they are preferentially oxidized to unsaturated fatty acids by interacting with free radicals or ROS. Preferential oxidation of proteins/peptides could occur when the amino acids are more oxidatively unstable than unsaturated fatty acids or other substrates, or when the physical location is near to free radical or ROS where the protein/peptide are able to quench the free radicals prior to the migration of the radical to lipids or other substrates. In addition to free radical scavenging, the antioxidant mechanism of protein/peptide can also derive from metal ion chelation, inactivation of ROS, hydroperoxide reduction, as well as aldehyde adduction.

ESM comprises cysteine, histidine, tryptophan, β -hydroxyl tryptophan (Huang et al., 2010; Yi et al., 2004), ovalbumin, ovotransferrin, and cystatin (Ahmed et al., 2017) that exhibit antioxidant activities (Nimalaratne et al., 2015; Uchida & Kawakishi, 1992), and CREMP which contains disulfide bonds and provides cysteine residues (Kodali et al., 2011). Therefore, we propose the hydrolysis of CREMPs and other ESM proteins contributed to the enhanced antioxidant activity of PEM-H.

However, the decline of total antioxidant activity of PEM-H < 53 μ m from 5 to 10 mg/mL can be ascribed to the kinetics of substrate consumption especially the accessibility between base and PEM. Thus, I selected the 5 mg/mL reaction system for further study so as to obtain the best antioxidant enhancement.

Next, I evaluated the specific antioxidant activities of PEM-H from various sizes PEM that were digested by 1.25 N NaOH after 24 h incubation at 37 °C. As illustrated in Figure 7-2b, PEM-Hs obtained from five sizes PEM exhibited a significant increase of antioxidant activity (at least $P < 0.001$ of each size) and demonstrated a size-dependent manner. Under these conditions, PEM-H < 15 and < 53 μ m showed the highest activity than the other three sizes of PEM-H with around 609.33 and 651.42 μ M TE/g protein. No significant difference was observed between PEM-H < 15 and < 53 μ m, so PEM-H < 53 μ m was selected for further analysis. This size-dependent antioxidant manner is similar to that of previously observed size-dependent antimicrobial activity. This suggests that we successfully increased the bioactivity of ESM and PEM and the top-down method to produce PEM is more favourable to obtain bioactive PEM-H than by direct hydrolysis from intact ESM.

The effects of hydrolyzing parameters including reaction time, base concentration and temperature on the total antioxidant activity and protein level of PEM-H were experimentally

evaluated, and their correlation with antioxidant index was assessed as well. The PEM<53 μm was hydrolyzed with 0.1, 0.3 and 1.25 N NaOH for up to 24 h at 37 and 50 °C. As shown in Figure 7-3 a) and c), the macroscopic turbidity changed under different hydrolysis conditions that indicated a distinctive hydrolysis phase for PEM<53 μm . The strongest TEAC levels for the soluble supernatant components produced at these two temperatures was achieved when the PEM-H<53 μm was hydrolyzed by 1.25 N NaOH for 24 h at 37 °C (499.66 μM TE) and 1.25 N NaOH for 6 h at 50 °C (575.68 μM TE). At these time points, the appearance of PEM-H<53 μm was pale yellow and clear.

Then, we assessed the specific antioxidant activity of PEM<53 μm by dividing the total activity by its associated protein concentration as shown in Figure 7-4. Interestingly, the specific antioxidant activity demonstrated a different profile as compared to the TEAC level (total antioxidant activity). As the highest specific antioxidant activity was achieved when PEM-H<53 μm was hydrolyzed by 1.25 N NaOH for 0.5 h at 37 °C (807.30 μM TE/g protein) and 0.1 N NaOH for 24 h at 50 °C (783.93 μM TE/g protein). To be noted, the huge jump of specific antioxidant activity of 1.25 N NaOH control groups was because of the low soluble protein concentration under these conditions. Thus, we were able to quantify the specific antioxidant activity in ESM hydrolysates for comparison to other sources. The specific antioxidant activity of PEM-H<53 μm (783.93 and 807.30 μM TE/g protein) was comparable to other antioxidants from the egg, such as egg yolk protein hydrolysates (720.5–867.8 μM TE/g protein) (Ting et al., 2011). But it was lower than the antioxidant activity reported for purified fractions from ESM hydrolysates, such as enzymatically hydrolyzed ESM (4400 μM TE/g hydrolyzed protein) (Santana et al., 2016) and Na₂SO₃-assisted protease hydrolyzed ESM (1725.1 μM ascorbic acid) (Zhao et al., 2019) [ascorbic acid shares similar TEAC as Trolox, (Marques et al., 2014)].

Therefore, this difference arouses the necessity for further steps to purify and identify PEM-H peptides and evaluate their individual antioxidant activity.

On the other hand, the hydrolysis time and NaOH concentration were positively correlated to TEAC level and specific antioxidant activity of PEM-H < 53 μm (Table 7-1). However, the temperature had no significant influence on these two indices which was in accord with the similar highest TEAC level and specific antioxidant activity of PEM-H obtained at 37 and 50 °C. Specifically, different temperatures (50°C and 37°C) could be compensated by elongated incubation time and increased NaOH concentration in order to achieve a similar hydrolysis effect.

ESM hydrolysates were reported with diverse bioactivities in several studies. For example, the ultrafiltered fractions of ESM hydrolysates (<5 kDa and 5-10 kDa) produced by enzyme alcalase and protease S possess increased antioxidant activity in human intestinal epithelial Caco-2 cells against oxidative damage (Shi, Kovacs-Nolan, et al., 2014b). Likewise, ESM hydrolysates were shown to inhibit pro-inflammatory cytokine IL-6 and anti-inflammatory cytokine IL-10 secretion *in vivo* (Shi, Rupa, et al., 2014). In another study, the alkaline water-miscible organic-solvent-hydrolyzed soluble eggshell membrane (ASESM) promoted the production of a young extracellular matrix (ECM) environment for human skin fibroblasts (HDF) *in vitro*, thereby facilitating the cell adhesion and wound healing process (Ohto-Fujita et al., 2011). Sodium hydroxide along with microbial fermented and enzymatically digested ESM presented a significant activation of NF- κ B in THP-1 cells (human leukemic monocyte), implying an enhanced immunomodulatory effect after hydrolysis (Ruff et al., 2015). Furthermore, concentrated peptides from ESM hydrolysate demonstrated a potential ability to

control cardiovascular diseases with high angiotensin-converting enzyme (ACE) and antioxidant activities (Santana et al., 2016).

In summary, we enhanced the antioxidant activity of PEM through alkaline hydrolysis with optimization of incubation time and base concentration. Further study is required to determine the amino acid and proteomic profile of PEM-H and its soluble peptides. The antioxidant activity needs to be confirmed by a more biologically relevant method both *in vitro* and *in vivo* (Jahandideh et al., 2016). As a potent antioxidant and bioactive ingredient, the multiple bioactivities of PEM-H worth to be studied for human health, such as the anti-hypertensive, antimicrobial, immune-modulating, anti-adhesive, antiviral and anticancer activities.

CHAPTER 8 CONCLUSIONS

This study describes a novel approach to upcycle environmental waste ESM by producing PEM in a submicron size range with enhanced solubility and bioavailability and provides a significant insight into the biomedical applications of PEM for skin health. In my study, the PEM demonstrated a dose- and size-dependent bacteriostatic effect against Gram-negative pathogen *E. coli* that enhanced the antimicrobial spectrum for PEM with our previous observations on *S. aureus* and *P. aeruginosa*. The PEM also displayed an effective anti-inflammatory activity against LPS-stimulated murine macrophages. Furthermore, the antioxidant activity of PEM was significantly improved by optimized alkaline hydrolysis with a size-dependent performance. Continued research with PEM and PEM-H can broaden our insight into their multifunctionality and *in vivo* behavior for human health applications. Eventually, we anticipate that this innovative ingredient will lead to new strategies to enrich topical cosmetics/skincare applications as well as pave a way forward for therapeutic alternatives for human health.

COPYRIGHTED CONTENT

Copyright and Trademark

Copyright

All rights regarding the reproduction of manuscripts, illustrations, and other materials presented in "Frontiers in Bioscience" are reserved and protected by the laws governing the copyright laws. The copyright laws provide exclusive right for reproduction and distribution of published materials. Apart from any personal use or for the purpose of review as permitted by the Copyright, Designs and Patent Act of 1988, this publication may not be reproduced, stored on microfilm or other electronic, optical or magnetic media or transmitted, in any form or by any means, without prior written permission of the Editorial Office of "Frontiers in Bioscience" in accordance with the terms of the licences issued by the Copyright Licensing agency. However, all individuals are free to access the information in this journal and print it for their personal use. The content of the journal should not be duplicated for purposes other than for personal use. For other uses, please contact the editorial office. The content of this journal or its individual components may not be altered or sold.

Trademark

"Frontiers in Bioscience" is the trademark of Frontiers in Bioscience, Inc. All rights reserved. Copyright © 1996-Present to the "Frontiers in Bioscience" by Dr S. Tabibzadeh. All rights reserved. No parts of this journal may be reproduced in any form or by any means without the prior written permission of the editorial office of "Frontiers in Bioscience."

SPRINGER NATURE LICENSE
TERMS AND CONDITIONS

Oct 28, 2020

This Agreement between Ling Wu ("You") and Springer Nature ("Springer Nature") consists of your license details and the terms and conditions provided by Springer Nature and Copyright Clearance Center.

License Number	4937990109018
License date	Oct 28, 2020
Licensed Content Publisher	Springer Nature
Licensed Content Publication	Nature Reviews Microbiology
Licensed Content Title	The skin microbiome
Licensed Content Author	Elizabeth A. Grice et al
Licensed Content Date	Mar 16, 2011
Type of Use	Thesis/Dissertation
Requestor type	academic/university or research institute
Format	print and electronic
Portion	figures/tables/illustrations
Number of figures/tables /illustrations	1
High-res required	no
Will you be translating?	no
Circulation/distribution	1 - 29
Author of this Springer Nature content	no
Title	Particalized eggshell membrane (PEM) for biomedical applications
Institution name	University of Ottawa
Expected presentation date	Nov 2020
Portions	Figure 1
Requestor Location	Ling Wu 451 Smyth Road Ottawa, ON K1H 8M5 Canada Attn: Miss Ling Wu
Total	0.00 CAD

ELSEVIER LICENSE
TERMS AND CONDITIONS

Oct 29, 2020

This Agreement between Ling Wu ("You") and Elsevier ("Elsevier") consists of your license details and the terms and conditions provided by Elsevier and Copyright Clearance Center.

License Number	4937870320495
License date	Oct 28, 2020
Licensed Content Publisher	Elsevier
Licensed Content Publication	Trends in Immunology
Licensed Content Title	Cutaneous Barriers and Skin Immunity: Differentiating A Connected Network
Licensed Content Author	Stefanie Eyerich,Kilian Eyerich,Claudia Traidl-Hoffmann,Tilo Biedermann
Licensed Content Date	Apr 1, 2018
Licensed Content Volume	39
Licensed Content Issue	4
Licensed Content Pages	13
Start Page	315
End Page	327
Type of Use	reuse in a thesis/dissertation
Portion	figures/tables/illustrations
Number of figures/tables /illustrations	1
Format	both print and electronic
Are you the author of this Elsevier article?	No
Will you be translating?	No
Title	Particalized eggshell membrane (PEM) for biomedical applications
Institution name	University of Ottawa
Expected presentation date	Nov 2020
Portions	Figure 1
Requestor Location	Ling Wu 451 Smyth Road Ottawa, ON K1H 8M5 Canada Attn: Miss Ling Wu
Publisher Tax ID	GB 494 6272 12
Total	0.00 CAD

Royal Society of Chemistry - License Terms and Conditions

This is a License Agreement between Ling Wu ("You") and Royal Society of Chemistry ("Publisher") provided by Copyright Clearance Center ("CCC"). The license consists of your order details, the terms and conditions provided by Royal Society of Chemistry, and the CCC terms and conditions.

All payments must be made in full to CCC.

Order Date	01-Nov-2020	Type of Use	Republish in a thesis/dissertation
Order license ID	1074335-1	Publisher	RSC Publishing
ISSN	2046-2069	Portion	Chart/graph/table/figure

LICENSED CONTENT

Publication Title	RSC advances	Publication Type	e-Journal
Article Title	Anti-inflammatory sesquiterpenes from the medicinal herb Tanacetum sinaicum	Start Page	44895
Date	01/01/2011	End Page	44901
Language	English	Issue	56
Country	United Kingdom of Great Britain and Northern Ireland	Volume	5
Rightsholder	Royal Society of Chemistry	URL	http://pubs.rsc.org/en/journals/journalss...

REQUEST DETAILS

Portion Type	Chart/graph/table/figure	Distribution	Worldwide
Number of charts / graphs / tables / figures requested	1	Translation	Original language of publication
Format (select all that apply)	Print, Electronic	Copies for the disabled?	No
Who will republish the content?	Academic institution	Minor editing privileges?	No
Duration of Use	Current edition and up to 5 years	Incidental promotional use?	No
Lifetime Unit Quantity	Up to 499	Currency	CAD
Rights Requested	Main product, any product related to main product, and other compilations/derivative products		

NEW WORK DETAILS

Title	Partalized eggshell membrane (PEM) for biomedical applications	Institution name	University of Ottawa
Instructor name	Maxwell Hincke	Expected presentation date	2020-11-06

ADDITIONAL DETAILS

Order reference number	N/A	The requesting person / organization to appear on the license	Ling Wu
------------------------	-----	---	---------

REUSE CONTENT DETAILS

Title, description or numeric reference of the portion(s)	Fig. 5	Title of the article/chapter the portion is from	Anti-inflammatory sesquiterpenes from the medicinal herb Tanacetum sinaicum
Editor of portion(s)	Hegazy, Mohamed-Elamir F.; Hamed, Ahmed R.; Mohamed, Tarik A.; Debbab, Abdessamad; Nakamura, Seikou; Matsuda, Hisashi; Paré, Paul W.	Author of portion(s)	Hegazy, Mohamed-Elamir F.; Hamed, Ahmed R.; Mohamed, Tarik A.; Debbab, Abdessamad; Nakamura, Seikou; Matsuda, Hisashi; Paré, Paul W.
Volume of serial or monograph	5	Issue, if republishing an article from a serial	56
Page or page range of portion	44895-44901	Publication date of portion	2015-01-01

Royal Society of Chemistry - License Terms and Conditions

This is a License Agreement between Ling Wu ("You") and Royal Society of Chemistry ("Publisher") provided by Copyright Clearance Center ("CCC"). The license consists of your order details, the terms and conditions provided by Royal Society of Chemistry, and the CCC terms and conditions.

All payments must be made in full to CCC.

Order Date	01-Nov-2020	Type of Use	Republish in a thesis/dissertation
Order license ID	1074334-1	Publisher	Royal Society of Chemistry
ISSN	2047-4830	Portion	Chart/graph/table/figure

LICENSED CONTENT

Publication Title	Biomaterials science	Rights holder	Royal Society of Chemistry
Article Title	A novel eco-friendly green approach to produce particalized eggshell membrane (PEM) for skin health applications.	Publication Type	Journal
Author/Editor	Kyoto Daigaku.Busshitsu-Saibō Tōgō Shisutemu Kyoten, Royal Society of Chemistry (Great Britain)	Start Page	5346
Date	01/01/2013	End Page	5361
Language	English	Issue	19
Country	United Kingdom of Great Britain and Northern Ireland	Volume	8

REQUEST DETAILS

Portion Type	Chart/graph/table/figure	Distribution	Worldwide
Number of charts / graphs / tables / figures requested	11	Translation	Original language of publication
Format (select all that apply)	Print, Electronic	Copies for the disabled?	No
Who will republish the content?	Academic institution	Minor editing privileges?	No
Duration of Use	Current edition and up to 5 years	Incidental promotional use?	No
Lifetime Unit Quantity	Up to 499	Currency	CAD
Rights Requested	Main product, any product related to main product, and other compilations/derivative products		

NEW WORK DETAILS

Title	Particalized eggshell membrane (PEM) for biomedical applications	Institution name	University of Ottawa
Instructor name	Maxwell Hincke	Expected presentation date	2020-11-06

ADDITIONAL DETAILS

Order reference number	N/A	The requesting person / organization to appear on the license	Ling Wu
------------------------	-----	---	---------

REUSE CONTENT DETAILS

Title, description or numeric reference of the portion(s)	Fig. 2; Fig.3; Table 2; Fig.4; Fig. 7; Fig.8; TableS1; Table S2; Table S3; Table S4; Figure S1	Title of the article/chapter the portion is from	A novel eco-friendly green approach to produce particalized eggshell membrane (PEM) for skin health applications.
Editor of portion(s)	Hincke, Maxwell T; Diep, Ty; Wu, Ling; Ahmed, Tamer A E; Kulshreshtha, Garima	Author of portion(s)	Hincke, Maxwell T; Diep, Ty; Wu, Ling; Ahmed, Tamer A E; Kulshreshtha, Garima
Volume of serial or monograph	8	Issue, if republishing an article from a serial	19
Page or page range of portion	5346-5361	Publication date of portion	2020-08-28

ELSEVIER LICENSE
TERMS AND CONDITIONS

Oct 29, 2020

This Agreement between Ling Wu ("You") and Elsevier ("Elsevier") consists of your license details and the terms and conditions provided by Elsevier and Copyright Clearance Center.

License Number	4937990900675
License date	Oct 28, 2020
Licensed Content Publisher	Elsevier
Licensed Content Publication	Journal of Proteomics
Licensed Content Title	In-depth comparative analysis of the chicken eggshell membrane proteome
Licensed Content Author	Tamer A.E. Ahmed, Henri-Pierre Suso, Maxwell T. Hincke
Licensed Content Date	Feb 23, 2017
Licensed Content Volume	155
Licensed Content Issue	n/a
Licensed Content Pages	14
Start Page	49
End Page	62
Type of Use	reuse in a thesis/dissertation
Portion	figures/tables/illustrations
Number of figures/tables /illustrations	1
Format	both print and electronic
Are you the author of this Elsevier article?	No
Will you be translating?	No
Title	Partalized eggshell membrane (PEM) for biomedical applications
Institution name	University of Ottawa
Expected presentation date	Nov 2020
Portions	Table 3
Requestor Location	Ling Wu 451 Smyth Road Ottawa, ON K1H 8M5 Canada Attn: Miss Ling Wu
Publisher Tax ID	GB 494 6272 12
Total	0.00 CAD

REFERENCES

- Afolabi, O. A., Salaudeen, A. G., Ologe, F. E., Nwabuisi, C., & Nwawolo, C. C. (2012). Pattern of bacterial isolates in the middle ear discharge of patients with chronic suppurative otitis media in a tertiary hospital in north central Nigeria. *African Health Sciences*.
<https://doi.org/10.4314/ahs.v12i3.18>
- Ageitos, J. M., Sánchez-Pérez, A., Calo-Mata, P., & Villa, T. G. (2017). Antimicrobial peptides (AMPs): Ancient compounds that represent novel weapons in the fight against bacteria. *Biochemical Pharmacology*, *133*, 117–138. <https://doi.org/10.1016/j.bcp.2016.09.018>
- Aguirre, A., Gil-Quintana, E., Fenaux, M., Erdozain, S., & Sarria, I. (2017). Beneficial Effects of Oral Supplementation With Ovoderm on Human Skin Physiology: Two Pilot Studies. *Journal of Dietary Supplements*, *14*(6), 706–714.
<https://doi.org/10.1080/19390211.2017.1310781>
- Ahlborn, G., & Sheldon, B. W. (2005). Enzymatic and microbiological inhibitory activity in eggshell membranes as influenced by layer strains and age and storage variables. *Poultry Science*, *84*(12), 1935–1941. <https://doi.org/10.1093/ps/84.12.1935>
- Ahmadinejad, F., Geir Møller, S., Hashemzadeh-Chaleshtori, M., Bidkhorji, G., & Jami, M.-S. (2017). Molecular Mechanisms behind Free Radical Scavengers Function against Oxidative Stress. *Antioxidants*, *6*(3), 51. <https://doi.org/10.3390/antiox6030051>
- Ahmed, T. A. E., Suso, H.-P., & Hincke, M. T. (2017). In-depth comparative analysis of the chicken eggshell membrane proteome. *Journal of Proteomics*, *155*, 49–62.
<https://doi.org/10.1016/j.jprot.2017.01.002>
- Ahmed, T. A. E., Suso, H.-P., & Hincke, M. T. (2019). Experimental datasets on processed eggshell membrane powder for wound healing. *Data in Brief*, *26*, 104457.

<https://doi.org/10.1016/j.dib.2019.104457>

Ahmed, T. A. E., Suso, H.-P., Maqbool, A., & Hincke, M. T. (2019). Processed eggshell membrane powder: Bioinspiration for an innovative wound healing product. *Materials Science and Engineering: C*, 95(July 2018), 192–203.

<https://doi.org/10.1016/j.msec.2018.10.054>

Akagawa, M., Wako, Y., & Suyama, K. (1999). Lysyl oxidase coupled with catalase in egg shell membrane. *Biochimica et Biophysica Acta - Protein Structure and Molecular Enzymology*.

[https://doi.org/10.1016/S0167-4838\(99\)00169-7](https://doi.org/10.1016/S0167-4838(99)00169-7)

Amundsen, S., Utgård, B., & Henri-Pierre, S. (2016). Method of processing eggshell residues (Patent No. US20160249666A1). In *Google Patents* (US20160249666A1).

Andersen, C. (2015). Bioactive Egg Components and Inflammation. *Nutrients*, 7(9), 7889–7913.

<https://doi.org/10.3390/nu7095372>

Apak, R., Güçlü, K., Özyürek, M., & Çelik, S. E. (2008). Mechanism of antioxidant capacity assays and the CUPRAC (cupric ion reducing antioxidant capacity) assay. *Microchimica Acta*, 160(4), 413–419. <https://doi.org/10.1007/s00604-007-0777-0>

Apak, R., Güçlü, K., Özyürek, M., & Karademir, S. E. (2004). Novel Total Antioxidant Capacity Index for Dietary Polyphenols and Vitamins C and E, Using Their Cupric Ion Reducing Capability in the Presence of Neocuproine: CUPRAC Method. *Journal of Agricultural and Food Chemistry*, 52(26), 7970–7981. <https://doi.org/10.1021/jf048741x>

Apel, K., & Hirt, H. (2004). Reactive oxygen species: Metabolism, oxidative stress, and signal transduction. *Annual Review of Plant Biology*, 55, 373–399.

<https://doi.org/10.1146/annurev.arplant.55.031903.141701>

Arai, K. (1994). *Production of re-formed egg shell membrane* (Patent No. JPH06192443A).

- Arias, J. L., Fernandez, M. S., Dennis, J. E., & Caplan, A. I. (1991). Collagens of the chicken eggshell membranes. *Connective Tissue Research*.
<https://doi.org/10.3109/03008209109152162>
- Arulseivan, P., Fard, M. T., Tan, W. S., Gothai, S., Fakurazi, S., Norhaizan, M. E., & Kumar, S. S. (2016). Role of Antioxidants and Natural Products in Inflammation. In *Oxidative Medicine and Cellular Longevity*. <https://doi.org/10.1155/2016/5276130>
- Baker, R. G., Hayden, M. S., & Ghosh, S. (2011). NF- κ B, inflammation, and metabolic disease. In *Cell Metabolism* (Vol. 13, Issue 1, pp. 11–22).
<https://doi.org/10.1016/j.cmet.2010.12.008>
- Baláž, M. (2014). Eggshell membrane biomaterial as a platform for applications in materials science. *Acta Biomaterialia*, 10(9), 3827–3843. <https://doi.org/10.1016/j.actbio.2014.03.020>
- Baláž, M., Daneu, N., Balážová, L., Dutková, E., Tkáčiková, L., Briančin, J., Vargová, M., Balážová, M., Zorkovská, A., & Baláž, P. (2017). Bio-mechanochemical synthesis of silver nanoparticles with antibacterial activity. *Advanced Powder Technology*, 28(12), 3307–3312.
<https://doi.org/10.1016/j.appt.2017.09.028>
- Battersby, A. J., Khara, J., Wright, V. J., Levy, O., & Kampmann, B. (2016). Antimicrobial Proteins and Peptides in Early Life: Ontogeny and Translational Opportunities. *Frontiers in Immunology*, 7. <https://doi.org/10.3389/fimmu.2016.00309>
- Benson, K., Newman, R., & Jensen, G. (2016). Water-soluble egg membrane enhances the immunoactivating properties of an Aloe vera-based extract of Nerium oleander leaves. *Clinical, Cosmetic and Investigational Dermatology*, Volume 9, 393–403.
<https://doi.org/10.2147/CCID.S114471>
- Berridge, M. J., Lipp, P., & Bootman, M. D. (2000). The versatility and universality of calcium

- signalling. In *Nature Reviews Molecular Cell Biology* (Vol. 1, Issue 1, pp. 11–21).
European Association for Cardio-Thoracic Surgery. <https://doi.org/10.1038/35036035>
- Bickers, D. R., & Athar, M. (2006). Oxidative stress in the pathogenesis of skin disease. *Journal of Investigative Dermatology*, *126*(12), 2565–2575. <https://doi.org/10.1038/sj.jid.5700340>
- Birben, E., Sahiner, U. M., Sackesen, C., Erzurum, S., & Kalayci, O. (2012). Oxidative Stress and Antioxidant Defense. *World Allergy Organization Journal*, *5*(1), 9–19.
<https://doi.org/10.1097/WOX.0b013e3182439613>
- Boscá, L., Zeini, M., Través, P. G., & Hortelano, S. (2005). Nitric oxide and cell viability in inflammatory cells: A role for NO in macrophage function and fate. *Toxicology*, *208*(2), 249–258. <https://doi.org/10.1016/j.tox.2004.11.035>
- Bosch, A. A. T. M., Biesbroek, G., Trzcinski, K., Sanders, E. A. M., & Bogaert, D. (2013). Viral and Bacterial Interactions in the Upper Respiratory Tract. In *PLoS Pathogens*.
<https://doi.org/10.1371/journal.ppat.1003057>
- Bursal, E., & Gülçin, I. (2011). Polyphenol contents and in vitro antioxidant activities of lyophilised aqueous extract of kiwifruit (*Actinidia deliciosa*). *Food Research International*, *44*(5), 1482–1489. <https://doi.org/10.1016/j.foodres.2011.03.031>
- Cannavò, S. P., Tonacci, A., Bertino, L., Marco, C., Francesco, B., & Gangemi, S. (2018). The role of oxidative stress in the biology of melanoma: a systematic review. *Pathology - Research and Practice*, *215*(October 2018), 21–28.
<https://doi.org/https://doi.org/10.1016/j.prp.2018.11.020>
- Celia, C., Trapasso, E., Locatelli, M., Navarra, M., Ventura, C. A., Wolfram, J., Carafa, M., Morittu, V. M., Britti, D., Di Marzio, L., & Paolino, D. (2013). Anticancer activity of liposomal bergamot essential oil (BEO) on human neuroblastoma cells. *Colloids and*

- Surfaces B: Biointerfaces*, 112, 548–553. <https://doi.org/10.1016/j.colsurfb.2013.09.017>
- Chen, Y. E., & Tsao, H. (2013). The skin microbiome: Current perspectives and future challenges. *Journal of the American Academy of Dermatology*, 69(1), 143-155.e3. <https://doi.org/10.1016/j.jaad.2013.01.016>
- Chi, Y., Wang, Y., Li, M. F., Ren, J., & Chi, Y. J. (2019). Numerical simulation and experimental study on eggshell membrane separation device. *International Journal of Agricultural and Biological Engineering*, 12(2), 173–183. <https://doi.org/10.25165/j.ijabe.20191202.3058>
- Chiller, K., Selkin, B. A., & Murakawa, G. J. (2001). Skin microflora and bacterial infections of the skin. *Journal of Investigative Dermatology Symposium Proceedings*. <https://doi.org/10.1046/j.0022-202x.2001.00043.x>
- Chiu, J., & Hogg, P. J. (2019). *Allosteric disulfides: Sophisticated molecular structures enabling flexible protein regulation*. <https://doi.org/10.1074/jbc.REV118.005604>
- Conner, E. M., & Grisham, M. B. (1996). Inflammation, free radicals and antioxidants. *Nutrition*, 12(4), 274–277. [https://doi.org/10.1016/S0899-9007\(96\)00000-8](https://doi.org/10.1016/S0899-9007(96)00000-8)
- Cordeiro, C. M. M., Esmaili, H., Ansah, G., & Hincke, M. T. (2013). Ovocalyxin-36 is a pattern recognition protein in chicken eggshell membranes. *PLoS ONE*, 8(12), 1–13. <https://doi.org/10.1371/journal.pone.0084112>
- Cordeiro, C. M. M., & Hincke, M. T. (2011). Recent Patents on Eggshell: Shell and Membrane Applications. *Recent Patents on Food, Nutrition & Agriculture*, 3(1), 1–8. <https://doi.org/10.2174/2212798411103010001>
- Cuperus, T., Coorens, M., van Dijk, A., & Haagsman, H. P. (2013). Avian host defense peptides. *Developmental & Comparative Immunology*, 41(3), 352–369.

<https://doi.org/10.1016/j.dci.2013.04.019>

Daengprok, W., Garnjanagoonchorn, W., & Mine, Y. (2002). Fermented pork sausage fortified with commercial or hen eggshell calcium lactate. *Meat Science*, *62*(2), 199–204.

[https://doi.org/10.1016/S0309-1740\(01\)00247-9](https://doi.org/10.1016/S0309-1740(01)00247-9)

Dávalos, A., Miguel, M., Bartolomé, B., & López-Fandiño, R. (2004). Antioxidant activity of peptides derived from egg white proteins by enzymatic hydrolysis. *Journal of Food Protection*, *67*(9), 1939–1944. <https://doi.org/10.4315/0362-028X-67.9.1939>

de Koning, H. D., Simon, A., Zeeuwen, P. L. J. M., & Schalkwijk, J. (2012). Pattern recognition receptors in infectious skin diseases. In *Microbes and Infection*.

<https://doi.org/10.1016/j.micinf.2012.03.004>

De Reu, K., Grijspeerdt, K., Messens, W., Heyndrickx, M., Uyttendaele, M., Debevere, J., & Herman, L. (2006). Eggshell factors influencing eggshell penetration and whole egg contamination by different bacteria, including *Salmonella enteritidis*. *International Journal of Food Microbiology*. <https://doi.org/10.1016/j.ijfoodmicro.2006.04.011>

Denamur, E., Clermont, O., Bonacorsi, S., & Gordon, D. (2020). The population genetics of pathogenic *Escherichia coli*. *Nature Reviews Microbiology*. <https://doi.org/10.1038/s41579-020-0416-x>

Denlinger, L. C., Fiset, P. L., Garis, K. A., Kwon, G., Vazquez-Torres, A., Simon, A. D., Nguyen, B., Proctor, R. A., Bertics, P. J., & Corbett, J. A. (1996). Regulation of inducible nitric oxide synthase expression by macrophage purinoreceptors and calcium. *Journal of Biological Chemistry*, *271*(1), 337–342. <https://doi.org/10.1074/jbc.271.1.337>

DeVore, D. P., & Long, F. D. (2013). Anti-inflammatory activity of eggshell membrane and processed eggshell membrane preparations (Patent No. US 8580315 B2). In *New York* (US

8580315 B2).

Dröge, W. (2002). Free Radicals in the Physiological Control of Cell Function. *Physiological Reviews*, 82(1), 47–95. <https://doi.org/10.1152/physrev.00018.2001>

Dröge, W. (2005). Oxidative stress and ageing: is ageing a cysteine deficiency syndrome? *Philosophical Transactions of the Royal Society B: Biological Sciences*, 360(1464), 2355–2372. <https://doi.org/10.1098/rstb.2005.1770>

Du, J., Hincke, M. T., Rose-Martel, M., Hennequet-Antier, C., Brionne, A., Cogburn, L. A., Nys, Y., & Gautron, J. (2015). Identifying specific proteins involved in eggshell membrane formation using gene expression analysis and bioinformatics. *BMC Genomics*, 16(1), 1–13. <https://doi.org/10.1186/s12864-015-2013-3>

Egg Farmers of Canada. (2020a). 2019 Annual Report. In *Egg Farmers of Canada*.

Egg Farmers of Canada. (2020b). *Canadian egg production*. Egg Farmers of Canada. <https://www.eggfarmers.ca/market-information-tables/#tableau-3>

Elias, P. M. (2007). The skin barrier as an innate immune element. *Seminars in Immunopathology*, 29(1), 3–14. <https://doi.org/10.1007/s00281-007-0060-9>

Elias, R. J., Kellerby, S. S., & Decker, E. A. (2008). Antioxidant Activity of Proteins and Peptides. *Critical Reviews in Food Science and Nutrition*, 48(5), 430–441. <https://doi.org/10.1080/10408390701425615>

Elmarakby, A. A., Pollock, D. M., & Imig, J. D. (2006). Renal dysfunction in hypertension and obesity. In *Comprehensive Medicinal Chemistry II* (Vol. 6, pp. 575–595). Elsevier Ltd. <https://doi.org/10.1016/b0-08-045044-x/00187-5>

Elsholz, F., Harteneck, C., Muller, W., & Friedland, K. (2014). Calcium - A central regulator of keratinocyte differentiation in health and disease. In *European Journal of Dermatology*.

<https://doi.org/10.1684/ejd.2014.2452>

- Eyerich, S., Eyerich, K., Traidl-Hoffmann, C., & Biedermann, T. (2018). Cutaneous Barriers and Skin Immunity: Differentiating A Connected Network. *Trends in Immunology*, 39(4), 315–327. <https://doi.org/10.1016/j.it.2018.02.004>
- Farjah, G. H., Heshmatian, B., Karimipour, M., & Saberi, A. (2013). Using eggshell membrane as nerve guide channels in peripheral nerve regeneration. *Iranian Journal of Basic Medical Sciences*. <https://doi.org/10.22038/ijbms.2013.1347>
- Fernandez, M. S., Moya, A., Lopez, L., & Arias, J. L. (2001). Secretion pattern, ultrastructural localization and function of extracellular matrix molecules involved in eggshell formation. *Matrix Biology*, 19(8), 793–803. [https://doi.org/10.1016/S0945-053X\(00\)00128-1](https://doi.org/10.1016/S0945-053X(00)00128-1)
- Finkel, T., & Holbrook, N. J. (2000). Oxidants, oxidative stress and the biology of ageing. *Nature*, 408(6809), 239–247. <https://doi.org/10.1038/35041687>
- Flores-Mireles, A. L., Walker, J. N., Caparon, M., & Hultgren, S. J. (2015). Urinary tract infections: Epidemiology, mechanisms of infection and treatment options. In *Nature Reviews Microbiology*. <https://doi.org/10.1038/nrmicro3432>
- Frantz, C., Stewart, K. M., & Weaver, V. M. (2010). The extracellular matrix at a glance. In *Journal of Cell Science*. <https://doi.org/10.1242/jcs.023820>
- Gautron, J., Hincke, M. T., Mann, K., Panhéleux, M., Bain, M., McKee, M. D., Solomon, S. E., & Nys, Y. (2001). Ovocalyxin-32, a Novel Chicken Eggshell Matrix Protein. *Journal of Biological Chemistry*, 276(42), 39243–39252. <https://doi.org/10.1074/jbc.M104543200>
- Gautron, J., Hincke, M. T., Panheleux, M., Garcia-Ruiz, J. M., Boldicke, T., & Nys, Y. (2001). Ovotransferrin is a Matrix Protein of the Hen Eggshell Membranes and Basal Calcified Layer. *Connective Tissue Research*, 42(4), 255–267.

<https://doi.org/10.3109/03008200109016840>

- Gautron, J., Murayama, E., Vignal, A., Morisson, M., McKee, M. D., Réhault, S., Labas, V., Belghazi, M., Vidal, M.-L., Nys, Y., & Hincke, M. T. (2007). Cloning of Ovocalyxin-36, a Novel Chicken Eggshell Protein Related to Lipopolysaccharide-binding Proteins, Bactericidal Permeability-increasing Proteins, and Plunc Family Proteins. *Journal of Biological Chemistry*, 282(8), 5273–5286. <https://doi.org/10.1074/jbc.M610294200>
- Gautron, J., Réhault-Godbert, S., Pascal, G., Nys, Y., & Hincke, M. T. (2011). Ovocalyxin-36 and other LBP/BPI/PLUNC-like proteins as molecular actors of the mechanisms of the avian egg natural defences. *Biochemical Society Transactions*, 39(4), 971–976. <https://doi.org/10.1042/BST0390971>
- Geoghegan, J. A., Irvine, A. D., & Foster, T. J. (2018). Staphylococcus aureus and Atopic Dermatitis: A Complex and Evolving Relationship. *Trends in Microbiology*, 26(6), 484–497. <https://doi.org/10.1016/j.tim.2017.11.008>
- Gharibi, H., & Abdolmaleki, A. (2018). Thermo-chemical modification of a natural biomembrane to induce mucoadhesion, pH sensitivity and anisotropic mechanical properties. *Journal of the Mechanical Behavior of Biomedical Materials*, 87(July), 50–58. <https://doi.org/10.1016/j.jmbbm.2018.07.014>
- Giry, V., Horiki, S., & Watanabe, K. (1989). *Manufacturing method of soluble eggshell membrane* (Patent No. JPH0621047B2).
- Glatz, P., & Miao, Z. (2009). High value products from hatchery waste. In *RIRDC* (Issue 09). RIRDC.
- Gong, D., Wilson, P. W., Bain, M. M., McDade, K., Kalina, J., Hervé-Grépinet, V., Nys, Y., & Dunn, I. C. (2010). Gallin; an antimicrobial peptide member of a new avian defensin

- family, the ovodefensins, has been subject to recent gene duplication. *BMC Immunology*, 11(1), 12. <https://doi.org/10.1186/1471-2172-11-12>
- Gonzalez, T., Biagini Myers, J. M., Herr, A. B., & Khurana Hershey, G. K. (2017). Staphylococcal Biofilms in Atopic Dermatitis. *Current Allergy and Asthma Reports*, 17(12), 81. <https://doi.org/10.1007/s11882-017-0750-x>
- Gordon, Y. J., Romanowski, E. G., & McDermott, A. M. (2005). Mini review: A review of antimicrobial peptides and their therapeutic potential as anti-infective drugs. In *Current Eye Research*. <https://doi.org/10.1080/02713680590968637>
- Gribbon, E. M., Cunliffe, W. J., & Holland, K. T. (1993). Interaction of *Propionibacterium acnes* with skin lipids in vitro. *Journal of General Microbiology*, 139(8), 1745–1751. <https://doi.org/10.1099/00221287-139-8-1745>
- Grice, E. A., Kong, H. H., Conlan, S., Deming, C. B., Davis, J., Young, A. C., Bouffard, G. G., Blakesley, R. W., Murray, P. R., Green, E. D., Turner, M. L., & Segre, J. A. (2009). Topographical and temporal diversity of the human skin microbiome. *Science*, 324(5931), 1190–1192. <https://doi.org/10.1126/science.1171700>
- Grice, E. A., & Segre, J. A. (2011). The skin microbiome. *Nature Reviews Microbiology*, 9(4), 244–253. <https://doi.org/10.1038/nrmicro2537>
- Grimble, R. F. (1999). Nutritional influences on inflammation. *Nestlé Nutrition Workshop Series. Clinical & Performance Programme*, 2, 63–81. <https://doi.org/10.1159/000061795>
- Guyot, N., Meudal, H., Trapp, S., Iochmann, S., Silvestre, A., Jousset, G., Labas, V., Reverdiau, P., Loth, K., Hervé, V., Aucagne, V., Delmas, A. F., Rehault-Godbert, S., & Landon, C. (2020). Structure, function, and evolution of Gga -AvBD11, the archetype of the structural avian-double- β -defensin family. *Proceedings of the National Academy of Sciences*, 117(1),

337–345. <https://doi.org/10.1073/pnas.1912941117>

Hambleton, J., Weinstein, S. L., Lem, L., & Defranco, A. L. (1996). Activation of c-Jun N-terminal kinase in bacterial lipopolysaccharide-stimulated macrophages. *Proceedings of the National Academy of Sciences of the United States of America*.

<https://doi.org/10.1073/pnas.93.7.2774>

Harper, J. C. (2020). Acne vulgaris: What's new in our 40th year. *Journal of the American Academy of Dermatology*, 82(2), 526–527. <https://doi.org/10.1016/j.jaad.2019.01.092>

Hasebe, Y. (2013). *Micro-powder containing eggshell membrane, tablet, preparation method for micro-powder containing eggshell membrane and preparation method for tablet* (Patent No. CN103300357A).

Hasebe, Y., Atomi, J., & Shimizu, M. (2018). *Hydrolyzed eggshell membrane powder and method for producing the same* (Patent No. JP6410229B2).

Hegazy, M.-E. F., Hamed, A. R., Mohamed, T. A., Debbab, A., Nakamura, S., Matsuda, H., & Paré, P. W. (2015). Anti-inflammatory sesquiterpenes from the medicinal herb *Tanacetum sinaicum*. *RSC Advances*, 5(56), 44895–44901. <https://doi.org/10.1039/C5RA07511D>

Hervé-Grépinet, V., Réhault-Godbert, S., Labas, V., Magallon, T., Derache, C., Lavergne, M., Gautron, J., Lalmanach, A.-C., & Nys, Y. (2010). Purification and Characterization of Avian β -Defensin 11, an Antimicrobial Peptide of the Hen Egg. *Antimicrobial Agents and Chemotherapy*, 54(10), 4401–4409. <https://doi.org/10.1128/AAC.00204-10>

Hervé, V., Meudal, H., Labas, V., Réhault-Godbert, S., Gautron, J., Berges, M., Guyot, N., Delmas, A. F., Nys, Y., & Landon, C. (2014). Three-dimensional NMR Structure of Hen Egg Gallin (Chicken Ovodefensin) Reveals a New Variation of the β -Defensin Fold. *Journal of Biological Chemistry*, 289(10), 7211–7220.

<https://doi.org/10.1074/jbc.M113.507046>

- Hincke, M. T., Gautron, J., Panheleux, M., Garcia-Ruiz, J., McKee, M. ., & Nys, Y. (2000). Identification and localization of lysozyme as a component of eggshell membranes and eggshell matrix. *Matrix Biology*, *19*(5), 443–453. [https://doi.org/10.1016/S0945-053X\(00\)00095-0](https://doi.org/10.1016/S0945-053X(00)00095-0)
- Hincke, M. T., Nys, Y., Gautron, J., Mann, K., Rodriguez-Navarro, A. B., & McKee, M. D. (2012). The eggshell: Structure, composition and mineralization. *Frontiers in Bioscience*, *17*(4), 1266–1280. <https://doi.org/10.2741/3985>
- Hirata, A., Iwakiri, R., & Okinami, S. (2013). A simulated eye for vitreous surgery using Japanese quail eggs. *Graefe's Archive for Clinical and Experimental Ophthalmology*. <https://doi.org/10.1007/s00417-012-2247-6>
- Hirsch, J. G. (1958). Bactericidal action of histone. *Journal of Experimental Medicine*, *108*(6), 925–944. <https://doi.org/10.1084/jem.108.6.925>
- Hogg, P. J. (2003). Disulfide bonds as switches for protein function. *Trends in Biochemical Sciences*, *28*(4), 210–214. [https://doi.org/10.1016/S0968-0004\(03\)00057-4](https://doi.org/10.1016/S0968-0004(03)00057-4)
- Hommel, D. W., Peppelenbosch, M. P., & Van Deventer, S. J. H. (2003). Mitogen activated protein (MAP) kinase signal transduction pathways and novel anti-inflammatory targets. *Gut*, *52*(1), 144–151. <https://doi.org/10.1136/gut.52.1.144>
- Huang, X., Zhou, Y., Ma, M., Cai, Z., & Li, T. (2010). Chemiluminescence evaluation of antioxidant activity and prevention of DNA damage effect of peptides isolated from soluble eggshell membrane protein hydrolysate. *Journal of Agricultural and Food Chemistry*, *58*(23), 12137–12142. <https://doi.org/10.1021/jf101728d>
- Ignarro, L. J. (2014). Nitric Oxide. In *Reference Module in Biomedical Sciences* (Vol. 71, Issue

- 7/8, pp. 398–406). Elsevier. <https://doi.org/10.1016/B978-0-12-801238-3.00245-2>
- Ino, T., Hattori, M., Yoshida, T., Hattori, S., Yoshimura, K., & TAKAHASHI, K. (2006). Improved Physical and Biochemical Features of a Collagen Membrane by Conjugating with Soluble Egg Shell Membrane Protein. *Bioscience, Biotechnology, and Biochemistry*, 70(4), 865–873. <https://doi.org/10.1271/bbb.70.865>
- Ishii, Y., Sugimoto, S., Izawa, N., Sone, T., Chiba, K., & Miyazaki, K. (2014). Oral administration of *Bifidobacterium breve* attenuates UV-induced barrier perturbation and oxidative stress in hairless mice skin. *Archives of Dermatological Research*, 306(5), 467–473. <https://doi.org/10.1007/s00403-014-1441-2>
- Jahandideh, F., Chakrabarti, S., Davidge, S. T., & Wu, J. (2016). Antioxidant Peptides Identified from Ovotransferrin by the ORAC Method Did Not Show Anti-Inflammatory and Antioxidant Activities in Endothelial Cells. *Journal of Agricultural and Food Chemistry*, 64(1), 113–119. <https://doi.org/10.1021/acs.jafc.5b04230>
- Jain, S., & Anal, A. K. (2016). Optimization of extraction of functional protein hydrolysates from chicken egg shell membrane (ESM) by ultrasonic assisted extraction (UAE) and enzymatic hydrolysis. *LWT - Food Science and Technology*, 69, 295–302. <https://doi.org/10.1016/j.lwt.2016.01.057>
- Jain, S., & Anal, A. K. (2018). Preparation of eggshell membrane protein hydrolysates and culled banana resistant starch-based emulsions and evaluation of their stability and behavior in simulated gastrointestinal fluids. *Food Research International*, 103, 234–242. <https://doi.org/10.1016/j.foodres.2017.10.042>
- Jensen, G., Shah, B., Holtz, R., Patel, A., & Lo, D. (2016). Reduction of facial wrinkles by hydrolyzed water-soluble egg membrane associated with reduction of free radical stress and

- support of matrix production by dermal fibroblasts. *Clinical, Cosmetic and Investigational Dermatology*, 9, 357–366. <https://doi.org/10.2147/CCID.S111999>
- Jia, H., Aw, W., Saito, K., Hanate, M., Hasebe, Y., & Kato, H. (2014). Eggshell membrane ameliorates hepatic fibrogenesis in human C3A cells and rats through changes in PPAR γ -Endothelin 1 signaling. *Scientific Reports*, 4(1), 7473. <https://doi.org/10.1038/srep07473>
- Jia, H., Hanate, M., Aw, W., Itoh, H., Saito, K., Kobayashi, S., Hachimura, S., Fukuda, S., Tomita, M., Hasebe, Y., & Kato, H. (2017). Eggshell membrane powder ameliorates intestinal inflammation by facilitating the restitution of epithelial injury and alleviating microbial dysbiosis. *Scientific Reports*, 7(1), 43993. <https://doi.org/10.1038/srep43993>
- Jia, H., Saito, K., Aw, W., Takahashi, S., Hanate, M., Hasebe, Y., & Kato, H. (2013). Transcriptional profiling in rats and an ex vivo analysis implicate novel beneficial function of egg shell membrane in liver fibrosis. *Journal of Functional Foods*. <https://doi.org/10.1016/j.jff.2013.07.003>
- Jia, J., Guo, Z., Yu, J., & Duan, Y. (2011). A new candidate for guided tissue regeneration: biomimetic eggshell membrane. *Journal of Medical Hypotheses and Ideas*, 5, 20.
- Jia, J., Liu, G., Guo, Z.-X., Yu, J., & Duan, Y. (2012). Preparation and Characterization of Soluble Eggshell Membrane Protein/PLGA Electrospun Nanofibers for Guided Tissue Regeneration Membrane. *Journal of Nanomaterials*, 2012, 1–7. <https://doi.org/10.1155/2012/282736>
- Jodoin, J., & Hincke, M. T. (2018). Histone H5 is a potent Antimicrobial Agent and a template for novel Antimicrobial Peptides. *Scientific Reports*, 8(1), 1–15. <https://doi.org/10.1038/s41598-018-20912-1>
- Kalman, D. S., & Hewlings, S. (2020). The effect of oral hydrolyzed eggshell membrane on the

- appearance of hair, skin, and nails in healthy middle-aged adults: A randomized double-blind placebo-controlled clinical trial. *Journal of Cosmetic Dermatology*, 19(6), 1463–1472. <https://doi.org/10.1111/jocd.13275>
- Kavarthapu, A., & Malaiappan, S. (2019). Comparative evaluation of demineralized bone matrix and type II collagen membrane versus eggshell powder as a graft material and membrane in rat model. *Indian Journal of Dental Research*. https://doi.org/10.4103/ijdr.IJDR_489_17
- Kelleher, B. P., Leahy, J. J., Henihan, A. M., O'Dwyer, T. F., Sutton, D., & Leahy, M. J. (2002). Advances in poultry litter disposal technology – a review. *Bioresource Technology*, 83(1), 27–36. [https://doi.org/10.1016/S0960-8524\(01\)00133-X](https://doi.org/10.1016/S0960-8524(01)00133-X)
- Khueychai, S., Jangpromma, N., Daduang, S., & Klaynongsruang, S. (2019). Effects of alkaline hydrolysis and storage conditions on the biological activity of ostrich egg white. *Journal of Food Processing and Preservation*, 43(4), 1–18. <https://doi.org/10.1111/jfpp.13921>
- Kim, P. K. M., Zamora, R., Petrosko, P., & Billiar, T. R. (2001). The regulatory role of nitric oxide in apoptosis. *International Immunopharmacology*, 1(8), 1421–1441. [https://doi.org/10.1016/S1567-5769\(01\)00088-1](https://doi.org/10.1016/S1567-5769(01)00088-1)
- Kim, Y., Chung, H., Kim, S., Han, J.-A., Yoo, Y., Kim, K., Lee, G., Yun, H., Green, A., Li, J., Simmons, R. L., & Billiar, T. R. (1999). Nitric Oxide Protects PC12 Cells from Serum Deprivation-Induced Apoptosis by cGMP-Dependent Inhibition of Caspase Signaling. *The Journal of Neuroscience*, 19(16), 6740–6747. <https://doi.org/10.1523/JNEUROSCI.19-16-06740.1999>
- King`ori, A. M. (2011). A Review of the Uses of Poultry Eggshells and Shell Membranes. *International Journal of Poultry Science*, 10, 908–912.
- Ko, W., Lee, S., Kim, S., Jo, M., Kumar, H., Han, I., & Sohn, S. (2017). Anti-inflammatory

effects of ursodeoxycholic acid by lipopolysaccharide-stimulated inflammatory responses in RAW 264.7 macrophages. *PLOS ONE*, *12*(6), e0180673.

<https://doi.org/10.1371/journal.pone.0180673>

Kobayashi, T., Naik, S., & Nagao, K. (2019). Choreographing Immunity in the Skin Epithelial Barrier. *Immunity*, *50*(3), 552–565. <https://doi.org/10.1016/j.immuni.2019.02.023>

Kobayashi, T., Voisin, B., Kim, D. Y., Kennedy, E. A., Jo, J. H., Shih, H. Y., Truong, A., Doebel, T., Sakamoto, K., Cui, C. Y., Schlessinger, D., Moro, K., Nakae, S., Horiuchi, K., Zhu, J., Leonard, W. J., Kong, H. H., & Nagao, K. (2019). Homeostatic Control of Sebaceous Glands by Innate Lymphoid Cells Regulates Commensal Bacteria Equilibrium. *Cell*, *176*(5), 982-997.e16. <https://doi.org/10.1016/j.cell.2018.12.031>

Kobayashi, Y., Rupa, P., Kovacs-Nolan, J., Turner, P. V., Matsui, T., & Mine, Y. (2015). Oral administration of hen egg white ovotransferrin attenuates the development of colitis induced by dextran sodium sulfate in mice. *Journal of Agricultural and Food Chemistry*. <https://doi.org/10.1021/jf505248n>

Kodali, V. K., Gannon, S. A., Paramasivam, S., Raje, S., Polenova, T., & Thorpe, C. (2011). A novel disulfide-rich protein motif from avian eggshell membranes. *PLoS ONE*. <https://doi.org/10.1371/journal.pone.0018187>

Kovacs-Nolan, J., Cordeiro, C. M. M., Young, D., Mine, Y., & Hincke, M. T. (2014). Ovocalyxin-36 is an effector protein modulating the production of proinflammatory mediators. *Veterinary Immunology and Immunopathology*, *160*(1–2), 1–11. <https://doi.org/10.1016/j.vetimm.2014.03.005>

Kulshreshtha, G., Ahmed, T. A. E., Wu, L., Diep, T., & Hincke, M. T. (2020). A novel eco-friendly green approach to produce partialized eggshell membrane (PEM) for skin health

applications. *Biomaterials Science*, 8(19), 5346–5361.

<https://doi.org/10.1039/D0BM01110J>

Kuwana, T., Mackey, M. R., Perkins, G., Ellisman, M. H., Latterich, M., Schneiter, R., Green, D. R., & Newmeyer, D. D. (2002). Bid, Bax, and lipids cooperate to form supramolecular openings in the outer mitochondrial membrane. *Cell*, 111(3), 331–342.

[https://doi.org/10.1016/S0092-8674\(02\)01036-X](https://doi.org/10.1016/S0092-8674(02)01036-X)

Łaniewski, P., & Herbst-Kralovetz, M. (2018). Vagina. In *Encyclopedia of Reproduction*.

<https://doi.org/10.1016/B978-0-12-801238-3.64406-9>

Lavergne, V., J. Taft, R., & F. Alewood, P. (2012). Cysteine-Rich Mini-Proteins in Human Biology. *Current Topics in Medicinal Chemistry*, 12(14), 1514–1533.

<https://doi.org/10.2174/156802612802652411>

Lee, M., Kovacs-Nolan, J., Yang, C., Archbold, T., Fan, M. Z., & Mine, Y. (2009). Hen egg lysozyme attenuates inflammation and modulates local gene expression in a porcine model of dextran sodium sulfate (DSS)-Induced Colitis. *Journal of Agricultural and Food Chemistry*. <https://doi.org/10.1021/jf803133b>

Lee, S. E., & Lee, S. H. (2018). Skin barrier and calcium. In *Annals of Dermatology*.

<https://doi.org/10.5021/ad.2018.30.3.265>

Leuner, K., Kraus, M., Woelfle, U., Beschmann, H., Harteneck, C., Boehncke, W. H., Schempp, C. M., & Müller, W. E. (2011). Reduced TRPC channel expression in psoriatic keratinocytes is associated with impaired differentiation and enhanced proliferation. *PLoS ONE*. <https://doi.org/10.1371/journal.pone.0014716>

Li, L. (1995). *Extracting process of egg membrane extract and application in cosmetics* (Patent No. CN1111514A).

- Lieleg, O., Lieleg, C., Bloom, J., Buck, C. B., & Ribbeck, K. (2012). Mucin Biopolymers As Broad-Spectrum Antiviral Agents. *Biomacromolecules*, *13*(6), 1724–1732.
<https://doi.org/10.1021/bm3001292>
- Lin, Z., Chen, Q., Lee, M., Cao, X., Zhang, J., Ma, D., Chen, L., Hu, X., Wang, H., Wang, X., Zhang, P., Liu, X., Guan, L., Tang, Y., Yang, H., Tu, P., Bu, D., Zhu, X., Wang, K., ... Yang, Y. (2012). Exome sequencing reveals mutations in TRPV3 as a cause of Olmsted syndrome. *American Journal of Human Genetics*.
<https://doi.org/10.1016/j.ajhg.2012.02.006>
- Liong, J. W. W., Frank, J. F., & Bailey, S. (1997). Visualization of Eggshell Membranes and Their Interaction with Salmonella enteritidis Using Confocal Scanning Laser Microscopy. *Journal of Food Protection*, *60*(9), 1022–1028. <https://doi.org/10.4315/0362-028X-60.9.1022>
- Liu, J., Huang, H., Huang, Z., Ma, Y., Zhang, L., He, Y., Li, D., Liu, W., Goodin, S., Zhang, K., & Zheng, X. (2019). Eriocitrin in combination with resveratrol ameliorates LPS-induced inflammation in RAW264.7 cells and relieves TPA-induced mouse ear edema. *Journal of Functional Foods*, *56*(February), 321–332. <https://doi.org/10.1016/j.jff.2019.03.008>
- Liu, T., Zhang, L., Joo, D., & Sun, S.-C. (2017). NF- κ B signaling in inflammation. *Signal Transduction and Targeted Therapy*, *2*(1), 17023. <https://doi.org/10.1038/sigtrans.2017.23>
- Liu, Y., Luo, C., & Liu, L. (2014). Comparison of eggshell membrane protein extracted effects by different methods. *Nongye Gongcheng Xuebao/Transactions of the Chinese Society of Agricultural Engineering*, *30*(7), 274–280.
- López-García, J., Lehocný, M., Humpolíček, P., & Sába, P. (2014). HaCaT Keratinocytes Response on Antimicrobial Atelocollagen Substrates: Extent of Cytotoxicity, Cell Viability

- and Proliferation. *Journal of Functional Biomaterials*. <https://doi.org/10.3390/jfb5020043>
- Louis, H. A., Pino, J. D., Schmeichel, K. L., Pomiès, P., & Beckerle, M. C. (1997). Comparison of three members of the cysteine-rich protein family reveals functional conservation and divergent patterns of gene expression. *Journal of Biological Chemistry*. <https://doi.org/10.1074/jbc.272.43.27484>
- Mackay, J. A., & Chilkoti, A. (2008). Temperature sensitive peptides: Engineering hyperthermia-directed therapeutics. In *International Journal of Hyperthermia*. <https://doi.org/10.1080/02656730802149570>
- Madamanchi, N. R., Vendrov, A., & Runge, M. S. (2005). Oxidative Stress and Vascular Disease. *Arteriosclerosis, Thrombosis, and Vascular Biology*, 25(1), 29–38. <https://doi.org/10.1161/01.ATV.0000150649.39934.13>
- Madhyastha, H., & Vatsala, T. M. (2010). Cysteine rich cyanopeptide β 2 from *Spirulina fusciformis* exhibits plasmid DNA pBR322 scission prevention and cellular antioxidant activity. *Indian Journal of Experimental Biology*.
- Maeda, K., & Sasaki, Y. (1982). An experience of hen-egg membrane as a biological dressing. *Burns*. [https://doi.org/10.1016/0305-4179\(82\)90029-8](https://doi.org/10.1016/0305-4179(82)90029-8)
- Mageed, A. M., Isobe, N., & Yoshimura, Y. (2008). Expression of Avian β -Defensins in the Oviduct and Effects of Lipopolysaccharide on Their Expression in the Vagina of Hens. *Poultry Science*, 87(5), 979–984. <https://doi.org/10.3382/ps.2007-00283>
- Makkar, S., Liyanage, R., Kannan, L., Packialakshmi, B., Lay, J. O., & Rath, N. C. (2015). Chicken Egg Shell Membrane Associated Proteins and Peptides. *Journal of Agricultural and Food Chemistry*, 63(44), 9897–9898. <https://doi.org/10.1021/acs.jafc.5b04266>
- Mann, K. (2007). The chicken egg white proteome. *Proteomics*, 7(19), 3558–3568.

<https://doi.org/10.1002/pmic.200700397>

Mann, K. (2008). Proteomic analysis of the chicken egg vitelline membrane. *PROTEOMICS*, 8(11), 2322–2332. <https://doi.org/10.1002/pmic.200800032>

Marcet, I., Salvadores, M., Rendueles, M., & Díaz, M. (2018). The effect of ultrasound on the alkali extraction of proteins from eggshell membranes. *Journal of the Science of Food and Agriculture*, 98(5), 1765–1772. <https://doi.org/10.1002/jsfa.8651>

Maritim, A. C., Sanders, R. A., & Watkins, J. B. (2003). Diabetes, oxidative stress, and antioxidants: A review. In *Journal of Biochemical and Molecular Toxicology*. <https://doi.org/10.1002/jbt.10058>

Marques, S., Magalhães, L., Tóth, I., & Segundo, M. (2014). Insights on Antioxidant Assays for Biological Samples Based on the Reduction of Copper Complexes—The Importance of Analytical Conditions. *International Journal of Molecular Sciences*, 15(7), 11387–11402. <https://doi.org/10.3390/ijms150711387>

Marshall, E., Costa, L. M., & Gutierrez-Marcos, J. (2011). Cysteine-Rich Peptides (CRPs) mediate diverse aspects of cell-cell communication in plant reproduction and development. *Journal of Experimental Botany*, 62(5), 1677–1686. <https://doi.org/10.1093/jxb/err002>

Masaki, H. (2010). Role of antioxidants in the skin: Anti-aging effects. In *Journal of Dermatological Science*. <https://doi.org/10.1016/j.jdermsci.2010.03.003>

Mascia, F., Denning, M., Kopan, R., & Yuspa, S. H. (2012). The Black Box Illuminated: Signals and Signaling. *Journal of Investigative Dermatology*, 132(3), 811–819. <https://doi.org/10.1038/jid.2011.406>

Matsuoka, R., Kurihara, H., Yukawa, H., & Sasahara, R. (2019). Eggshell membrane protein can be absorbed and utilised in the bodies of rats. *BMC Research Notes*, 12(1), 258.

<https://doi.org/10.1186/s13104-019-4306-0>

- Matthias, L. J., Yam, P. T. W., Jiang, X. M., Vandegraaff, N., Li, P., Pountourios, P., Donoghue, N., & Hogg, P. J. (2002). Disulfide exchange in domain 2 of CD4 is required for entry of HIV-I. *Nature Immunology*. <https://doi.org/10.1038/ni815>
- May, A. K., Stafford, R. E., Bulger, E. M., Heffernan, D., Guillaumondegui, O., Bochicchio, G., & Eachempati, S. R. (2009). Treatment of Complicated Skin and Soft Tissue Infections. *Surgical Infections*, *10*(5), 467–499. <https://doi.org/10.1089/sur.2009.012>
- McSorley, S. J., & Liew, F. Y. (1998). Nitric Oxide. In *Encyclopedia of Immunology* (pp. 1859–1861). Elsevier. <https://doi.org/10.1006/rwei.1999.0466>
- Medzhitov, R. (2008). Origin and physiological roles of inflammation. In *Nature*. <https://doi.org/10.1038/nature07201>
- Mendis, E., Rajapakse, N., & Kim, S.-K. (2005). Antioxidant Properties of a Radical-Scavenging Peptide Purified from Enzymatically Prepared Fish Skin Gelatin Hydrolysate. *Journal of Agricultural and Food Chemistry*, *53*(3), 581–587. <https://doi.org/10.1021/jf048877v>
- Mine, Y., Ma, F., & Lauriau, S. (2004). Antimicrobial Peptides Released by Enzymatic Hydrolysis of Hen Egg White Lysozyme. *Journal of Agricultural and Food Chemistry*, *52*(5), 1088–1094. <https://doi.org/10.1021/jf0345752>
- Mine, Y., Oberle, C., & Kassaify, Z. (2003). Eggshell Matrix Proteins as Defense Mechanism of Avian Eggs. *Journal of Agricultural and Food Chemistry*, *51*(1), 249–253. <https://doi.org/10.1021/jf020597x>
- Mogoşanu, G. D., & Grumezescu, A. M. (2014). Natural and synthetic polymers for wounds and burns dressing. *International Journal of Pharmaceutics*, *463*(2), 127–136. <https://doi.org/10.1016/j.ijpharm.2013.12.015>

- Mosser, D. M., & Edwards, J. P. (2008). Exploring the full spectrum of macrophage activation. *Nature Reviews Immunology*, 8(12), 958–969. <https://doi.org/10.1038/nri2448>
- Muñoz, A., Dominguez-Gasca, N., Jimenez-Lopez, C., & Rodriguez-Navarro, A. B. (2015). Importance of eggshell cuticle composition and maturity for avoiding trans-shell Salmonella contamination in chicken eggs. *Food Control*. <https://doi.org/10.1016/j.foodcont.2015.02.028>
- Nestle, F. O., Di Meglio, P., Qin, J. Z., & Nickoloff, B. J. (2009). Skin immune sentinels in health and disease. *Nature Reviews Immunology*, 9(10), 679–691. <https://doi.org/10.1038/nri2622>
- Nimalaratne, C., Bandara, N., & Wu, J. (2015). Purification and characterization of antioxidant peptides from enzymatically hydrolyzed chicken egg white. *Food Chemistry*, 188, 467–472. <https://doi.org/10.1016/j.foodchem.2015.05.014>
- Ohto-Fujita, E., Konno, T., Shimizu, M., Ishihara, K., Sugitate, T., Miyake, J., Yoshimura, K., Taniwaki, K., Sakurai, T., Hasebe, Y., Atomi, Y., Ohto-Fujita, E., Shimizu, M., Konno, T., Ishihara, : K, Sugitate, T., Miyake, J., Ishihara, K., Yoshimura, K., ... Atomi, Y. (2011). Hydrolyzed eggshell membrane immobilized on phosphorylcholine polymer supplies extracellular matrix environment for human dermal fibroblasts. *Cell and Tissue Research*, 345, 177–190. <https://doi.org/10.1007/s00441-011-1172-z>
- Omana, D. A., Wang, J., & Wu, J. (2010). Ovomucin – a glycoprotein with promising potential. *Trends in Food Science & Technology*, 21(9), 455–463. <https://doi.org/10.1016/j.tifs.2010.07.001>
- Otberg, N., Richter, H., Schaefer, H., Blume-Peytavi, U., Sterry, W., & Lademann, J. (2004). Variations of Hair Follicle Size and Distribution in Different Body Sites. *Journal of*

- Investigative Dermatology*, 122(1), 14–19. <https://doi.org/10.1046/j.0022-202X.2003.22110.x>
- Özyürek, M., Güçlü, K., Tütem, E., Bakan, K. S., Erçağ, E., Esin Çelik, S., Baki, S., Yildiz, L., Karaman, Ş., & Apak, R. (2011). A comprehensive review of CUPRAC methodology. In *Analytical Methods*. <https://doi.org/10.1039/c1ay05320e>
- Paczosa, M. K., & Meccas, J. (2016). *Klebsiella pneumoniae*: Going on the Offense with a Strong Defense. *Microbiology and Molecular Biology Reviews*. <https://doi.org/10.1128/membr.00078-15>
- Pahwa, R., & Jialal, I. (2019, June 4). *Chronic Inflammation*. StatPearls; StatPearls Publishing. <http://www.ncbi.nlm.nih.gov/pubmed/29630225>
- Peña-Ramos, E. A., & Xiong, Y. L. (2002). Antioxidant Activity of Soy Protein Hydrolysates in a Liposomal System. *Journal of Food Science*, 67(8), 2952–2956. <https://doi.org/10.1111/j.1365-2621.2002.tb08844.x>
- Pereira, L. B. (2014). Impetigo - Review. *Anais Brasileiros de Dermatologia*, 89(2), 293–299. <https://doi.org/10.1590/abd1806-4841.20142283>
- Petkovšek, Ž., Eleršič, K., Gubina, M., Žgur-Bertok, D., & Erjavec, M. S. (2009). Virulence potential of *Escherichia coli* isolates from skin and soft tissue infections. *Journal of Clinical Microbiology*. <https://doi.org/10.1128/JCM.01421-08>
- Phaniendra, A., Jestadi, D. B., & Periyasamy, L. (2015). Free Radicals: Properties, Sources, Targets, and Their Implication in Various Diseases. In *Indian Journal of Clinical Biochemistry*. <https://doi.org/10.1007/s12291-014-0446-0>
- Pillai, M. M., Akshaya, T. R., Elakkiya, V., Gopinathan, J., Sahanand, K. S., Rai, B. K. D., Bhattacharyya, A., & Selvakumar, R. (2015). Egg shell membrane-a potential natural

- scaffold for human meniscal tissue engineering: An in vitro study. *RSC Advances*, 5(93), 76019–76025. <https://doi.org/10.1039/c5ra09959e>
- Pinto, M., Hundi, G., Bhat, R., Bala, N., Dandekeri, S., Martis, J., & Kambil, S. (2016). Clinical and epidemiological features of coryneform skin infections at a tertiary hospital. *Indian Dermatology Online Journal*. <https://doi.org/10.4103/2229-5178.182351>
- Poland, A. L., & Sheldon, B. W. (2001). Altering the Thermal Resistance of Foodborne Bacterial Pathogens with an Eggshell Membrane Waste By-Product. *Journal of Food Protection*, 64(4), 486–492. <https://doi.org/10.4315/0362-028X-64.4.486>
- Pund, S., Borade, G., & Rasve, G. (2014). Improvement of anti-inflammatory and anti-angiogenic activity of berberine by novel rapid dissolving nanoemulsifying technique. *Phytomedicine*, 21(3), 307–314. <https://doi.org/10.1016/j.phymed.2013.09.013>
- Ralph, P., & Nakoinz, I. (1977). Antibody-Dependent Killing of Erythrocyte and Tumor Targets by Macrophage-Related Cell Lines: Enhancement by PPD and LPS. *The Journal of Immunology*, 119(3), 950 LP – 954.
- Rath, N. C., Liyanage, R., Makkar, S. K., & Lay, J. O. (2016). Protein profiles of hatchery egg shell membrane. *Proteome Science*, 15(1), 4. <https://doi.org/10.1186/s12953-017-0112-6>
- Réhault-Godbert, S., Hervé-Grépinet, V., Gautron, J., Cabau, C., Nys, Y., & Hincke, M. T. (2011). Molecules involved in chemical defence of the chicken egg. In *Improving the Safety and Quality of Eggs and Egg Products: Egg Chemistry, Production and Consumption*. <https://doi.org/10.1533/9780857093912.2.183>
- Rendon, A., & Schäkel, K. (2019). Psoriasis pathogenesis and treatment. In *International Journal of Molecular Sciences*. <https://doi.org/10.3390/ijms20061475>
- Rinnerthaler, M., Bischof, J., Streubel, M., Trost, A., & Richter, K. (2015). Oxidative Stress in

- Aging Human Skin. *Biomolecules*, 5(2), 545–589. <https://doi.org/10.3390/biom5020545>
- Rose-Martel, M., & Hincke, M. T. (2017). The Eggshell Proteome Yields Insight Into Its Antimicrobial Protection. In *Egg Innovations and Strategies for Improvements* (pp. 157–163). Elsevier. <https://doi.org/10.1016/B978-0-12-800879-9.00015-9>
- Rose-Martel, M., Kulshreshtha, G., Ahferom Berhane, N., Jodoin, J., & Hincke, M. T. (2017). Histones from Avian Erythrocytes Exhibit Antibiofilm activity against methicillin-sensitive and methicillin-resistant *Staphylococcus aureus*. *Scientific Reports*, 7(1), 45980. <https://doi.org/10.1038/srep45980>
- Rose-Martel, M., Smiley, S., & Hincke, M. T. (2015). Novel identification of matrix proteins involved in calcitic biomineralization. *Journal of Proteomics*, 116, 81–96. <https://doi.org/10.1016/j.jprot.2015.01.002>
- Ruff, K. J., DeVore, D. P., Leu, M. D., & Robinson, M. A. (2009). Eggshell membrane: a possible new natural therapeutic for joint and connective tissue disorders. Results from two open-label human clinical studies. *Clinical Interventions in Aging*, 4, 235–240. <https://doi.org/10.2147/cia.s5797>
- Ruff, K. J., Durham, P., O'Reilly, A., & Long, D. (2015). Eggshell membrane hydrolyzates activate NF- κ B in vitro: possible implications for in vivo efficacy. *Journal of Inflammation Research*, 49. <https://doi.org/10.2147/JIR.S78118>
- Ruff, K. J., Winkler, A., Jackson, R. W., DeVore, D. P., & Ritz, B. W. (2009). Eggshell membrane in the treatment of pain and stiffness from osteoarthritis of the knee: a randomized, multicenter, double-blind, placebo-controlled clinical study. *Clinical Rheumatology*, 28(8), 907–914. <https://doi.org/10.1007/s10067-009-1173-4>
- Ruszczak, Z. (2003). Effect of collagen matrices on dermal wound healing. *Advanced Drug*

- Delivery Reviews*. <https://doi.org/10.1016/j.addr.2003.08.003>
- Sah, M. K., & Pramanik, K. (2014). Soluble-eggshell-membrane-protein-modified porous silk fibroin scaffolds with enhanced cell adhesion and proliferation properties. *Journal of Applied Polymer Science*, *131*(8). <https://doi.org/10.1002/app.40138>
- Sah, M. K., & Rath, S. N. (2016). Soluble eggshell membrane: A natural protein to improve the properties of biomaterials used for tissue engineering applications. *Materials Science and Engineering: C*, *67*, 807–821. <https://doi.org/10.1016/j.msec.2016.05.005>
- Sakanaka, S., & Tachibana, Y. (2006). Active oxygen scavenging activity of egg-yolk protein hydrolysates and their effects on lipid oxidation in beef and tuna homogenates. *Food Chemistry*, *95*(2), 243–249. <https://doi.org/10.1016/j.foodchem.2004.11.056>
- Salinas, G., Pellizza, L., Margenat, M., Fló, M., & Fernández, C. (2011). Tuned Escherichia coli as a host for the expression of disulfide-rich proteins. *Biotechnology Journal*, *6*(6), 686–699. <https://doi.org/10.1002/biot.201000335>
- Santana, A., Melo, A., Tavares, T., & Ferreira, I. M. P. L. V. O. (2016). Biological activities of peptide concentrates obtained from hydrolysed eggshell membrane byproduct by optimisation with response surface methodology. *Food and Function*, *7*(11), 4597–4604. <https://doi.org/10.1039/c6fo00954a>
- Sarmadi, B. H., & Ismail, A. (2010). Antioxidative peptides from food proteins: A review. *Peptides*, *31*(10), 1949–1956. <https://doi.org/10.1016/j.peptides.2010.06.020>
- Schön, A., Clarkson, B. R., Jaime, M., & Freire, E. (2017). Temperature stability of proteins: Analysis of irreversible denaturation using isothermal calorimetry. *Proteins: Structure, Function and Bioinformatics*. <https://doi.org/10.1002/prot.25354>
- Sekirov, I., Russell, S. L., Caetano M Antunes, L., & Finlay, B. B. (2010). Gut microbiota in

- health and disease. In *Physiological Reviews*. <https://doi.org/10.1152/physrev.00045.2009>
- Seo, M., Won, H., Kim, J., Mishig-Ochir, T., & Lee, B. (2012). Antimicrobial Peptides for Therapeutic Applications: A Review. *Molecules*, *17*(10), 12276–12286. <https://doi.org/10.3390/molecules171012276>
- Shahbandeh, M. (2017). *Growth of demand for animal protein worldwide 2015-2035*. Statista. <https://www.statista.com/statistics/739502/changes-in-global-demand-for-animal-protein/>
- Shahidi, F., & Zhong, Y. (2008). Bioactive peptides. *Journal of AOAC International*, *91*(4), 914–931.
- Shahidi, F., & Zhong, Y. (2010). Novel antioxidants in food quality preservation and health promotion. *European Journal of Lipid Science and Technology*. <https://doi.org/10.1002/ejlt.201000044>
- Shapouri-Moghaddam, A., Mohammadian, S., Vazini, H., Taghadosi, M., Esmaeili, S. A., Mardani, F., Seifi, B., Mohammadi, A., Afshari, J. T., & Sahebkar, A. (2018). Macrophage plasticity, polarization, and function in health and disease. *Journal of Cellular Physiology*, *233*(9), 6425–6440. <https://doi.org/10.1002/jcp.26429>
- Shi, Y., Kovacs-Nolan, J., Jiang, B., Tsao, R., & Mine, Y. (2014a). Antioxidant activity of enzymatic hydrolysates from eggshell membrane proteins and its protective capacity in human intestinal epithelial Caco-2 cells. *Journal of Functional Foods*, *10*, 35–45. <https://doi.org/10.1016/j.jff.2014.05.004>
- Shi, Y., Kovacs-Nolan, J., Jiang, B., Tsao, R., & Mine, Y. (2014b). Peptides derived from eggshell membrane improve antioxidant enzyme activity and glutathione synthesis against oxidative damage in Caco-2 cells. *Journal of Functional Foods*, *11*, 571–580. <https://doi.org/10.1016/j.jff.2014.08.017>

- Shi, Y., Rupa, P., Jiang, B., & Mine, Y. (2014). Hydrolysate from eggshell membrane ameliorates intestinal inflammation in mice. *International Journal of Molecular Sciences*. <https://doi.org/10.3390/ijms151222728>
- Strohbehn, R. E., Etzel, L. R., & Figgins, J. I. (2010). *Solubilized protein composition obtained from eggshell membrane* (Patent No. US8211477B2).
- Strohbehn, R. E., & Figgins, J. I. (2012). *Method of separating components of technical eggs, edible eggs, yolk and whites and products therefrom* (Patent No. US20120052552A1).
- Stulberg, D. L., Penrod, M. A., & Blatny, R. A. (2002). Common bacterial skin infections. *American Family Physician*, 66(1), 119–125.
- Taciak, B., Białasek, M., Braniewska, A., Sas, Z., Sawicka, P., Kiraga, Ł., Rygiel, T., & Król, M. (2018). Evaluation of phenotypic and functional stability of RAW 264.7 cell line through serial passages. *PLoS ONE*, 13(6). <https://doi.org/10.1371/journal.pone.0198943>
- Takahashi, K., Shirai, K., Kitamura, M., & Hattori, M. (1996). Soluble Egg Shell Membrane Protein as a Regulating Material for Collagen Matrix Reconstruction. *Bioscience, Biotechnology, and Biochemistry*, 60(8), 1299–1302. <https://doi.org/10.1271/bbb.60.1299>
- Tanaka, S. (2013). *Eggshell membrane solubilization method using enzymes* (Patent No. US10526423B2).
- Tavassoli, M. (1983). Effect of the substratum on the growth of CFU-c in continuous marrow culture t. *Experientia*, 39(4), 411–412. <https://doi.org/10.1007/BF01963153>
- Taylor, M. J., & Richardson, T. (1980). Antioxidant activity of cysteine and protein sulfhydryls in a linoleate emulsion oxidized by hemoglobin. *Journal of Food Science*, 45(5), 1223–1227. <https://doi.org/10.1111/j.1365-2621.1980.tb06526.x>
- Thomson, A., Hemphill, D., & Jeejeebhoy, K. N. (1998). Oxidative Stress and Antioxidants in

- Intestinal Disease. *Digestive Diseases*, 16(3), 152–158. <https://doi.org/10.1159/000016859>
- Thoroski, J. H. (2003). Eggshell processing methods and apparatus (Patent No. US 6649203 B1).
In *United States Patent* (US 6649203 B1).
- Ting, B. P. C. P., Mine, Y., Juneja, L. R., Okubo, T., Gauthier, S. F., & Pouliot, Y. (2011).
Comparative composition and antioxidant activity of peptide fractions obtained by
ultrafiltration of egg yolk protein enzymatic hydrolysates. *Membranes*, 1(3), 149–161.
<https://doi.org/10.3390/membranes1030149>
- Traber, M. G., & Stevens, J. F. (2011). Vitamins C and E: Beneficial effects from a mechanistic
perspective. In *Free Radical Biology and Medicine*.
<https://doi.org/10.1016/j.freeradbiomed.2011.05.017>
- Trouba, K. J., Hamadeh, H. K., Amin, R. P., & Germolec, D. R. (2002). Oxidative Stress and Its
Role in Skin Disease. *Antioxidants & Redox Signaling*, 4(4), 665–673.
<https://doi.org/10.1089/15230860260220175>
- Turin, S. Y., Ledwon, J. K., Bae, H., Buganza-Tepole, A., Topczewska, J., & Gosain, A. K.
(2018). Digital analysis yields more reliable and accurate measures of dermal and epidermal
thickness in histologically processed specimens compared to traditional methods.
Experimental Dermatology, 27(6), 687–690. <https://doi.org/10.1111/exd.13534>
- Uchida, K., & Kawakishi, S. (1992). Sequence-Dependent Reactivity of Histidine-Containing
Peptides with Copper(II)/Ascorbate. *Journal of Agricultural and Food Chemistry*.
<https://doi.org/10.1021/jf00013a003>
- Ůrgeová, E., & Vulganová, K. (2016). Comparison of Enzymatic Hydrolysis of Polysaccharides
from Eggshells Membranes. *Nova Biotechnologica et Chimica*, 15(2), 133–141.
<https://doi.org/10.1515/nbec-2016-0014>

- Usal, M., & Sahan, Y. (2020). In vitro evaluation of the bioaccessibility of antioxidative properties in commercially baby foods. *Journal of Food Science and Technology*, *57*(9), 3493–3501. <https://doi.org/10.1007/s13197-020-04384-8>
- Uttara, B., Singh, A., Zamboni, P., & Mahajan, R. (2009). Oxidative Stress and Neurodegenerative Diseases: A Review of Upstream and Downstream Antioxidant Therapeutic Options. *Current Neuropharmacology*, *7*(1), 65–74. <https://doi.org/10.2174/157015909787602823>
- van Dijk, A., Veldhuizen, E. J. A., & Haagsman, H. P. (2008). Avian defensins. *Veterinary Immunology and Immunopathology*, *124*(1–2), 1–18. <https://doi.org/10.1016/j.vetimm.2007.12.006>
- van Dijk, A., Veldhuizen, E. J. A., Kalkhove, S. I. C., Tjeerdsma-van Bokhoven, J. L. M., Romijn, R. A., & Haagsman, H. P. (2007). The β -Defensin Gallinacin-6 Is Expressed in the Chicken Digestive Tract and Has Antimicrobial Activity against Food-Borne Pathogens. *Antimicrobial Agents and Chemotherapy*, *51*(3), 912–922. <https://doi.org/10.1128/AAC.00568-06>
- Vuong, T. T., Rønning, S. B., Ahmed, T. A. E., Brathagen, K., Høst, V., Hincke, M. T., Suso, H. P., & Pedersen, M. E. (2018). Processed eggshell membrane powder regulates cellular functions and increase MMP-activity important in early wound healing processes. *PLOS ONE*, *13*(8), 1–23. <https://doi.org/10.1371/journal.pone.0201975>
- Vuong, T. T., Rønning, S. B., Suso, H. P., Schmidt, R., Prydz, K., Lundström, M., Moen, A., & Pedersen, M. E. (2017). The extracellular matrix of eggshell displays anti-inflammatory activities through NF- κ B in LPS-triggered human immune cells. *Journal of Inflammation Research*, *10*, 83–96. <https://doi.org/10.2147/JIR.S130974>

- Wang, M., Thakur, M., Peng, M., Jiang, Y., Frantz, L. A. F., Li, M., Zhang, J., Wang, S., Peters, J., Otecko, N. O., Suwannapoom, C., Guo, X., Zheng, Z., Esmailizadeh, A., Hirimuthugoda, N. Y., Ashari, H., Suladari, S., Zein, M. S. A., Kusza, S., ... Zhang, Y.-P. (2020). 863 genomes reveal the origin and domestication of chicken. *Cell Research*, 30(8), 693–701. <https://doi.org/10.1038/s41422-020-0349-y>
- Wang, P., Hung, Y., Lin, T., Fang, J., Yang, P., Chen, M., & Pan, T. (2019). Comparison of the Biological Impact of UVA and UVB upon the Skin with Functional Proteomics and Immunohistochemistry. *Antioxidants*, 8(12), 569. <https://doi.org/10.3390/antiox8120569>
- WHO. (2016). United Nations meeting on antimicrobial resistance. *Bulletin of the World Health Organization*, 94(9), 638–639. <https://doi.org/10.2471/BLT.16.020916>
- WHO. (2017). *Global priority list of antibiotic-resistant bacteria to guide research, discovery, and development of new antibiotics*. World Health Organization. <https://www.who.int/medicines/publications/global-priority-list-antibiotic-resistant-bacteria/en/>
- WHO. (2020a). *Antimicrobial resistance*. World Health Organization. <https://www.who.int/news-room/fact-sheets/detail/antimicrobial-resistance>
- WHO. (2020b). *Global Antimicrobial Resistance and Use Surveillance System (GLASS) report*. World Health Organization. <https://www.who.int/glass/resources/publications/early-implementation-report-2020/en/>
- Williams, C. M., Barker, J. C., & Sims, J. T. (1999). Management and utilization of poultry wastes. *Reviews of Environmental Contamination and Toxicology*. https://doi.org/10.1007/978-1-4612-1528-8_3
- Wilson, G., & Garthwaite, J. (2009). Nitric Oxide. In *Encyclopedia of Neuroscience* (pp. 1151–

- 1156). Elsevier. <https://doi.org/10.1016/B978-008045046-9.00684-7>
- Wu, P. Y., Lin, T. Y., Hou, C. W., Chang, Q. X., Wen, K. C., Lin, C. Y., & Chiang, H. M. (2019). 1,2-bis[(3-methoxyphenyl)methyl]ethane-1,2-dicarboxylic acid reduces UVB-induced photodamage in vitro and in vivo. *Antioxidants*, 8(10), 1–19. <https://doi.org/10.3390/antiox8100452>
- Xu, H., Timares, L., & Elmetts, C. A. (2018). Host Defenses in Skin. In *Clinical Immunology: Principles and Practice*. Elsevier Ltd.
- Yacoub, H. A., Elazzazy, A. M., Abuzinadah, O. A. H., Al-Hejin, A. M., Mahmoud, M. M., & Harakeh, S. M. (2015). Antimicrobial activities of chicken β -defensin (4 and 10) peptides against pathogenic bacteria and fungi. *Frontiers in Cellular and Infection Microbiology*, 5. <https://doi.org/10.3389/fcimb.2015.00036>
- Yahfoufi, N., Alsadi, N., Jambi, M., & Matar, C. (2018). The immunomodulatory and anti-inflammatory role of polyphenols. *Nutrients*, 10(11), 1–23. <https://doi.org/10.3390/nu10111618>
- Yang, G., Lu, Y., Bomba, H. N., & Gu, Z. (2019). Cysteine-rich Proteins for Drug Delivery and Diagnosis. *Current Medicinal Chemistry*, 26(8), 1377–1388. <https://doi.org/10.2174/0929867324666170920163156>
- Yang, Jinming, Amiri, K. I., Burke, J. R., Schmid, J. A., & Richmond, A. (2006). BMS-345541 targets inhibitor of κ B kinase and induces apoptosis in melanoma: Involvement of nuclear factor κ B and mitochondria pathways. *Clinical Cancer Research*, 12(3 I), 950–960. <https://doi.org/10.1158/1078-0432.CCR-05-1220>
- Yang, Juiyung, Chuang, S., Yang, W., & Tsay, P. (2003). Egg membrane as a new biological dressing in split-thickness skin graft donor sites: a preliminary clinical evaluation. *Chang*

Gung Medical Journal, 26(3), 153–159.

- Yang, M., Zhang, C., Zhang, X., Zhang, M. Z., Rottinghaus, G. E., & Zhang, S. (2016). Structure-function analysis of Avian β -defensin-6 and β -defensin-12: role of charge and disulfide bridges. *BMC Microbiology*, 16(1), 210. <https://doi.org/10.1186/s12866-016-0828-y>
- Yarlagadda, K., Hassani, J., Foote, I. P., & Markowitz, J. (2017). The role of nitric oxide in melanoma. *Biochimica et Biophysica Acta - Reviews on Cancer*, 1868(2), 500–509. <https://doi.org/10.1016/j.bbcan.2017.09.005>
- Yeom, M., Kim, J. H., Min, J. H., Hwang, M. K., Jung, H. S., & Sohn, Y. (2015). Xanthii fructus inhibits inflammatory responses in LPS-stimulated RAW 264.7 macrophages through suppressing NF- κ B and JNK/p38 MAPK. *Journal of Ethnopharmacology*, 176, 394–401. <https://doi.org/10.1016/j.jep.2015.11.020>
- Yeom, M., Park, J., Lim, C., Sur, B., Lee, B., Han, J. J., Choi, H. D., Lee, H., & Hahm, D. H. (2015). Glucosylceramide attenuates the inflammatory mediator expression in lipopolysaccharide-stimulated RAW264.7 cells. *Nutrition Research*, 35(3), 241–250. <https://doi.org/10.1016/j.nutres.2015.01.001>
- Yi, F., Guo, Z. X., Zhang, L. X., Yu, J., & Li, Q. (2004). Soluble eggshell membrane protein: Preparation, characterization and biocompatibility. *Biomaterials*, 25(19), 4591–4599. <https://doi.org/10.1016/j.biomaterials.2003.11.052>
- Yi, F., Yu, J., Guo, Z. X., Zhang, L. X., & Li, Q. (2003). Natural bioactive material: A preparation of soluble eggshell membrane protein. *Macromolecular Bioscience*, 3(5), 234–237. <https://doi.org/10.1002/mabi.200390030>
- Yi, F., Yu, J., Li, Q., & Guo, Z. (2007). Soluble eggshell mebrane protein: Antibacterial property

- and biodegradability. *Journal Wuhan University of Technology, Materials Science Edition*, 22(1), 117–119. <https://doi.org/10.1007/s11595-005-1117-z>
- Yoo, J., Kim, J., Yang, H., & Park, K. (2015). Effects of egg shell membrane hydrolysates on UVB-radiation-induced wrinkle formation in SKH-1 hairless mice. *Korean Journal for Food Science of Animal Resources*, 35(1), 58–70. <https://doi.org/10.5851/kosfa.2015.35.1.58>
- Yoo, J., Park, K., Yoo, Y., Kim, J., Yang, H., & Shin, Y. (2014). Effects of egg shell membrane hydrolysates on anti-inflammatory, anti-wrinkle, anti-microbial activity and moisture-protection. *Korean Journal for Food Science of Animal Resources*, 34(1), 26–32. <https://doi.org/10.5851/kosfa.2014.34.1.26>
- Zadik, Y. (2007). Self-Treatment of Full-Thickness Traumatic Lip Laceration with Chicken Egg Shell Membrane. *Wilderness & Environmental Medicine*, 18(3), 230–231. <https://doi.org/10.1580/06-WEME-LE-082R1.1>
- Zhai, X. T., Zhang, Z. Y., Jiang, C. H., Chen, J. Q., Ye, J. Q., Jia, X. Bin, Yang, Y., Ni, Q., Wang, S. X., Song, J., & Zhu, F. X. (2016). *Nauclea officinalis* inhibits inflammation in LPS-mediated RAW 264.7 macrophages by suppressing the NF- κ B signaling pathway. *Journal of Ethnopharmacology*. <https://doi.org/10.1016/j.jep.2016.01.018>
- Zhao, Q. C., Zhao, J. Y., Ahn, D. U., Jin, Y. G., & Huang, X. (2019). Separation and identification of highly efficient antioxidant peptides from eggshell membrane. *Antioxidants*, 8(10), 1–16. <https://doi.org/10.3390/antiox8100495>
- Zhou, Q., Mrowietz, U., & Rostami-Yazdi, M. (2009). Oxidative stress in the pathogenesis of psoriasis. *Free Radical Biology and Medicine*, 47(7), 891–905. <https://doi.org/10.1016/j.freeradbiomed.2009.06.033>

Zhou, X., Hao, Y., Yuan, L., Pradhan, S., Shrestha, K., Pradhan, O., Liu, H., & Li, W. (2018).

Nano-formulations for transdermal drug delivery: A review. *Chinese Chemical Letters*.

<https://doi.org/10.1016/j.ccllet.2018.10.037>